Techno-Economic Feasibility and Business Case for the Offshore Green FPSO

Towards a Net-Zero Green Hydrogen Supply Chain

TIL5060: TIL Thesis

Piotr Kaczmarek

Delft University of Technology

TU Delft

Techno-Economic Feasibility and Business Case for the Offshore Green FPSO

Towards a Net-Zero Green Hydrogen Supply Chain

by

Piotr Kaczmarek

Student Name	Student Number
Piotr Kaczmarek	5539986

University Supervisors:	E. van Hassel
	J. Pruijn
	J. A. Annema
Commissioner:	J. de Wilde
Project Duration:	March 2024 - February 2025
Faculty:	Faculty of Civil Engineering and Geosciences, Delft

Cover: Offshore wind power systems off the western coast of Taiwan by BING-JHEN HONG from Canva®

TU Delft

Preface

As a Masters student of Transport, Infrastructure, and Logistics, I have developed an interest in mathematical optimization models as well as how these models can be used to underpin strategic decision making in supply chains and logistics. I was eager to apply the theory I have learned to a practical example, and I am grateful for the opportunity to do this here. Throughout my studies I have also been passionate about topics surrounding climate change and sustainability, and I have aimed to incorporate this into my projects. At the time of writing, it is known that 2024 has been the warmest year on record, breaching the $1.5^{\circ}C$ level above the pre-industrial mean temperature. But I believe that should not discourage the efforts to decarbonize our future. The following report aims to investigate a possible component of the pathway towards carbon neutrality by the year 2050. Could a green FPSO concept feasibly provide a carbon-free energy source in the future? I hope that this thesis provides insight into the topic.

I would like to extend my sincere gratitude toward the members of the thesis committee: Jaap de Wilde, Edwin van Hassel, Jan Anne Annema, and Jeroen Pruyn. Thank you for all the valuable insight, patience, and guidance throughout the process. It has been a pleasure to work with you and I wish you all the best. I am also very grateful for my family for all the support and motivation they have provided me, as well as to my friends for the encouragement and staying by my side.

Piotr Kaczmarek
Delft, February 2025

Summary

Green hydrogen has the potential to contribute in decarbonization efforts and achieving a net-zero emission economy by 2050. This report investigates the potential for production of green hydrogen offshore, using a Floating Production Storage and Offloading (FPSO) vessel. The aim is to determine a techno-economically feasible strategy for deploying this Green FPSO (GFPSO) and in turn its holistic hydrogen supply chain. State of the art literature is reviewed to define the knowledge gap to address and delineate the scope of the research. This is encapsulated by the main research question: ”What strategy could be used to deploy a GFPSO supply chain and ensure techno-economically feasible outcomes?”. To answer this question, a methodology is devised involving the breakdown of the strategy into key decisions, the outline of the criteria by which the strategy can be scored against, and the formulation of an MILP model. The model encapsulates the supply chain from energy generation, hydrogen production, storage, and transport to destination. Technical and economic parameters are implemented in a North Sea business case context, assuming 4 scenarios which represent how each implemnentation strategy varies. This comes down to the configuration of energy vector of gaseous hydrogen (GH2), liquid hydrogen (LH2), and ammonia (NH3), as well as the transport mode of either shipping vessels or a pipiline, used to deliver the medium from production to demand location. Based on the MILP model result, the optimal locations in the discretized region for energy generation within each scenario, as well as comparison across scenarios using the calculated levelised cost of hydrogen (LCOH) in [€/kg].

The results of the study reveal LCOH values of 4.05-6.52[€/kg] for the time period of 2020-2050. The lowest cost was observed in the GH2 pipeline configuration, followed by NH3 shipping. The pipeline configuration required implementation closer to shore, while the shipping configuration correlates with the location of highest energy availability in the weather data. The greatest portion of the overall costs in all scenarios originated from wind turbines used for energy generation. Conversion process costs formed another significant component of the total costs in the scenarios involving NH3 and LH2. Sufficient reduction of these conversion costs could enable a more competitive performance from the corresponding configurations. Based on the criteria framework, the strategy utilizing GH2 pipeline supply chain configuration performs best in terms of LCOH, CO2 emissions, and access, while NH3 shipping performs better in Commercial Readiness Index (CRI), Technological Readiness Index (TRL), Ease of Implementation (EoI), and in existing regulations. The significance of these strengths and weaknesses will vary depending on the weight attributed to the importance of the criterion by the decision making entity.

Contents

1

Introduction

The energy transition is an ambitious global undertaking as a means to limit the impact of climate change, contributing to slowing of the average temperature increase of earth's atmosphere. Carbon dioxide has been identified as a significant cause for the enhanced greenhouse effect, with emissions observed in the atmosphere since 1850 exhibiting correlation to the elevation in average temperatures measured in the global climate [31].

To this end, the Maritime Research Institute (MARIN) in Wageningen is interested in the potential of floating production of offshore green hydrogen, through a novel green Floating Production Storage and & Offloading (FPSO) vessel such as those commonly applied in the oil & gas industries. This is in line with the strategy of MARIN, specifically as part of their mission stated as accelerating "sustainability and climate adaptation at sea" [46]. Previous research done for the institute by [49] suggests that this may be a feasible solution for the net-zero carbon emission economy by 2050 in certain scenarios, with a cost of hydrogen in the range of 3.17 - 4.29 [€/kg] across the studied scenarios. With this result in mind, further development of the green FPSO solution can be investigated to continue the pursuit towards achieving net-zero emissions by 2050.

1.1. Research Questions

An interesting knowledge gap emerges from literature, with its relevance explained more comprehensively later in Chapter 2, where a holistic value chain modeling approach involving a combination of wind and solar energy generation, while considering different combinations of transport modes and energy vectors in a floating offshore hydrogen production for regions spanning large location potential has not been presented. As such, the research objective can be formulated as: "Determine a feasible strategy for implementation of an offshore GFPSO supply chain by developing an accessible holistic techno-economic assessment model and applying it in a comprehensive business case spanning until 2050". Clarifying the terminology used, the "GFPSO" is a combination of production, storage, and offloading systems on a floating vessel for green hydrogen, while the GFPSO supply chain also encompasses the wind and solar technology used upstream as well as the logistical processes present downstream until reaching the demand node. The strategy refers to the key decisions which must be made by stakeholders in the process of setting up and operating a GFPSO supply chain. In the formulation, the keyword "feasible" is used instead of "optimal" deliberately, since optimality can imply a single best output or outcome, however a strategy's performance can vary depending on the weight attributed to the criteria used for assessment, and not necessarily purely on optimization model results. These weights could plausibly be subjective to the stakeholder and should be considered in a case specific manner. Finally, "holistic" is used similarly to [20] in order to specify that the techno-economic model represents the complete supply chain, spanning from energy generation to delivery, and "accessible" to attempt to make the model as user-friendly as possible. The objective is dissected further in the research questions.

The questions were formulated on the basis of the corroborative knowledge type approach from [74],

where it is asserted that a knowledge type can be ranked, and a higher-rank question can only be answered through questions of lower or equal rank. The ranks and descriptions are shown in Appendix A. The core question in this project is ”prescriptive”, which is the highest possible rank discussed in [74]. This question is subdivided into lower-rank questions. The knowledge type is indicated in parentheses beside the question.

What strategy could be used to deploy a GFPSO supply chain and ensure techno-economically feasible outcomes? (Prescriptive)

1. What key decisions must be made in a GFPSO supply chain deployment strategy? (Descriptive)
2. What criteria can be used to evaluate the success of the GFPSO deployment strategy in a business case? (Descriptive)
3. What model can be used to easily, effectively, and efficiently determine a realistic techno-economic feasibility at varying locations on a large-scale? (Evaluative)
4. To what extent can additional solutions enhance techno-economic potential of the GFPSO? (Evaluative)
5. Which transport mode and energy medium combinations offer optimal outcomes? (Evaluative)
6. What are the preferable scenarios for deployment of a GFPSO? (Evaluative)

The questions serve the purposes of addressing gaps, steering towards the methodology, and efficiently answering the core question through knowledge obtained from the sub-questions (SQs). The core question aims to bring focus to the end purpose of creating a realistic business case for an offshore GFPSO project, prescribing future action required to facilitate a successful implementation of a value chain. This business case must be broken down into key stakeholder decisions, which is targeted by SQ (1), in order to lay the foundation for the industry perspective that the research aims to produce knowledge for. Having understood this, the SQ (2) can be used to develop a framework to assess the degree of success of the strategy at attaining the desired outcomes of the stakeholders. The deliverable for this could be in the form of an assessment criteria framework similar to [32], categorized by technological, economic, environmental, and geopolitical considerations. SQ (3) steers toward the reproduction of the modeling approach from [49] which can be used to underpin the decisions qualitatively. Specific keywords were chosen in the question to describe the model requirements, namely ”easily” pertaining to accessibility and usability of the implemented mathematical model, ”effectively” to provide relevant insight based on an accurate, validated and verified formulation, and finally ”efficiently” to achieve a reasonable computation time. The deliverable for this question should be a mathematical model formulation, an implementation in python, with preliminary results and analysis. In SQ (4), novel contribution adaptations to the modeling should be considered. This includes additional energy mediums, and transport modes. The deliverable should be an updated model implementation with adjusted objective function, constraints, decision variables, and parameters as necessary, as well as an analysis of the model behavior. SQ (5) extends the novel contribution by consideration of the results of the additional transport modalities as well as energy mediums introduced into the model. Similarly to the previous question, the deliverable should be an analysis of the impacts on model output behavior and sensitivity based on parameters applied. Finally, SQ (6) aims to circle back to the business case, making use of the developed model and insights from the analyses to perform a location scan for study, apply knowledge to develop strategies, outlining the key decisions previously determined in SQ (1), and evaluating the alternatives based on the criteria established previously in SQ (2).

In Chapter 2 the literature review approach is formulated. The state of the art literature is investigated, underpinning the knowledge gaps targeted in the research questions. Chapter 3 delves into the methodology used to answer the proposed research questions, with Section 3.1 outlining the context for preparation of the strategy of a GFPSO supply chain, involving the breakdown of decisions and the criteria which can be used to evaluate the strategy. Section 3.2 provides the mathematical model and implementation, together with an analysis of the initial results from prior data. Once this is complete, Chapter 4 presents a business case in the North-Sea region for the strategy of a GFPSO supply chain, with relevant input parameters, results, analysis, and discussion of limitations. Finally, Chapter 5 provides conclusions from the research, implications and recommendations based on the results, as well

as further research suggestions.

2

Literature Review

The purpose of this section is to first outline the approach for collecting literature material, as shown in Section 2.1. This is followed by the review of the found literature in Section 2.2, used to characterize the project context and state of the art surrounding the topic of far offshore floating green hydrogen production and storage. The literature is critically reviewed to identify knowledge gaps in existing research and position the project in the knowledge domain.

2.1. Literature Collection Strategy

The collection of literature begins from the master thesis [49], where the author has developed a foundation for investigating offshore green hydrogen floating production and storage. The main articles cited in his research must be reviewed. Through this initial exploration, a list of relevant concept groups emerges, allowing to build up a conceptual understanding of the current state of the knowledge in the topic through a search in scientific article database of SCOPUS. The primary groups are ”Offshore” and ”Green Hydrogen”, which are contained in every search, while the secondary groups are used in combination with the primary groups for searching the databases. Each group can be broken down into keywords, which are used in conjunction with the concept group in the search in article database, as well as being used to determine relevance of the articles found. The concept groups and corresponding keywords are compiled in Table 2.1.

2.2. Literature Review

An overview is first presented of the thesis done by [49] for MARIN, followed by a discussion of possible areas for development. The areas are categorized into concept groups, each of which is further researched and reviewed for knowledge gap identification. Finally, the gaps are discussed and evaluated for determining the research objective.

2.2.1. Overview

The thesis by [49] carried out a techno-economic feasibility analysis of floating far offshore green hydrogen production for years 2020-2050, to understand the role of green hydrogen in the 2050 net-zero economy. This was done by determining the technologies to be applied in the offshore green hydrogen system, constructing a mathematical model to optimize the costs of energy generation, production of the hydrogen energy carrier, and transporting the energy to the demand node. The resulting mathematical model was a Mixed Integer Quadratically Constrained Programming (MIQCP) model, which was implemented in python using the Gurobi solver. The author chose floating wind turbines and solar platforms as the energy generation method, due to their technological feasibility having been demonstrated, and accessibility of cost development information. Far offshore was defined as a location which is characterized by a depth of more than 50m. Wave energy conversion was excluded as an energy generation method due to relatively uncertain cost and ability to implement such technology far offshore. In the modeling, energy generation is given a time period of 10 months from hourly weather data to

Table 2.1: Summary of concept groups and their corresponding keywords to be researched.

Concept Groups	Keywords
Offshore	Far offshore, deep offshore, FPSO, Ports
Green hydrogen	Hydrogen, Fuel Cell, Electrolysis, Ammonia, NH3, Liquid, Gaseous, H2
Energy Generation	Energy sources, wind turbines, solar panels, fuels, availability, seasonality, energy transition, renewable, sustainable
Production	Electrolysis, PEM, Electrolyzer, intermittency, start-up time, operation time, efficiency, matching demand
Storage	Battery, Peak shaving, peak balancing, load balancing, seasonality, P2X, PtX, Power-to-Gas, Conversion, Reconversion, location, matching demand
Transport	Modes, Hydrogen pipeline, hydrogen tanker, vessel, ship, fleet, AIS, routes, route choice, shipping, logistics, freight
Optimization	Python, gurobi, MILP, MIQCP, Stochastic Programming, recourse, scipy, pulp, operations research, chance constraints, location theory, VRP, multi-objective, modal choice, freight, meta-heuristic
Economic	Feasibility, potential, NPV, LCOH, LCOA, LCOE, risk, investment, CAPEX, OPEX, capital, operations, business case
Policy	Subsidies, investment, climate change, targets, ambitions, goals, governments, ports, competition, sectors

represent the variability of wind and solar source availability. The number of wind turbines and solar platforms is determined by the optimization, resulting in a total hourly power produced, which can be used for the production of green hydrogen. The modeling approach from [63] was used as a foundation for modeling energy generation in [49].

Green hydrogen was defined by [49] as hydrogen produced through renewable energy, in contrast to gray hydrogen produced through steam methane reforming (SMR) which makes use of fossil fuels such as natural gas, and blue hydrogen which uses SMR in combination with carbon capture and storage (CCS) to achieve net-zero carbon emissions. The green hydrogen production methods available are electrolysis based, with 3 leading types considered. These include Alkaline Electrolysis (AEL), Proton Exchange Membrane (PEM) electrolysis, and High-Temperature Electrolysis (HTEL). The technology chosen was PEM due to technology readiness level and scalability considerations. PEM does require a desalination plant, which is included in the cost optimization in the mathematical model. The model considers the cost optimization based on the number of electrolyzers, the number of desalination plants, the storage volume on the FPSO, the volume of the FPSO vessel, and the amount of conversion and reconversion devices. The (re)conversion varies depending on the energy medium of the hydrogen carrier, therefore binary decision variables are implemented, such that the optimization determines which medium is preferable cost-wise.

The transport of hydrogen was investigated through energy medium and transport modes over land and sea. The mediums considered were gaseous, liquid, liquid organic hydrogen carriers (LOHC), ammonia and methanol. For storage during transport, gaseous hydrogen requires high pressure compression, liquid hydrogen requires very low temperatures, LOHC requires large volumes, while ammonia and methanol require conversion and reconversion. The economic advantages and disadvantages of each medium was considered and the focus was placed on liquid hydrogen and ammonia as the mediums for study. Regarding transport modes, electrical cables are not considered due infeasibility of transport over distances in the order of magnitude required. For maritime transport, ships and pipelines are discussed. Pipeline transport is done with gaseous hydrogen, while ship transport can be done through for each medium. The author suggests sea pipelines may be technologically feasible, however dismissed them from the scope on the basis of excessive costs at large depths. In the modeling, the transport cost is determined by obtaining the transport distance from a selected supply node to a selected demand node, representing the production location and usage location respectively. This distance is separated into kilometers traveled over sea and land, with a geodesic between the nodes. If the line crosses over land during the sea transport, a correction factor is applied. The total transport cost is a combination

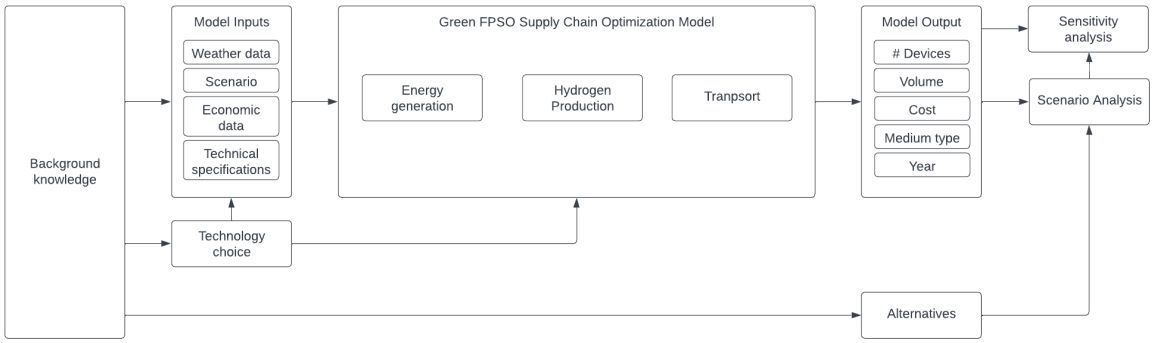

Figure 2.1: Conceptual framework representing the research process in [49]

of the total yearly hydrogen demand multiplied by a base sea rate (for 10,000 or 20,000 km) and the further rate for distance transported by sea, then summed with the land transport cost.

The model created is applied to 6 selected scenarios in differing geographical locations. Each scenario has corresponding data for input, (including start year, period, time steps, production, port, and usage locations, water depth, and the sea distance correction factor). The scenarios for study were determined based on strongest wind resources identified by [63], and low potential onshore production identified from [75]. Global demand for hydrogen varies based on different studies, therefore the values chosen for model input were determined from [75], due to similar assumptions regarding a net-zero economy in 2050, decarbonized options and conventional alternatives, and feasibility of application as well as supply chain considerations. The results for all scenarios fell within a cost of 7.73 - 11.93 [€/kg] hydrogen delivered in 2020, and decreased to 3.17 - 4.29 [€/kg] hydrogen delivered in 2050. The transport medium determined by the optimizer was ammonia in every scenario.

A sensitivity analysis was conducted by varying input parameters by $\pm$50% from the baseline model input, and looking into the effect on hydrogen costs. The most sensitive parameter was floating offshore wind cost, which exhibits variations of a maximum +21% hydrogen cost [€/kg] if wind platform cost is increased and -29% hydrogen cost [€/kg] if wind platform cost is decreased (spanning 2020-2050). The interest rate has the second most sensitive behavior, with +28% and -15% variation, followed by floating offshore platform cost at +5% and -19% for increase and decrease respectively.

Based on the former overview provided, a general visual representation of the conceptual framework demonstrating the research process in the thesis by [49] is portrayed in Figure 2.1. This framework can serve to understand how the research was carried out, and where to position further developments.

2.3. Discussion

While the author of [49] has introduced a novel model for estimating costs of the offshore green hydrogen supply chain, it is important to discuss the limitations of the study in order to clarify where and when an offshore green hydrogen production can serve as a feasible solution for decarbonization. One such limitation is the narrow scope of scenarios considered in the study. This leaves room for possible scenarios where an improved optimal cost could be achieved, which would be valuable knowledge for strategic decision making surrounding implementation of the solution. The scenarios considered were based primarily on presumed energy source availability, preferring areas with abundant offshore wind and solar while avoiding areas with abundant onshore wind and solar where competitors are expected to dominate. While this criteria is certainly significant, it does not offer a complete insight into optimal cost on a global scale, thus not fully addressing the knowledge gap based on [63]. Ideally, a heat map similar to [63] could be created which would encompass all possible scenarios globally. This would require an expansion on the model from the simplification mentioned in chapter 2.3.1 of [49] concerning optimization of demand and supply balancing. The author chose to simplify this in order focus on production and technology combinations. Since the technology choice has been made and production has been represented, the model could be used for gathering data to use as parameters for a new model investigating supply and demand node interactions. Additionally, in [49] the terms representing

the transport cost in the current objective function in reality act as a parameter rather than a decision variable, since each scenario has one constant distance between the nodes, and the demand given as an input parameter. If more demand/usage nodes were considered, the amount of hydrogen produced at the origin supply node could be split between port and destination nodes, resulting in a different optimal solution. With more possible nodes, characteristics of locations could also be investigated to determine how various water depths in different regions would influence the cost, and what locations result in optimal costs. This could be combined with regional set up and operational costs of the green hydrogen production. This would be useful for companies to make decisions on location choice for green FPSO implementation.

If computation time is excessive, there are also possibilities for adjustment of the original model by [49] to reduce this. For instance, the MIQCP model could possibly be reformulated into a Mixed Integer Linear Programming (MILP) model, by attempting to rewrite the quadratic constraints and implementing sets. The variable representing the number of (re)conversion devices could be treated as a parameter, effectively eliminating the quadratic behavior in the model. Another way to remove this quadratic behavior would be to change the binary decision variable T into a parameter and run the model for both transport mediums separately, then compare which one performed better in terms of resulting costs.

Given that local hydrogen demand was considered in the scenarios, and ammonia was chosen as a medium in each scenario analyzed, in could be reasonable to look further into the market, demand, and competitors in ammonia. The shipping industry has decarbonization targets, with the International Maritime Organization (IMO) greenhouse gas strategy including an ambition for net-zero GHG emissions from international shipping near 2050 [13]. Companies have been working on ammonia fueled freight ships, with Yara International expecting to have an ammonia fueled ship set on the trade route between Norway and Germany as early as 2026 [30]. With this in mind, there may be a scenario possible where the converted ammonia from the green FPSO is used directly to satisfy ammonia demand rather than being converted into hydrogen, thus reducing the need for some reconversion devices and in turn reducing costs. Another possible situation would arise from placing the FPSO along a shipping route, allowing ships to bunker for fuel directly, eliminating transport costs to ports. The routes could be attained through Automatic Identification System (AIS) vessel data. These considerations could be implemented in an extended techno-economic model of the green FPSO supply chain.

Another potentially interesting knowledge gap emerges from the seasonality and variability of energy generation. The thesis by [49] suggests the possible solution of a storage system, such as a battery, to smoothen the power curve and perform load balancing. This would have the potential to reduce cost of electrolyzers in the production of hydrogen, since fewer electrolyzers could be required if power could be stored while they are at full capacity and then fed in during a trough. [76] has developed an energy management system with an integrated battery energy storage system (BESS) onboard a vessel. The study considers the uncertainty of wind generation, and uses stochastic programming to determine the charging decisions for the battery on the basis of electricity prices from the grid. While this was applied to reduce load on a grid, it could be useful to adopt the approach and adapt it to the model for green hydrogen floating offshore production. The effects of economies of scale should also be considered in the production design, as these can be leveraged to reduce cost, however on the other hand scale effects such as losses due to longer cable infrastructure can contribute to higher costs. Aside from energy generation, there are other uncertainties in parameters relevant to attaining the cost of hydrogen. While some, like cost of floating wind, were dealt with through the sensitivity analysis in [49], others like the learning rate could also be investigated.

Various transport modes and mediums were considered and evaluated by [49], however only some were selected for implementation in the mathematical model. There could be further mediums such as gaseous hydrogen included for a more comprehensive model. In addition, pipelines were dismissed for sea transport due to the depths involved increasing the investment cost, however this could be investigated explicitly by extending the model to consider refurbishing existing infrastructure, and perhaps new dedicated hydrogen pipelines in certain locations could be feasible. While pipelines do increase initial investment cost, the operational cost is reduced in the long term. Understanding if current infrastructure, such as natural gas pipelines, could feasibly be repurposed for hydrogen and what is required to facilitate this, could prove to be a significant reduction in operational transport cost. According to [5], ”pipelines are the preferred option for large quantities and long distances” regarding gaseous and

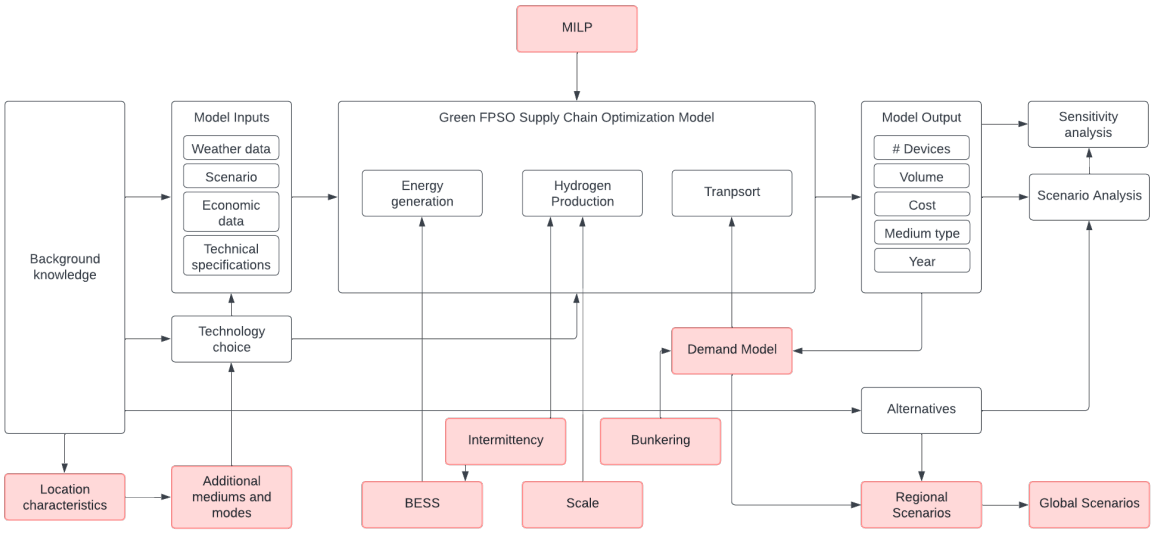

Figure 2.2: Conceptual framework including identified further research possibilities

liquid hydrogen, and have been used for over 50 years. The Langeled natural gas pipeline reaches depths of 360 [m] [25], therefore it is conceivable that this could be technologically feasible. There are however many considerations for the implementation of such a submarine hydrogen pipeline, including pressures, maintenance, and materials, particularly given that [25] states this technology is not yet commercially mature.

Based on the discussion, the topics for further developments are visualized on the conceptual framework in Figure 2.2.

2.3.1. State of the art

Based on the previous discussion of limitations identified, the concepts addressed are summarized in Table 2.1. These concept groups aim to represent the knowledge required for further research in the gaps identified in the discussion of [49]. The search, as described in Section 2.1, resulted in the number of documents shown in Table 2.2. It is noted that the topic has gained significant research in the past 2 years, with majority of literature having been published within or after 2022 for each search term combination. For the purposes of the preliminary literature review, the most recent (by date) and most relevant (by keywords) articles were chosen for review. There is some overlap of articles across the search terms.

Starting with [72], a combination of energy generation offshore and onshore through wind was done by investigating PEM and Alkaline Water Electrolysis (AWE) for techno-economic feasibility. The study showed an LCOH of 9.69 [$/kg] with a payback rate exceeding 25 years for offshore, which was higher than the alternatives. PEM and AWE technologies are considered sufficiently technologically mature, with PEM having higher Capital Expenditure (CAPEX) and lower Operational Expenditure (OPEX), while the reverse for AWE. [9] assessed offshore and onshore electrolyzers, resulting in LCOH of 6 [€/kg] in 2020, 3-4 [€/kg] in 2030, and 2 [€/kg] in 2050. The case study performed for Galicia, Spain, resulted in onshore electrolyzers being more attractive than offshore counterparts economically. When looking at the transport, pipeline installation was concluded to have smaller losses than power cables, with cheaper installation and preferable scalability. The study optimized energy generation with hourly optimization algorithms through neural network forecasting for wind power. Proposed hydrogen fuel cell to assist in regulation of feed-in power to the electrolyzer onshore. [71] performed a critical review of green hydrogen production, looking at Solid Oxide Electrolysis (SOE), AWE, and PEM as well as deslination technologies of Reverse Osmosis (RO), thermal deslaination, and membrane desalination. The review concluded that PEM stood out as the most suitable current electrolysis method, while RO providing the lowest investment and operation costs with lower energy demand. It was noted that RO has the potential to harm the marine environment due to the brine discharge, and this should be dealt

Table 2.2: Documents available on SCOPUS for the search terms based on Concept Groups as of March 2024.

Search Terms	All time	2022+
offshore AND green AND hydrogen AND energy AND generation	87	72
offshore AND green AND hydrogen AND production	206	147
offshore AND green AND hydrogen AND storage	80	59
offshore AND green AND hydrogen AND transport	39	24
offshore AND green AND hydrogen AND optimization	39	27
offshore AND green AND hydrogen AND economic	76	53
offshore AND green AND hydrogen AND policy	31	21

with in system implementations. [36] and [35] explore the potential of green hydrogen production in Canada based on solar and wind energy respectively. The studies illustrated a potential of 39.54 [Mt] at the highest and 0.34 [Mt] at the lowest region with solar Photovoltaic (PV) technology. Offshore solar only contributed 2.93% to this potential, and it was noted that between 520-660 [Mt] of hydrogen must be produced globally to reach net zero emission targets. For offshore wind, a potential of 37.29 [Mt] was concluded. [20] assessed various hydrogen energy mediums through a techno-economic model involving wind generation, conversion, transport and storage, in a similar manner as in [49], however not including far offshore (>1000 [km] from shore), nor floating solar panels in the scope. Wind availability was deemed crucial for economic feasibility, while direct electric energy vector through High-Voltage Direct Current (HVDC) terminals was found to be less expensive to any H2 vector. Gaseous H2 exhibited 2-3x lower costs as compared to liquid H2 and ammonia. Notably, for liquid H2 and ammonia were deemed to require shipping rather than other transport modes. [59] simulated optimal electrolyzer plant size for minimized cost in the coast of Galicia, Spain, with offshore wind and solar PV. The electrolyzer technologies considered were PEM, Anion Exchange Membrane (AEM), and SOE. The cost of hydrogen was estimated at 4 [$/kg] in 2020, dropping to 2 [$/kg] in 2050. The study suggested that 5.5 [$/kg] is the boundary under which production of green hydrogen becomes profitable, with solar energy resulting in a profit 3x higher than wind energy. [19] analyzed the CAPEX and OPEX of both offshore and onshore H2 production, including storage and transport medium considerations, in the location of the North Sea for context of the UK. It was found that by 2030, cost reduction can reach competitive levels against grey and blue hydrogen. Compressed H2 was stated as most cost-effective when started in 2025, depending on storage period and distance to the shore. Liquid H2 and methylcyclohexane were expected to enter cost-effectiveness from 2050 at an LCOH of 2 [£/kg]. For the compressed H2 medium a compressor device is necessary, and the medium can be stored or transported in a pipeline. Pipeline learning rates were identified as 8.0% and 14.2% with respect to material and labor cost reductions across the relevant time frame. The distance to shore and energy generation were most significant in determination of most cost-effective scenarios. It was further discussed that pipelines remain effective between 60 - 380 [km], however not likely beyond 1000 [km] distances. Cost of electrolyzer had a significant share. [62] considered wind and floating PV integration in to the hydrogen economy, with a focus on pipelines and subsea cables for transport, as well as storage on onshore bunkering. It was found that at low capacities of $\tilde{1}$00 [GWh/y] the subsea cables performed preferably, while at high capacities in [TWh/y] scale the pipelines were competetive above 750 [km] distance to shore. The cost was largely dependent on the distance to shore, and the comparison was made through a Levelized Cost of Energy Transport [LCOET]. Finally, [57] reviewed offshore green hydrogen production, concluding that hydrogen is useful as a storage medium for renewable energy over long durations, with possible applications of electricity (through power-to-hydrogen), renewable heat, long-haul transport, shipping, aviation, and decarbonization of industrial processes. The cost is dominated by electricity used for electrolyzer, and a bottleneck to capacity is identified as operation of

electrolyzers solely during periods of low electricity prices, which limits utilization of investment. Offshore was estimated to increase capacity by 60-70% in relation to onshore, and in short-medium terms RO is advised for desalination. AWE was found to have a slower response time in comparison to PEM for production. [1] reviews production methods and identifies the key issues pertaining to the scale up of these methods, namely lack of a green hydrogen value chain, the storage and transport considerations, a significant cost of production, international standards are not present, large risks in investment with uncertainty, and flammability.

2.4. Conclusion & Discussion on Literature

It is clear that specific single regions are selected for scenarios when investigating offshore green hydrogen in the current literature, as can be seen in [72] with a case study on Uribia, Colombia, [9] considering floating offshore in Galicia, Spain, [36][35] focusing on Canada, [20] focusing on the Iberian peninsula, and [19] performing a UK case study. Aside from [63], there is a gap in attempting to perform a techno-economic analysis on a large scale. Onshore storage and bunkering is investigated in [20] and [62], however in the offshore case there is limited knowledge. Feeding power into the electrolyzers from produced hydrogen is proposed in [9] but only in the case of near offshore and onshore, leaving a gap for possible investigation in energy storage for feed in power (hydrogen or BESS) in offshore production. [9] also identified the uncertainty of green hydrogen floating production and storage installation costs, while [19] suggested that stochastic modelling for uncertainties in parameters would be a suitable further development. Pipelines seem to be beneficial to cost in certain scenarios identified in [9][20][19], however the costs rise with distance to shore, with feasibility uncertain beyond 1000 [km] as stated in [19]. Furthermore, this restricts the medium to gaseous H2, requiring compression devices according to [19]. It is possible to investigate this further, while remaining cautious with the expectations. Regarding the absence of a value chain mentioned by [1], all the studies have in some form proposed, discussed, and/or evaluated various relevant technologies, transport modes, energy mediums, supply chain structures, however a techno-economically feasible business case proposition for a comprehensive, holistic chain involving both solar and wind sources, while considering various transport modes and energy carriers, in the floating offshore hydrogen context has not been presented. With [49] providing the foundation for such a supply chain, it is possible to extend this and aim to close the gap toward achieving a feasible offshore green hydrogen FPSO supply chain in reality.

3

Methodology

To investigate the research questions proposed and achieve the objective of determining an feasible offshore GFPSO supply chain, the appropriate methodology must be outlined. This begins with the Preparation in Section 3.1, where the context of the GFPSO system is investigated, key decisions in the supply chain design are listed, and a framework with criteria for evaluation is determined. Once this is established, the next step is the Modeling and Verification Section 3.2, where a new MILP formulation is created on the basis of the model from [49], with the purpose of reducing computation time to enable larger scale location analysis. This can be done by investigating the parameters, variables, objective, and constraints. The mathematical model notation is standardized and formulated, the relevant constraints and components of the objective function are linearized, and finally the remaining redundancies are identified and removed. The model is verified against the results of [49], and initial results can be produced as a baseline. Once this is complete, the Model contribution Section 3.2.2 presents the investigation into transport modalities and energy vectors. This is incorporated into the mathematical model and the resulting effects are analyzed. The model can be found in the GitHub repository [34]. Finally, the parameters are collected and the model is applied to support a business case for the implementation of a GFPSO supply chain, which is presented in the dedicated Chapter 4, and each scenario is evaluated against the previously established criteria.

3.1. Preparation

This section will discuss what a deployment strategy for a GFPSO consists of identifying the key decisions which need to be determined, as well as developing a criteria framework based on which the strategy can be evaluated.

3.1.1. Key Decisions

The key decisions of the GFPSO deployment strategy consist of equipment, energy medium, transport mode, and logistics decisions. The decisions lead to different costs for each supply chain configuration, which are considered in terms of CAPEX and OPEX.

There are various possibilities for equipment, which ultimately impact the configuration and costs in the supply chain. When considering the upstream section of the supply chain, wind energy requires wind turbines which must be either fixed or floating depending on water depth. Currently fixed structures have been applied in practice, with mounting options using monopiles and jackets, while floating technology such as spar-buoys, semi-submersible and tension-leg platforms still being developed [48][49]. Wind power capacity per turbine must be specified to determine the amount of turbines required to satisfy demand. Regarding the costs, the initial investment of CAPEX can be categorized into turbine, foundation, electrical grid, project, and decommissioning costs [43]. The OPEX will depend on the operational hours of the wind farm (with a maximum of 8760 hours per year at 100% capacity factor), and consists of maintenance, administration, insurance, grid, site costs [43].

For solar energy, a combination of solar PV modules form a solar platform, with various concepts

being deployed [48]. The solar platforms enhance upstream energy generation by filling empty space between wind turbines, separated due to wake effects [48]. A floating PV platform will have a specified capacity, typically represented as nominal power in [kWp]. Additionally, inverter type, azimuth, tilt, and albedo, and temperature will affect the yield delivered by the PV system. The CAPEX consists of structural materials, tracking system, PV module, mooring and anchorage, electrical components, development and consent, as well as installation costs [48]. The OPEX includes maintenance such as cleaning and inspections [48].

After the upstream energy generation, the next section of the supply chain concerns the FPSO vessel. The equipment required includes the production using electrolyzers, conversion of the product depending on energy medium, storage in the hull of the vessel, and offloading depending on the transport mode. The electrolyzer type selected by [49] was PEM, although AWE and HTEL are also possible. PEM and AWE were seen as preferable to HTEL due to higher technological readiness and no need for high temperature resistant materials [49]. The disadvantage of PEM is the high cost of catalysts, while AWE requires the management of highly-corrosive electrolytes. Typically in large scale applications AWE is deployed in industry, for instance in the Shell Holland Hydrogen 1 project applying a ThyssenKrupp Nucera supplied AWE unit with 20[MW] capacity, scaled to gigawatt levels [61][53]. Examples of PEM units provided include units provided by nel of 1.2 - 10 [MW] capacity, Fortescue's 1 [MW] capacity units scalable to 50 [MW], or ITM's 20[MW] Poseidon units. PEM electrolyzers are typically offered as modular units, with the possibility of combining units to increase overall production capacity [71]. In the context of offshore production, PEM has the advantage over AWE of lower complexity and compactness, making it suitable for stacking in an offshore application. While AWE may be a competitive alternative due to its large scale application benefits, following from the reasoning in [49] the PEM technology will be considered for this study.

Regarding the PEM electrolyzer, the specification must include capacity, lifetime, water and energy input requirements, as well as hydrogen output. The FPSO vessel is suitable for housing the electrolyzer equipment on the topsides. The costs of CAPEX and OPEX with future estimations, following from the reasoning in [49], can be based on the research into the hydrogen value chain elements by [69], where CAPEX is represented by the total direct cost and OPEX is estimated as a fraction of CAPEX.

The conversion equipment decision is based on the energy medium applied. The product of the electrolyzers comes in the form of gaseous hydrogen, therefore if another medium is used for storage and offloading, a conversion step is added to the process. The energy vectors in concern are gaseous hydrogen (GH2), liquid hydrogen (LH2), and ammonia (NH3). GH2 is in the same medium as the output from the electrolyzer, therefore no conversion must be done (compression must occur, however this will be addressed in the next stages of the process). LH2 requires liquefaction of the product, necessitating an extremely low temperature of -240[°C]. Conversion to ammonia is typically done using the Haber-Bosch processes, with the product remaining in liquid phase at a comparatively less extreme -33.1[°C]. The demand at the final location may not match the energy mode selected, therefore a reconversion step may be necessary once the product is delivered to shore. This will be addressed when considering the transport mode.

The storage equipment depends on the energy medium and transport mode applied. In general, the hull of the vessel should offer a suitable space for the storage of the material. LH2 will require the cold temperatures previously mentioned, with safety valves for boil-off. When considering liquid phase vectors with shipping transport, the storage space on the vessel must be sufficient to match the offloading frequencies to the incoming vessels [16]. When pipeline is selected, the main storage can be within the pipeline itself due to its considerable volume, although the hull may need to be utilized for buffer storage during maintenance to facilitate continuous production.

Figure 3.1: Trident PEM stack by ITM at the World Hydrogen Summit 2024 in Rotterdam

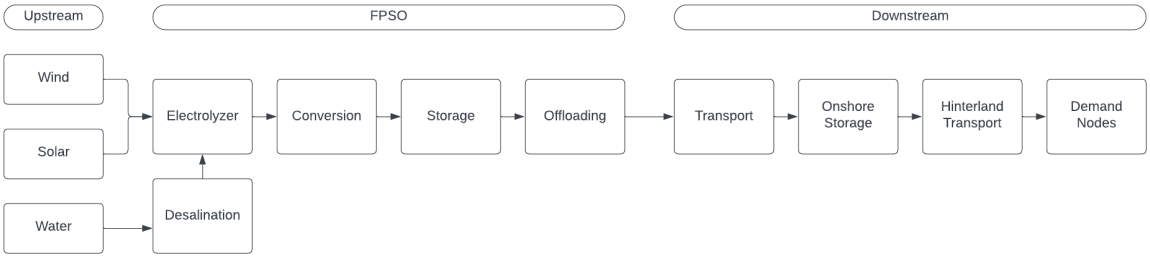

Figure 3.2: Map of Supply Chain

The logistics decisions can be dissected into 4 stages: Location, Topology, Allocation, and Routing. Typically a logistics network design problem involves several supply and demand nodes, with possible transshipment nodes in between which it is possible to reduce costs due to consolidation and economies of scale. The location decision would pertain to the placement of transshipment nodes, topology would consider which transshipment nodes are connected, allocation would assign supply/demand nodes to the transshipment nodes, and finally routing would determine which connections are used for the delivery of the demand. In the case of the GFPSO supply chain, the situation is simplified by considering a single production node to be placed. The transshipment node is predetermined as the port. The transport mode can vary, which impacts the cost of the connection between the nodes and thus the decision on which connection ought to be chosen. Furthermore, allocation and routing will not be considered in the scope of the research, therefore from this point on the transshipment node will be considered the final demand node.

In order to compare between the different supply chain strategies/configurations emerging from the decisions previously discussed, certain criteria must be determined to evaluate the performance of each strategy. This is investigated in the following Section 3.1.2.

3.1.2. Criteria Framework

To evaluate the GFPSO supply chain, the criteria which determine its success must be denoted. The approach in [32] identified 4 relevant categories (economic, technological, social, & environmental) of considerations for determining an optimal configuration for a renewable energy source pathway, with each category requiring at least one corresponding criterion to enable evaluation of performance. In the case of the GFPSO, the social category is removed due to lack of direct interaction of external members from society with the supply chain, compared to the case of a business park in [32]. The deployment of the GFPSO would likely impact social prosperity indirectly through environmental benefits like CO2 reductions. In turn, the category of Geopolitical considerations is added. This is due to [49] highlighting the importance of geopolitical dynamics on the feasibility of a GFPSO. This permits for the identification of the 4 categories: Economic, Technological, Environmental, and Geopolitical. These categories and how they pertain to the supply chain configurations is discussed in the following subsections.

Economic

Economic aspects are key in driving the attractiveness and possibility of deployment of a GFPSO supply chain. Such a project requires significant investments to instate each element, with investors typically seeking some form of returns and to limit risks. In renewable energy sectors, risk is not only common (for instance seen with Shell cutting 200 jobs in their Low Carbon Solutions division [56]), but expected, particularly with prevalent uncertainties regarding production capacities, prices, lack of dominant designs, and limited dedicated infrastructure. When attempting to quantify the value of an investment, the Net Present Value (NPV) provides a number based on expected cash inflows (revenue streams R_l) and outflows (costs C_l) in the lifetime $l \in L$ of a project adjusted for interest d (shown in Eq. 3.1). Revenue will depend on the prices at which the energy can be sold in the market, which requires forecasting methods out of scope of the model considered in this study, however the costs will be calculated and compared through the Levelized Cost of Energy (LCOE). The elements of the supply chain configurations can also be evaluated based on their commercial readiness, using the Commercial Readiness Index (CRI) criterion.

$$NPV = \sum_{l \in L} \frac{R_l}{(1+d)^l} - \sum_{l \in L} \frac{C_l}{(1+d)^l} \tag{3.1}$$

Levelised Cost of Hydrogen (LCOH) This criterion pertains to the cost of the energy when considering the lifetime of the equipment used. It is based on the Levelised Cost of Energy (LCOE) approach from [11]:

$$LCOE = \frac{\sum_{n=0}^{N} \frac{(I_n + M_n + F_n)}{(1+r)^n}}{\sum_{n=0}^{N} \frac{E_n}{(1+r)^n}} \tag{3.2}$$

Here n is the year in the N lifetime of the project, r is the discount rate, I is the initial investment cost, M is the operations and maintenance cost, F is the fuel cost, and E is the energy produced. As can be seen, the numerator represents the NPV of the costs, while the denominator represents the NPV of the energy produced. The LCOE provides the cost per unit, and is typically represented by euros per kilowatthour [€/kWh], however in the case of this project it can be more useful to look at the levelised cost of hydrogen (LCOH) in euros per kilogram of hydrogen [€/kgH2] specifically when comparing between hydrogen producing solutions. In this case E is replaced by $H2$ produced. This metric is common in literature when performing techno-economic analyses. Each supply chain configuration will result in a different levelized cost. The model in [49] already considers costs of CAPEX and OPEX using an amortization factor over the lifetime and a learning rate to estimate relevant values. As such, the LCOH value taken in this research will be based on the NPV of the total yearly cost (omitting revenue), divided by the NPV of the production.

Commercial Readiness Index (CRI) The CRI, as portrayed in Figure 3.3, is a tool developed by [2] to measure how commercially ready a renewable energy solution is. It contains levels from 1-6, ranging from a ”Hypothetical Commercial Proposition” to a ”Bankable Asset Class”. This represents

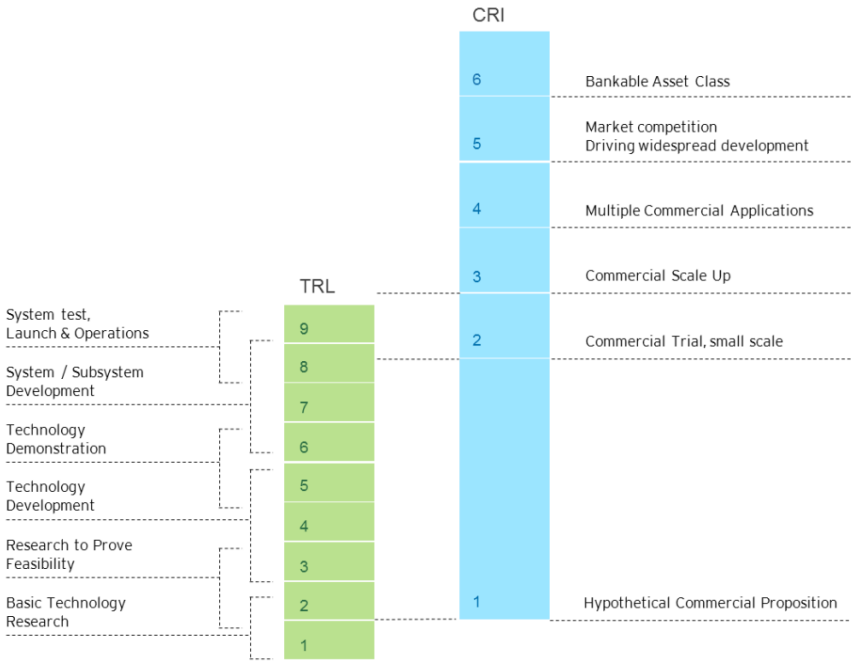

Figure 3.3: CRI and TRL from [2]

the maturity of the solution in terms of its application in the market. At the first level, a technology may be ready for deployment but have no prior implementations, therefore there is a lack of evidence or data to prove and verify its commercial success. At the highest level, the solution has established standards and expectations, readily supported by investments, and typical market forces acting on it.

Technological

Technology Readiness Level (TRL) The TRL, as visualized in Figure 3.3, is a measure of the readiness of a technology originating from NASA to determine if a technology is ready for space deployment [23]. In the years after its conception, the scale has been adapted to apply to further areas of innovation. The scale ranges from 1 to 9, starting with early research of a basic technology, and reaching up to an operational system which has been tested and is ready for applications (stages are illustrated in Figure 3.3). Notably, CRI cannot exceed level 2 unless the TRL is considered at least 9.

Ease of Implementation (EoI) The Ease of implementation criterion, based on ”Ease pf spatial integration” from [32], serves to capture the characteristic difficulty to setup and deploy the supply chain configuration. This is because other economic and technological criteria may omit certain barriers to entry, such as additional surveying, permits, and construction of infrastructure. While it may be possible to infer this from the ratio of early setup CAPEX to the overall project lifetime costs, this criterion serves to explicitly address such concerns.

Environmental

CO2 Emissions For this criterion the amount of CO2 required for setup and operation of the supply chain can be estimated and compared between solutions. Scope 1, 2, and 3 emissions can be considered to ensure a complete analysis of the supply chain. Scope 1 focuses on the direct emissions due to fuel usage in operation, scope 2 focuses on indirect emissions due to energy used, such as electricity from the grid which is sourced from certain fuel, and scope 3 pertains to upstream and downstream emissions adjacent to the project. The estimation will depend on the specific elements in the supply chain configuration, as determined in the business case.

Geopolitical

Access Access to the location is a prerequisite to enable the supply chain operations. When considering the access of the location, political borders can be taken into account as determined in the

”Convention on the Continental Shelf” [50]. Aside from having an agreement to operate within a certain country’s territorial waters (if applicable), the location must be accessible by a GFPSO vessel and have sufficient space for installation of wind turbines, solar panels, as well as possible pipelines, without interfering with other activities.

Regulations The regional regulatory context for different renewable energy projects can have an impact on the degree of support for the deployment of the supply chain based on the configuration used. The literature can be reviewed to determine how the equipment combinations relate to the policies and strategies being enacted in the region.

3.1.3. Framework Table

The framework for evaluation takes on the form of a Table (3.1), where all the criteria for each category are listed on the left hand side, and the supply chain configurations/scenarios (for example C1 and C2) are listed in the topmost row. The value of each criterion is determined for each configuration, allowing for attribution of a ranking. The dominant supply chain configuration is based on the overall final ranking.

Category	Criterion	Value C1	Value C2	Rank C1	Rank C2	Final
Economic	LCOH					
	CRI					
Technological	TRL					
	EoI					
Environmental	CO2 Reduction					
Geopolitical	Access					
	Regulations					

Table 3.1: Framework for Evaluating Supply Chain Configurations

3.2. Modeling & Verification

In this chapter the model is presented for investigating the techno-economic feasibility of the GFPSO. The model from [49] is investigated and reformulated in Section 3.2.1. This updated formulation is then applied to previous data used in the first scenario from [49] to verify whether the updated model behavior provides the same results as observed previously. The following Section 3.2.2 introduces the contribution of pipeline into the model, which will later be used for investigation in the business case. The pipeline approach based on [16] is investigated, and applied into the model as a basis for the pipeline techno-economic analysis. This is verified and implemented into the model formulation, with adjustments in notation being provided.

3.2.1. Mathematical Model Formulation

The complete model overview is outlined in section 3.1.2 of [49]. A summarized overview is portrayed in Figure 3.4a. The modeling approach involves importing a dataset from excel which provides input parameters, as well as Era5 weather data for calculating the power output of the wind turbines and solar platforms using the ”windpowerlib” and ”pvlib” python libraries respectively. Once the data is imported, the Gurobi platform is used, with parameters and variables are denoted in python, and constraints are formulated. The objective function of minimizing total yearly cost, and the optimization is ran for a set time period in certain time steps. Once the optimization has found the optimal solution for each time step, the data is processed and exported for analysis. In Figure 3.4b, the approach has been re-adapted to allow for analysis of an increased number of locations per optimization run. The transport cost parameter calculation, as well as the solar and wind power calculations are implemented into functions, such that they can easily be called for in the parameters section. A location loop is introduced, using a ”for loop” to iterate over a set number of location coordinates. This allows for data collection of several locations in one run. The detailed formulation is presented in Table 3.2.

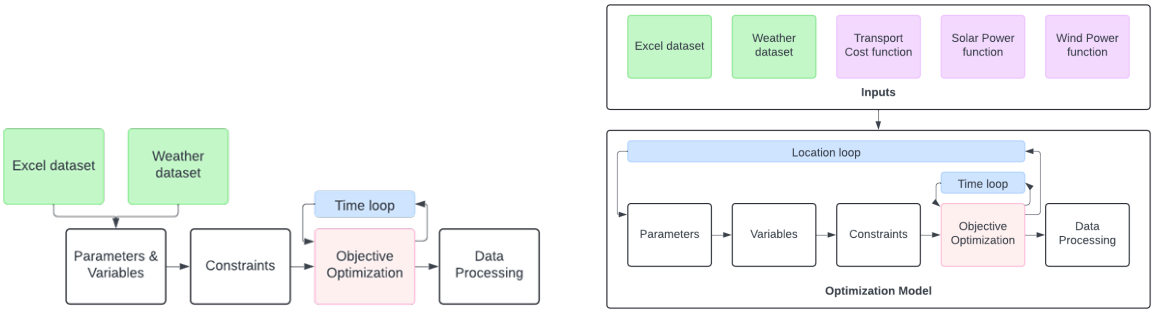

(a) Former Model **(b)** Updated Model

Figure 3.4: Model Overview Comparison

Table 3.2: Notation

Sets and indices		
I	Set for conversion and re-conversion devices	$i \in I$
J	Set for energy mediums	$j \in J$
K	Set for wind, solar, electrolysis, and desalination devices	$k \in K$
L	Set for years in studied time period	$l \in L$
N	Set for volume-based equipment	$n \in N$
T	Set for hours in year	$t \in T$
Parameters		
A_{lij}	Cost for device i in medium j for year l	[€/device/y]
B_{lk}	Cost for device k for year l	[€/device/y]
C_{lnj}	Cost of volume based device n in medium j for year l	[€/m^3/y]
D	Yearly demand of hydrogen	[t/y]
E	Choice of energy medium	[-]
PS_t	Solar energy generated at hour t at given location	[W/device/h]
PW_t	Wind energy generated at hour t at given location	[W/device/h]
TC_{lj}	Transport Cost for medium j in year l	[€/y]
WC_{lj}	Total cost of conversion devices for medium j	[€/y]
w_{ij}	number of devices i in medium j	[devices]
α_j	Fraction of generated energy in medium j used in electrolysis	[-]
β	Hourly output hydrogen production capacity of an electrolyzer	[t/device/h]
γ	Energy requirement of an electrolyzer to produce ton of hydrogen	[Wh/t]
ϵ	Time required to produce ton of hydrogen	[h/t]
η_{ij}	Efficiency of conversion device i in medium j	[-]
ϕ_j	Ratio of storage required for medium j	[-]
ν_j	Scale parameter for FPSO volume to fit electrolyzer with medium j	[m^3/device]
Variables		
x_k	Number of devices k needed,	[devices]
y_n	Volume of equipment n needed	[m^3]
PU_t	Power used by electrolyzers at hour t	[W/h]
PG_t	Power generated by wind and solar at hour t	[W/h]
h_t	Hydrogen produced at hour t	[t/h]

The sets consist of:

$$i = \begin{cases} 1 & \text{if } Converter \\ 2 & \text{if } Reconverter \end{cases}$$

$$j = \begin{cases} 1 & \text{if } Ammonia \\ 2 & \text{if } LiquidHydrogen \end{cases}$$

$$k = \begin{cases} 1 & \text{if } Wind \\ 2 & \text{if } Solar \\ 3 & \text{if } Electrolyzer \\ 4 & \text{if } Desalinator \end{cases}$$

$$n = \begin{cases} 1 & \text{if } Storage \\ 2 & \text{if } FPSO \end{cases}$$

And choice in E is represented by a choice of medium in set J:

$$E = \begin{cases} 1 & \text{if } Ammonia \\ 2 & \text{if } LiquidHydrogen \end{cases}$$

Objective:

$$\min(\sum_{k \in K} x_k B_{lk} + \sum_{n \in N} y_n C_{lnE} + WC_{lE} + TC_{lE}) \qquad \forall l \in L \tag{3.3}$$

Subject to:

$$PG_t = PW_t x_1 + PS_t x_2 \qquad \forall t \in T \tag{3.4}$$
$$PU_t \leq \alpha_E PG_t \qquad \forall t \in T \tag{3.5}$$
$$(\Delta t) PU_t \leq \beta \gamma x_3 \qquad \forall t \in T \tag{3.6}$$
$$h_t = \frac{PU_t}{\gamma} \qquad \forall t \in T \tag{3.7}$$
$$\sum_{t \in T} h_t \geq \frac{D}{\eta_{1E} \eta_{2E}} \tag{3.8}$$
$$x_4 \geq \beta \epsilon x_3 \tag{3.9}$$
$$y_2 = x_3 \nu_E \tag{3.10}$$
$$y_1 = y_2 \phi_E \tag{3.11}$$
$$x_k \geq 0 \qquad \forall k \in K \tag{3.12}$$
$$y_n \geq 0 \qquad \forall n \in N \tag{3.13}$$
$$PU_t \geq 0 \qquad \forall t \in T \tag{3.14}$$
$$PG_t \geq 0 \qquad \forall t \in T \tag{3.15}$$
$$h_t \geq 0 \qquad \forall t \in T \tag{3.16}$$

The objective function 3.3 minimizes the total cost in a given year l, for each year in set L. The first term minimizes the costs associated with wind, solar, electrolyzer, and desalination equipment. The second term minimizes the cost of volume based equipment, namely storage and vessel size. The third and fourth term are simply parameters representing conversion and transport cost, added depending on the transport medium and year. Constraint 3.4 combines the sum of the power generated from a single wind turbine PW_t multiplied by the number of wind turbines x_1 and the power generated from a single solar panel PS_t multiplied by the number of solar panels x_2, resulting in the total power generated at hour t in the form of variable PG_t. This is done for each hour t in T. The constraint 3.5 takes the power generated PG_t multiplied by the fraction which will be utilized by the electrolyzers α_E in order to limit power actually used by the electrolyzers at given hour t, represented by the variable PU_t. The constraint 3.6 also limits the power used PU_t by the maximum capacity of the electrolyzers at every

hour t, as represented by the product of hourly electrolyzer output capacity β, the energy requirement of a single electrolyzer γ, and the number of electrolyzers x_3. The hour difference Δt [h], which will always be 1 hour since the model runs for discrete hourly time steps, is multiplied by PU_t in order to match the units. Constraint 3.7 ensures that the amount of hydrogen produced h_t at hour t is defined by the power used in the electrolysis PU_t divided by the power required to produce one ton of hydrogen γ. The demand balancing constraint 3.8 takes the sum of hydrogen produced at every hour in the operational year, and ensures that this is sufficient to satisfy the total yearly demand D, accounting for the efficiency losses due to conversion η_{1E} and reconversion η_{2E}. The water desalination constraint 3.9 ensures that the number of desalination devices x_4 is at least enough to maintain the maximum capacity of the electrolysis process, as represented by the product of hourly electrolyzer capacity β, the time required to produce one ton of hydrogen ϵ, and the number of electrolyzers x_3. The constraint 3.10 pertains to the FPSO volume y_2, based on the number of electrolyzers x_3 and the medium dependent scaling parameter ν_E. Constraint 3.11 sets the storage volume y_1 equal to the FPSO volume y_2 multiplied by a storage ratio parameter ϕ_E. Finally, constraints 3.12 - 3.16 are the domain restrictions.

It is important to note that number of conversion and re-conversion devices is not a decision variable in the model. As such, these are set as parameters prior to optimization. To ensure that these do not cause a bottleneck for hydrogen supply, the demand is divided by the conversion capacity to arrive at the number of each unit, enforcing that these devices are never the limiting element in the supply chain. With a constant device number, the costs will not vary within each run, and can be precomputed as follows in Equation 3.17:

$$WC_{lj} = \sum_{i \in I} w_{ij} A_{lij} \qquad \forall j \in J, l \in L \tag{3.17}$$

Initial Results & Verification

Based on the updated mathematical formulation, the optimization model is implemented in python using the Gurobi platform. With the implementation in place, the previously used parameters can be applied in order to verify the model against that of [49] to ensure consistency with prior findings after removal of quadratic constraints. The output should also be investigated to determine if the behavior is matching expectations. Furthermore, additional results can be computed to illustrate the capabilities of the model for further results to be collected in the business case.

Given the parameters of Tokyo: Scenario 1 from [49], the results of the former model can be seen in Table 3.3 and the corresponding results from the updated model can be seen in Table 3.4. As can observed, both results match identically across all considered years for every variable considered. This suggests that the models exhibit the same behaviour under the same conditions, and thus the updated model can reliably output significant results for further investigations.

Additionally, the updated model significantly reduces computational time, as illustrated in Table 3.5. The computation times vary between 2.7 - 4.5 seconds across 11 runs done in Scenario 1, shown in Figure 3.5.

It is necessary to further verify model behavior based on location. This can be done by running the optimization for several adjacent locations in order to check whether the weather data has the expected impact on the number of electrolyzers (x_3) being chosen in the objective function. This run is portrayed in Figure 3.6, demonstrating that the electrolyzer number varies by location, with a greater number of electrolyzers on land, as can be expected with the lower wind availability. This is further conveyed in Figure 3.7, where total wind power produced over the weather dataset is shown in blue, while the number of electrolyzers is shown in orange.

3.2.2. Model Contribution

The model from [49] applied shipping as a transport mode for all scenarios. This can be extended further to include pipelines to investigate the implications on cost. Pipelines are common in high volume applications, which is relevant for a large scale production case.

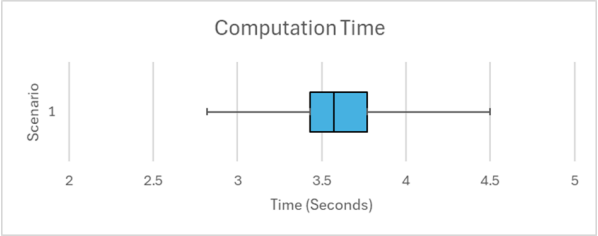

Figure 3.5: Computation Time Distribution - Scenario 1 runs

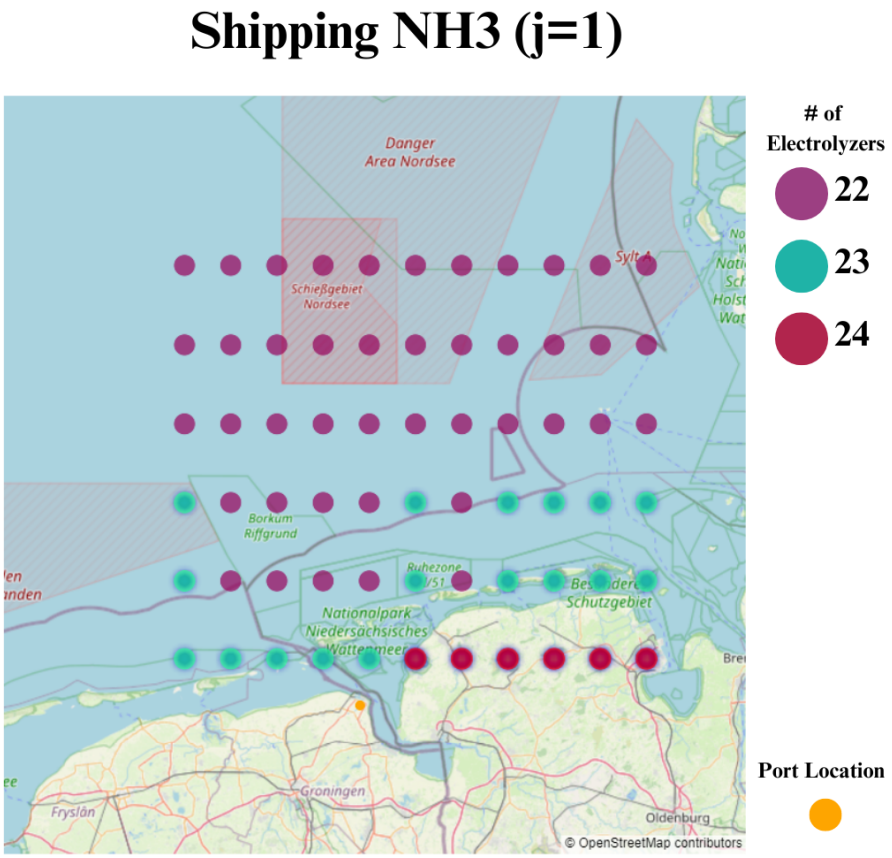

Figure 3.6: Number of Electrolyzers varying by location in the North-Sea at demand of 50000[tH2], for region spanning (54.55,6.08) to (53.55,8.08) in steps of 0.2°

Year	2020	2023	2026	2029	2032	2035	2038	2041	2044	2047	2050
Total costs per year (euros)	5.96E+08	5.33E+08	4.72E+08	4.12E+08	3.52E+08	2.88E+08	2.72E+08	2.57E+08	2.43E+08	2.29E+08	2.14E+08
Costs per kg hydrogen (euros)	11.93	10.65	9.44	8.23	7.04	5.76	5.44	5.14	4.86	4.57	4.29
Wind turbines	39	41	44	46	49	59	60	60	60	63	63
Solar platforms	1464	1328	1111	939	663	0	30	30	30	5	5
Electrolyzers	27	26	25	25	26	28	27	27	27	26	26
Desalination equipment	26	25	24	24	25	27	26	26	26	25	25
Storage volume (m^3)	4.79E+04	4.61E+04	4.44E+04	4.44E+04	4.61E+04	4.97E+04	4.79E+04	4.79E+04	4.79E+04	4.61E+04	4.61E+04
Conversion devices	9	9	9	9	9	9	9	9	9	9	9
Reconversion devices	5	5	5	5	5	5	5	5	5	5	5
Transport medium	AMMONIA	AMMONIA	AMMONIA	AMMONIA	AMMONIA	AMMONIA	AMMONIA	AMMONIA	AMMONIA	AMMONIA	AMMONIA
FPSO volume (m^3)	4.86E+05	4.68E+05	4.50E+05	4.50E+05	4.68E+05	5.04E+05	4.86E+05	4.86E+05	4.86E+05	4.68E+05	4.68E+05
Distance sea (km)	1566	1566	1566	1566	1566	1566	1566	1566	1566	1566	1566
Distance land (km)	0	0	0	0	0	0	0	0	0	0	0

Table 3.3: Output from [49] Model of Tokyo: Scenario 1

Index	2020	2023	2026	2029	2032	2035	2038	2041	2044	2047	2050
Demand (tons of hydrogen)	50000	50000	50000	50000	50000	50000	50000	50000	50000	50000	50000
Usage location	Tokyo	Tokyo	Tokyo	Tokyo	Tokyo	Tokyo	Tokyo	Tokyo	Tokyo	Tokyo	Tokyo
Year	2020	2023	2026	2029	2032	2035	2038	2041	2044	2047	2050
Production location	East Chinese Sea	East Chinese Sea	East Chinese Sea	East Chinese Sea	East Chinese Sea	East Chinese Sea	East Chinese Sea	East Chinese Sea	East Chinese Sea	East Chinese Sea	East Chinese Sea
Transfer port	Tokyo	Tokyo	Tokyo	Tokyo	Tokyo	Tokyo	Tokyo	Tokyo	Tokyo	Tokyo	Tokyo
Total costs per year (euros)	5.96413e+08	5.32651e+08	4.72103e+08	4.11585e+08	3.52181e+08	2.87803e+08	2.71953e+08	2.56783e+08	2.42963e+08	2.28742e+08	2.1448e+08
Costs per kg hydrogen (euros)	11.9283	10.653	9.44207	8.23171	7.04363	5.75605	5.43906	5.13565	4.85926	4.57483	4.2896
Wind turbines	39	41	44	46	49	59	60	60	60	63	63
Solar platforms	1464	1328	1111	939	663	0	30	30	30	5	5
Electrolyzers	27	26	25	25	26	28	27	27	27	26	26
Desalination equipment	26	25	24	24	25	27	26	26	26	25	25
Storage volume (m^3)	47918	46143.3	44368.5	44368.5	46143.3	49692.7	47918	47918	47918	46143.3	46143.3
Conversion devices	9	9	9	9	9	9	9	9	9	9	9
Reconversion devices	5	5	5	5	5	5	5	5	5	5	5
Transport medium	Ammonia	Ammonia	Ammonia	Ammonia	Ammonia	Ammonia	Ammonia	Ammonia	Ammonia	Ammonia	Ammonia
FPSO volume (m^3)	486430	468414	450398	450398	468414	504446	486430	486430	486430	468414	468414
Distance sea (km)	1565.84	1565.84	1565.84	1565.84	1565.84	1565.84	1565.84	1565.84	1565.84	1565.84	1565.84
Distance land (km)	0	0	0	0	0	0	0	0	0	0	0

Table 3.4: Output from updated model for Tokyo: Scenario 1

The transport cost parameter TC [€] was originally represented in the model as follows:

$$TC = X_{base}C_{base} + X_{kmsea}C_{kmsea} + X_{kmland}C_{kmland} \tag{3.18}$$

- X_{base} is the hydrogen demand [tons]
- C_{base} is the base cost of transporting hydrogen [€/ton]
- X_{kmsea} is the sea freight distance transported [tonkm]
- C_{kmsea} is the cost of sea transport above the base rate [€/tonkm]
- X_{kmland} is the land freight distance transported [tonkm]
- C_{kmland} is the cost of land transport above the base rate [€/tonkm]

This is useful for estimating costs for shipping, and has been previously verified. To begin with extending the parameter to include pipeline, the approach from [16] offers an approach for estimating costs of offshore pipelines for energy medium of gaseous hydrogen (GH2) and ammonia (NH3). This is discussed in the following subsections.

Subsea Pipeline

In large scale applications, pipeline transport offers the most cost effective solution for transmitting large volumes of material once it has been installed [51]. Gaseous, liquid, and slush hydrogen can be transported by pipeline, however liquid and slush must be carried at extremely low temperatures and due to latent heat is prone to evaporation [68]. With this in mind, pipeline transport with these phases is particularly inefficient with current methods, and therefore only gaseous hydrogen and ammonia are considered for subsea pipeline transport in this modeling approach.

Gaseous Hydrogen Pipeline The approach from [16] considers an offshore pipeline based on onshore pipeline cost estimations, scaled by a factor of 2 to represent expected offshore costs. The method involves calculating the CAPEX and OPEX of the pipe, which together with the throughput of GH2 provides the Levelized Cost of Transmission (LCOT) used for comparison of solutions. To align the approach with the modeling approach of the GFPSO, the calculations for CAPEX and OPEX can be recreated and verified through LCOT, after which the CAPEX and OPEX can be applied to the model through the yearly cost C_{yearly} Equation 3.19 applied in [49], which will later be modified to be a function of distance:

Model, Scenario, Year	Computation Time [s]
Former, Tokyo, 2047	399.7
Current Tokyo, 2047	4.27

Table 3.5: Computation Time Comparison

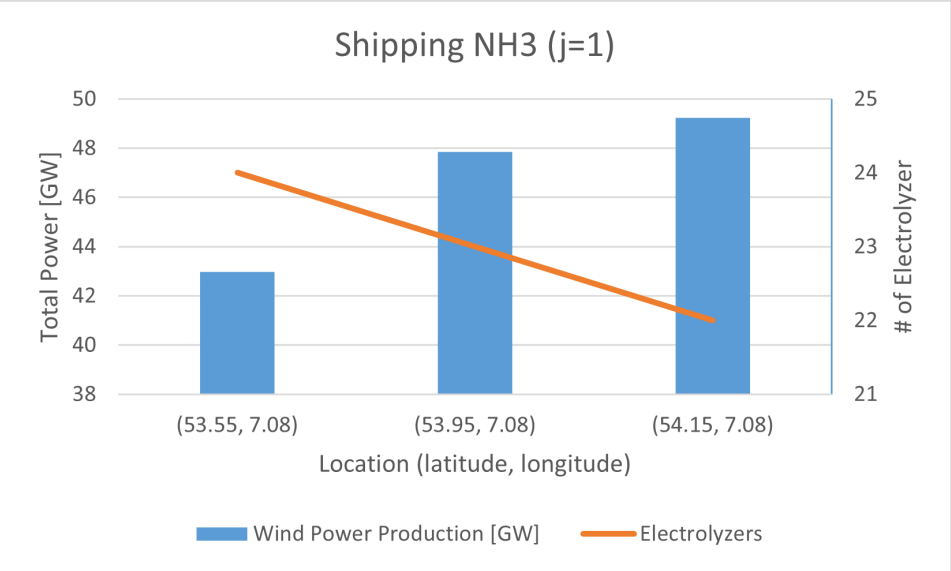

Figure 3.7: Wind Power Output in [GW] at locations of constant longitude, alongside electrolyzer number for shipping NH3

$$C_{yearly} = a * CAPEX + OPEX \tag{3.19}$$

$$a = \frac{r * (1+i)^{lifetime}}{(1+i)^{lifetime} - 1} \tag{3.20}$$

Where a is the amortization factor to account for the spread of the costs of capital across the lifetime of the project, based on interest rate i[%/100] and project lifetime.

The LCOT of GH2 in [16] is calculated as follows in Equation 3.21:

$$LCOT_{GH2pipe} = \frac{CAPEX_{GH2pipe} * d + \sum_{l \in L} \frac{OPEX_{GH2pipe}}{(1+r)^l}}{\sum_{l \in L} \frac{Prod_{GH2pipe}}{(1+r)^l}} \tag{3.21}$$

- $CAPEX_{GH2pipe}$ is in [€/km]
- OF is the Offshore Factor, 1 for an onshore pipeline, and 2 for an offshore pipeline
- d is the distance in [km]
- $OPEX_{GH2pipe}$ is 2% of $CAPEX_{GH2pipe}$
- l is the year in the lifetime L of the project
- r is the discount rate of the project in [%/100]

The former equation is based on the following equations adapted from [7]:

$$CAPEX_{GH2pipe} = OF * (4000000 * D^2_{GH2pipe} + 598600 * D_{GH2pipe} + 329000) \tag{3.22}$$

$$D_{GH2pipe} = \sqrt{\frac{4 * F}{\pi * v}} \tag{3.23}$$

$$F = \frac{Q}{\rho} \tag{3.24}$$

$$Q = E_{cap} * P_{rate} \tag{3.25}$$

- $D_{GH2pipe}$ is the diameter of the pipeline in [m]
- F is the volumetric flow rate in [m^3/s]
- v is the average fluid velocity in [m/s]
- Q is the peak mass flow rate in [kg/s]
- ρ is the mass density in [kg/m^3]
- E_{cap} is the total capacity of electrolyzer plant in [MW]
- P_{rate} is the production rate of GH2 by the electrolyzers in [kg/s/MW]

Ammonia Pipeline The LCOT of NH3 in [16] is calculated as follows in Equation 3.26:

$$LCOT_{NH3pipe} = \frac{CAPEX_{NH3pipe} + \sum_{l \in L} \frac{OPEX_{NH3pipe}}{(1+r)^l}}{\sum_{l \in L} \frac{Prod_{NH3pipe}}{(1+r)^l}} \tag{3.26}$$

- $CAPEX_{NH3pipe}$ is in [€]
- OF is the Offshore Factor, 1 for an onshore pipeline, and 2 for an offshore pipeline
- $OPEX_{NH3pipe}$ is 2% of $CAPEX_{NH3pipe}$
- l is the year in the lifetime L of the project

$$CAPEX_{NH3pipe} = OF * (C_{NH3pipe} * d + C_{NH3pump} * n_{pump}) \tag{3.27}$$

$$n_{pump} = \lceil d / Pump_{distance} \rceil \tag{3.28}$$

- $C_{NH3pipe}$ is the NH3 pipeline cost per kilometer, dependent on diameter [€/km]
- d is the distance in [km]
- $C_{NH3pump}$ is the cost of 1 pumping station in [€/station]
- n_{pump} is the number of pumping stations required at the given distance, and is a ceiling function of distance and maximum distance between pumping stations [# of stations]
- $Pump_{distance}$ is the maximum distance between the pump stations to maintain sufficient pressure [km]

Model Implementation To include the pipeline costs in the model, the set of energy mediums J is extended to contain both the medium and transport mode, such that:

$$j = \begin{cases} 1 & \text{if} \quad NH3_{Shipping} \\ 2 & \text{if} \quad LH2_{Shipping} \\ 3 & \text{if} \quad GH2_{Pipeline} \\ 4 & \text{if} \quad NH3_{Pipeline} \end{cases}$$

Each value of j represents a possible scenario for the GFPSO supply chain, which can be investigated in the business case. The implications on model notation include each variable and parameter containing j as an index now being extended to include the specific transport mode. Additionally, when choosing parameter E, now the choice of energy medium and transport mode are both included.

$$TC_{lj} = X_{base}C_{base} + X_{kmsea}C_{kmsea} + X_{kmland}C_{kmland} \qquad j \in \{1,2\} \qquad (3.29)$$

$$TC_{lj} = a * CAPEX_{GH2pipe} + OPEX_{GH2pipe} \qquad j \in \{3\} \qquad (3.30)$$

$$TC_{lj} = a * CAPEX_{NH3pipe} + OPEX_{NH3pipe} \qquad j \in \{4\} \qquad (3.31)$$

Verification Applying the data provided from [26] to the mentioned approaches results in the plots in Figure 3.9, with Figure 3.9a for the LCOT of a GH2 (onshore) pipeline and with Figure 3.9b for the NH3 (onshore) pipeline. These can be compared with the results presented in [16], demonstrating estimations from [16] and [26].

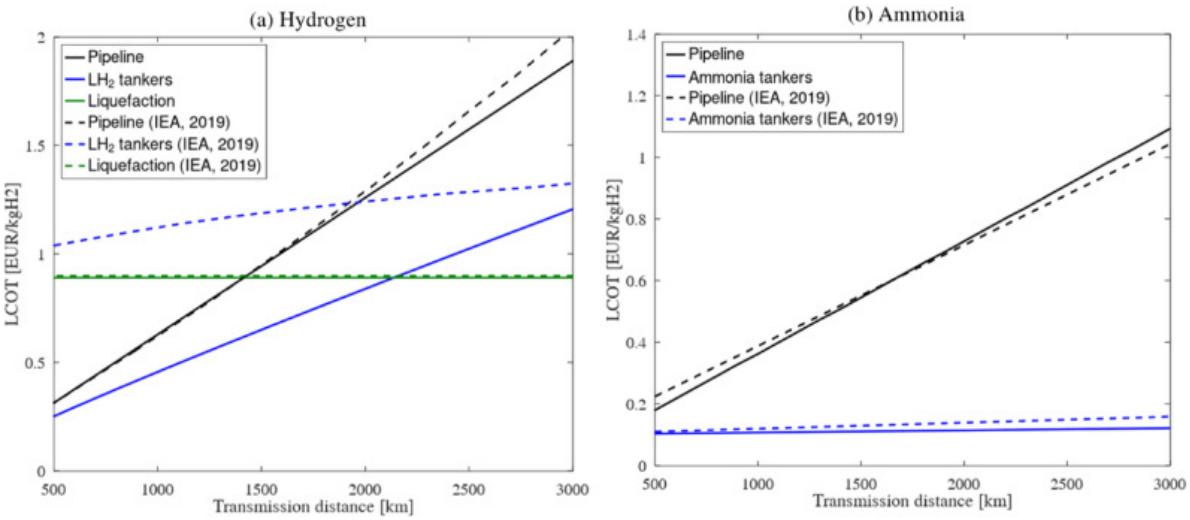

Figure 3.8: GH2 and NH3 Pipeline LCOT from [16]

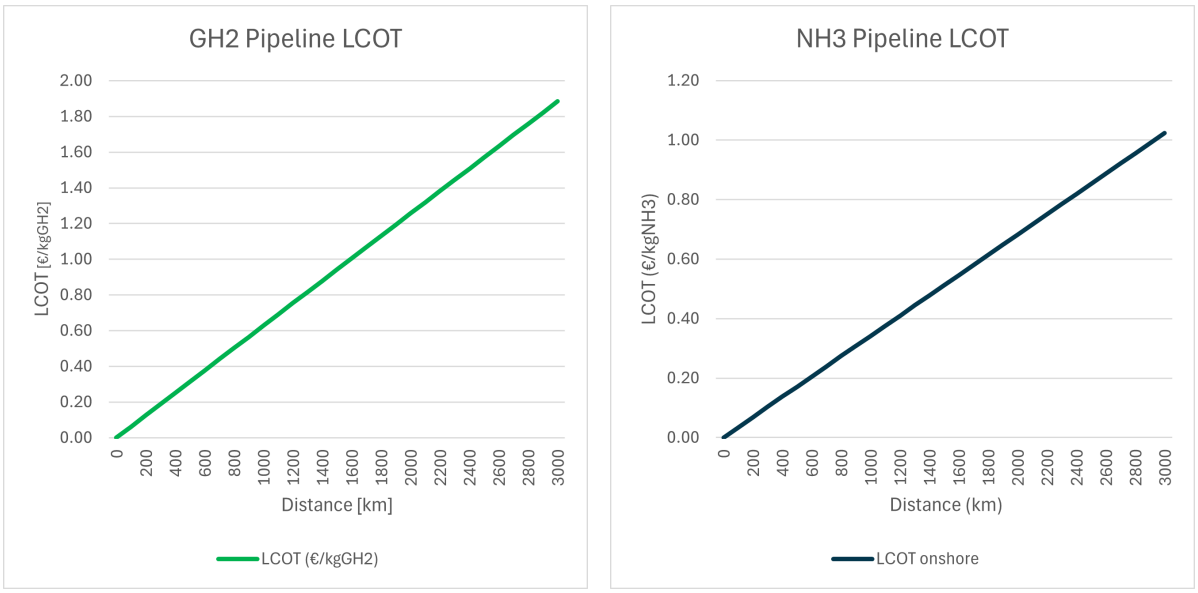

(a) GH2 Pipeline LCOT

(b) NH3 Pipeline LCOT

Figure 3.9: LCOT calculation recreation using [16] based on parameters from [26]

4

Business Case

4.1. North-Sea Case Context

Inspired by the Dutch government plans for a 700[MW] capacity wind farm "Ten Noorden van de Waddeneilanden" [52], a case can be prepared for utilizing the wind farm for production of offshore hydrogen.

Due to the demand being an input in the model, the case will estimate the maximum possible output of a 700 [MW] plant and assume this as the input demand.

$$Capacity * OperationalHours = EnergyOuput$$
$$700[MW] * 8760[h/y] = 6132000[MWh/y]$$

At Capacity Factor of 100%:

$$\frac{6132000}{\gamma} = 121[ktH2/y]$$

4.2. Parameters:

In the following section the input parameters used for the model will be denoted. The general parameters which apply to the overall case study are presented here:

- Production Location: Region spanning from 58.35° latitude, 2.78° longitude to 53.35° latitude, 7.78° longitude, in steps of 1° as visualized in Figure 4.1.
- Demand location: port of Eemshaven in Groningen at 53.43° latitude and 6.84° longitude. The range of distances from production to demand location is 594[m]
- Demand: 121 [ktH2/y]
- Discount rate: 8[%] [16]
- Interest rate: 8[%] [49][8]
- Time period: 2020 - 2050
- Time step: 3 [y]

4.2.1. Wind

In the case of the North-Sea the depths are relatively shallow, around 56[m] [52]. This allows for fixed structures to used for the wind turbines, thus costs are lower than in the floating case, with proven technology applied. The values from [44] suggest a CAPEX of 1900[€/kW] above the Wadden islands excluding decommission since only a 25 year lifetime was in scope, with an OPEX of 64[€/kW/y]. The

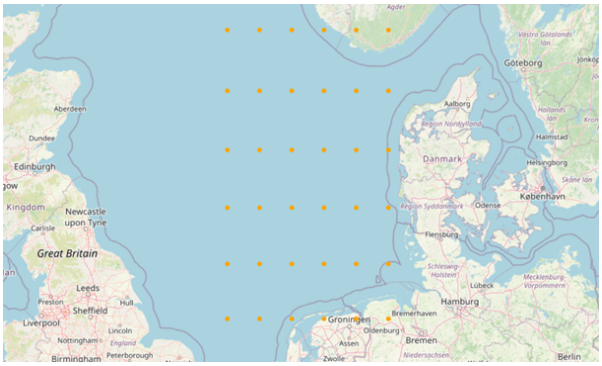

Figure 4.1: Location for study of North-Sea case

decommission cost of 44[€/kW] from [43] can be added to make the total CAPEX of 1944[€/kW], since this case will consider a time period exceeding the lifetime. The turbine capacity is set as 12[MW] [67][49]. The learning rates in [49] were set at 0.35 and 0.5 for floating wind technology between 2025-2035 and 2035-2050 respectively, however in the North-Sea case we apply bottom fixed turbines which will have a different learning rate [65]. The empirically calculated learning rate from [65] is 8.8[%] (with 6.3[%] lower bound and 11.2[%] upper bound) for fixed-bottom offshore wind projects. This learning rate is based on a doubling of global cumulative capacity of wind turbines. If we assume a linear growth of global cumulative capacity as in [65], we can estimate an annual capacity increase of $\approx$ 14.29[GW], based on Figure 5 in [65] with capacities of 50[GW] in 2021 and 250[GW] in 2031. With this we can estimate the CAPEX as follows in Equation 4.1:

$$CAPEX_{year} = CAPEX_{initial} * (\frac{CumulativeCapacity_{year}}{50[GW]})^{log_2(1-0.088)} \tag{4.1}$$

$$CumulativeCapacity_{year} = 50[GW] + (year - 2021) * 14.29[GW/y] \tag{4.2}$$

The parameters are summarized in Table 4.1 including the amortization factor a calculated from Equation 3.20, which can be used to determine model parameter $B_{l,k=1}$ for the total cost of wind turbine (k=1) in [€/device/y] in year l. The complete table of cost parameters used in the model can be found in Appendix B.

Parameters	Value	Units	Source
Depth	56.0	[m]	[52]
Turbine Capacity	12.0	[MW]	[49]
Lifetime	25.0	[y]	[49]
Learning rate	8.80	[%]	[65]
a	0.094	[-]	Eq. 3.20
Development cost	212	[€/kW]	[43]
Turbine cost	1060	[€/kW]	[43]
Foundation cost	350	[€/kW]	[43]
Other investment costs	278	[€/kW]	[43][44]
Decommission cost	44.0	[€/kW]	[43]
$CAPEX_{initial}$	1944	[€/kW]	[43][44]
OPEX	64.0	[€/kW/y]	[44]

Table 4.1: Wind Parameters

4.2.2. Solar

The solar PV platforms are assumed to be floating platforms placed between wind turbines to improve space utilization. These platforms consist of modules, which add up to 524 [kWp] nominal capacity

per platform based on the concept by [17] as considered prior in [49]. To ensure this value is still comparable to alternatives considered by state of the art literature, consider another study on offshore solar farms which used an installed capacity value of 6.762[MW] for 100 structures [48], which results in 67.62[kWp] per structure. When considering the Solar Duck concept which specifies a 524[kWp] nominal capacity for a platform consisting of 6 units of 131 panels [17], this results in a comparable 87.33[kWp] per unit. The CAPEX is the average of the baseline onshore solar costs calculated in [8], multiplied by an offshore factor OF to adjust for the additional cost due to the offshore installation. The lifetime of a platform is set at 25 years [49].

Within the solar energy generation function in the model, there are parameters within the pvlib python library which are necessary to determine solar power output. These parameters include inverter type, which is set to the "ABB MICRO 0 25 I OUTD US 208 208V" from [40] for consistency with [49], the angles of azimuth at 180° pointing south and tilt at 30° to again follow from [49], and albedo is set to 0.075, which is the average of the ocean reflection range of 0.05-0.1 [64]. Temperature is determined by the Era5 weather data [40]. The solar energy parameters are summarized in Table 4.2.

Parameters	**Value**	**Units**	**Source**
Platform Capacity	524	[kWp]	[49][17]
Lifetime	25.0	[years]	[49]
a	0.097	[-]	Eq. 3.20
OF	2.00	[-]	[49]
CAPEX	Average(PV_{cost})*OF	[€/kW]	[8][49]
OPEX	2.00	[%ofCAPEX]	[49]

Table 4.2: Solar Platform Parameters

4.2.3. Electrolyzers

The electrolyzer parameters include the energy requirement to produce a ton of hydrogen denoted as γ based on the data sheet from [69]. This γ is used to calculate the electrolyzer power consumption ratio α_j, which represents how much of the power generated must be dedicated to the electrolyzer for hydrogen production. This is calculated by dividing γ by the estimated total energy requirement as a sum of each equipment, as shown in Equation 4.3:

$$\alpha_j = \frac{\gamma}{Energy_{Desalination} + Energy_{Conversion,j} + Energy_{Storage,j} + \gamma} \tag{4.3}$$

The energy requirements are calculated in the respective equipment sections. The β parameter represents the hourly hydrogen output of PEM electrolyzer unit, while the PEM unit is scaled at a capacity of 20[MW], as retrieved from [69]. The lifetime of a PEM electrolyzer is 15 years according to [10]. The CAPEX and OPEX are calculated based on findings from [49], with a linear interpolation between the values provided by [69] for 2020, 2030, and 2040, with an estimated value for 2050 assuming cost decline continues at 3[%] annually after 2040. The parameters are summarized in Table 4.3.

Parameters	Value	Units	Source
$\alpha_{j=1}$ (NH3)	0.92	[-]	Eq. 4.3
$\alpha_{j=2}$ (LH2)	0.82	[-]	Eq. 4.3
$\alpha_{j=3}$ (GH2)	0.99	[-]	Eq. 4.3
$\alpha_{j=4}$ (NH3)	0.92	[-]	Eq. 4.3
β	0.40	[tH2/h]	[69]
γ	50.5	[MWh/tH2]	[69]
Capacity electrolyzer	20.0	[MW]	[69]
Lifetime	15.0	[y]	[10]
a	0.12	[-]	Eq. 3.20
CAPEX	Function of year	[€]	[49][69]
OPEX	Function of year	[€]	[49][69]

Table 4.3: Electrolyzer Parameters

4.2.4. Desalination

The desalination equipment required for providing processed seawater into the PEM electrolyser is based on the unit offered by [22]. The daily capacity offered by one such device amounts to 100[m^3/d], or equivalently 4.17[m^3/h]. The daily capacity of the plant described in [37] is larger by a factor of 1000, thus in order to use the investment cost of 120[M$] we scale down by this amount to arrive at the CAPEX, which is then converted to [€] [49]. Based on the hourly energy requirement of 3.5[kWh/m^3] and the water requirement for the electrolyzer we can estimate that $Energy_{Desalination}$ = 35[kWh/tH2] [49]. An OPEX of 2[%ofCAPEX] and an equipment lifetime of 30[y] is given in [37]. Finally, we estimate ϵ as follows in Equation 4.4:

$$\epsilon = \frac{WaterRequirementforElectrolyzer}{HourlyCapacityDesalinationDevice} = \frac{10}{4.17} = 2.40[h/t] \tag{4.4}$$

Parameters	Value	Units	Source
ϵ	2.40	[h/t]	Eq. 4.4
Hourly Capacity Desalination Device	4.17	[m^3/h]	[22][37]
Hourly Energy Requirement	3.50	[kWh/m^3]	[37][49]
Water Requirement for Electrolyzer	10.0	[m^3]	[69]
$Energy_{Desalination}$	35.0	[kWh/tH2]	[37][49][69]
Investment cost	121	[M$]	[37][49]
Lifetime	30.0	[y]	[37][49]
Currency conversion	0.94	[€/$]	[49]
CAPEX	0.113	[M€]	[37]
OPEX	2.00	[%ofCAPEX]	[49]

Table 4.4: Desalination Equipment Parameters

4.2.5. NH3

Regarding the parameters relevant for ammonia transmission, we can categorize by conversion, re-conversion, and transport modes. The (re-)conversion and transport parameters along with sources are provided in Table 4.5, with calculations previously shown in Sections 3.2.1 and 3.2.2 respectively.

Parameters	Value	Units	Source
Conversion			
a	0.094	[-]	Eq. 3.20
Device capacity	10.0	[ktH2/y]	[49]
Throughput conversion	274	[tNH3/day]	[49][69]
Total direct costs conversion	80.0	[M€]	[49][69]
$\eta_{i=1,j=1,4}$	0.98	[-]	[49][69]
Cost Ratio	5.56	[-]	[49]
Lifetime	25.0	[y]	
Reconversion			
a	0.094	[-]	
Device capacity	10.0	[ktH2/y]	
Throughput reconversion	1.20	[ktNH3/day]	[49][69]
Total direct costs reconversion	63.0	[M€]	[49][69]
$\eta_{i=2,j=1,4}$	0.98	[-]	[49][69]
CAPEX	94.5	[M€]	[49][69]
OPEX	1.60	[M€/y]	[49][69]
Lifetime	25.0	[y]	
Transport			
Mode	**Shipping**		
CostNH3 10000km	47.0	[€/tNH3]	[49][27]
CostNH3 20000km	65.8	[€/tNH3]	[49][27]
CostH2 10000km	261	[€/tH2]	[49]
CostH2 20000km	367	[€/tH2]	[49]
Price per km	0.0104	[€/tkm]	[49]
Base price	157	[€/tH2]	[49]
Mode	**Pipeline**		
a	0.089	[-]	Eq. 3.20
Project Lifespan	30.0	[y]	[16]
$CAPEX_{pipe}$	function(d, n_{pump})	[€]	Eq. 3.27
OF	2.00	[-]	[16]
$C_{pipeNH3}$	0.771	[M€/km]	[16]
$C_{pumpNH3}$	1.80	[M€/pump]	[16]
n_{pump}	$\lceil d/Pump_{distance} \rceil$	[pumps]	[16]
$Pump_{distance}$	128	[km]	[6]
$\nu_{j=1,4}$	18.0	[m^3/kW]	[49]
$\phi_{j=1}$	0.0985	[-]	[49]
$\phi_{j=4}$	0.00	[-]	[49]

Table 4.5: Ammonia Parameters

4.2.6. LH2

The parameters relevant for liquid hydrogen transmission are categorized by conversion, re-conversion, and transport mode, similarly to Section 4.2.5. The (re-)conversion and transport parameters along with sources are provided in Table 4.6, with relevant calculations previously shown in Sections 3.2.1 and 3.2.2.

Parameters	Value	Units	Source
a	0.089	[-]	Eq. 3.20
Conversion			
Device capacity	10.0	[ktH2/y]	[49]
$\eta_{i=1,j=2}$	1.00	[-]	[49]
Lifetime	30.0	[years]	[49]
Reconversion			
Device capacity	10.0	[ktH2/y]	
Cost Ratio	0.20	[-]	[49][45]
$\eta_i = 2, j = 2$	1.00	[-]	[49]
CAPEX		[€]	[49][8]
OPEX		[€/y]	[49][8]
Lifetime	30.0	[years]	[49]
Transport			
Mode	Shipping		
CostH2 10000km	1110	[€/tH2]	[49][27]
CostH2 20000km	1440	[€/tH2]	[49][27]
Price per km	0.0329	[€/tkm]	[49]
Base price	780	[€/tH2]	[49]

Table 4.6: Liquid Hydrogen Parameters

4.2.7. GH2

The parameters for gaseous hydrogen transmission include the amortization factor and transport, with the assumption of no conversion required leading to $\eta_{i=1,2,j=3}$=1. The transport parameters for the pipeline along with sources are provided in Table 4.7, with relevant calculations previously shown in Section 3.2.2.

Parameters	Value	Units	Source
a	0.089	[-]	Eq. 3.20
Transport			
Mode	Pipeline		
Lifetime	30.0	[years]	[16]
$CAPEX_{GH2pipe}$	0.615	[M€/km]	Eq. 3.25
OF	2	[-]	[16]
$D_{pipeGH2}$	0.203	[m]	Eq. 3.23
$v_{pipeGH2}$	15.0	[m/s]	[16]
$F_{pipeGH2}$	0.49	[kg/m^3]	Eq. 3.24
$Q_{pipeGH2}$	3.90	[kg/s]	[49]
$\rho_{pipeGH2}$	8.00	[kg/m^3]	[16]
OPEX per km	2.00	[%ofCAPEX]	[16]
Assumed plant capacity	700	[MW]	[52]
$\eta\_i = 1, j = 3$	1.00	[-]	No conversion assumption
$\eta_i = 2, j = 3$	1.00	[-]	No reconversion assumption
P_{rate}	5.50	[kgH2/s/kW]	[16]

Table 4.7: Gaseous Hydrogen Parameters

4.2.8. Storage

The storage parameters, summarized in Table 4.8, are categorized by energy medium. The parameters are the same as in [49] when considering scenarios j=1 and j=2, while the previously discussed assumption of pipelines serving as storage themselves leading to the cost already being considered in their respective transport CAPEX for both scenarios j=3 and j=4.

Parameters	Value	Units	Source
NH3 (j=1)			
Mode	Shipping		
Lifetime	25.0	[y]	
Tank Capacity	25.0	[kt]	[51]
Density NH3	682	[kg/m^3]	[49]
Tank Volume Capacity	3.66×10^4	[m^3]	[49][51]
$CAPEX_{NH3tank}$	24.5	[M€]	[51]
$OPEX$	3.00	[% of CAPEX]	[51]
Learning Rate 2030	0.90	[-]	[49]
Learning Rate 2050	0.50	[-]	[49]
$CAPEX_{NH3}$	$\frac{CAPEX_{NH3tank}*LearningRate}{TankVolumeCapacity}$	[€/m3]	
LH2 (j=2)			
Mode	Shipping		
Lifetime	25.0	[years]	
Tank Capacity	3.19	[kt]	[8]
Density LH2	71.0	[kg/m^3]	[49]
Tank Volume Capacity	4.49×10^4	[m^3]	[49]
$CAPEX_{LH2tank}$	273	[M€]	[8]
$CAPEX_{LH2}$	$\frac{CAPEX_{LH2tank}*LearningRate}{TankVolumeCapacity}$	[€/m3]	
$OPEX$	4.00	[%ofCAPEX]	[8]
GH2 (j=3)			
Mode	Pipeline		
Cost	0.00	[€]	[16]
NH3 (j=4)			
Mode	Pipeline		
Cost	0.00	[€]	[16]

Table 4.8: Storage Parameters

4.2.9. FPSO size

The FPSO size is determined based on volumes required to accommodate electrolyzers and storage. This is captured through the ratio parameters ν_j and ϕ_j respectively. Due to the assumption that pipelines can be considered as storage, $\phi_{j=3,4}$=0, since the vessel is purely utilized for production and offloading. The $\nu_{j=3}$ parameter is assumed to be equal to the $\nu_{j=2}$ due to the study in [42] not considering gaseous hydrogen specifically, while $\nu_{j=4}$ is assumed equal to $\nu_{j=1}$ due to both producing the same energy medium.

Parameters	Value	Units	Source
Lifetime	25.0	[y]	[49]
a	0.094	[-]	Eq. 3.20
C_{ship}	106	[kg/m^3]	[42]
C_{FPSO}	7.52	[€/kg]	[49]
$CAPEX$	797	[€/m^3]	$C_{FPSO} \times C_{ship}$
$OPEX$	2.00	[%ofCAPEX]	[49]
Total yearly	90.6	[€/m^3]	Eq. 3.19
$\phi_{j=1}$	0.0985	[-]	[49]
$\phi_{j=2}$	0.138	[-]	[49]
$\phi_{j=3}$	0.00	[-]	[16]
$\phi_{j=4}$	0.00	[-]	[16]
$\nu_{j=1,4}$	1110	[m^3/electrolyzer]	[42]
$\nu_{j=2,3}$	901	[m^3/electrolyzer]	[49]

Table 4.9: Parameters FPSO size

4.2.10. Weather Data

The weather data applied in the model comes from the ERA5 hourly data on single levels dataset from [24]. The time frame selected is 2020, with the region applied as discussed previously, shown in Figure 4.1. The dataset is restricted to a period of 9 months due to download limits made by the website [24], which is smaller than the previous limit of 10 months in [49]. Following the same approach as [49], the parameters will be scaled to this dataset (such that yearly costs are multiplied by a factor of 0.75) and later assumed to be extended to a whole year in the results for analysis. The weather data is processed into wind and solar power using the python library by [40] to arrive at the PW and PS parameters.

4.3. Modelling Results

The results are presented in 4 scenarios for each of the relevant energy medium and transport mode combinations. The full location-based cost results are provided in Appendix C. The scenarios are then compared together in the results analysis, followed by a sensitivity analysis of the parameters and a discussion of limitations.

4.3.1. Scenario 1: NH3 Shipping (j=1)

In this scenario the energy medium of ammonia and is chosen, with shipping as the transport medium. The model runtime data is summarized in Table 4.10, with the average runtime of 2.94[s] along with maximum runtime of 7.38[s]. On average, the runtime matches the falls under the expected median computation time from Section 3.2.1. The cost results for each location is compiled in Table C.1 of Appendix C, where the optimal location is most relevant to discuss. The optimization resulted in an optimal LCOH of 5.290[€/kg] at location (57.35, 7.78), at a distance of 440[km] from the port. The cost provided in 2020 begin with 6.06 [€/kg], dropping in 2050 to 4.41 [€/kg], with a total cost over the time period summing up to 6,610[M€]. This cost is achieved with 96 wind turbines, 34 solar platforms, 53 electrolyzers, and 51 desalination units. The storage volume is 94,100[m^3], and the FPSO volume is 955,000[m^3]. Based solely on the energy generation, the number of units of wind and solar equipment would reach a theoretical peak capacity of 1.17 [GW].

The costs per kg in 2050 and electrolyzer number are mapped out for each location as portrayed in Figure 4.2. As can be seen, the cost per kg values in 2050 range between 4.41-6.09[€/kg], with the land locations exhibiting higher costs due to lower energy generation availability, which requires more wind and solar turbines in order to produce enough to satisfy demand. The land locations result in unrealistically high equipment numbers, for instance sometimes up to 3000 units of solar platforms, however the model only considers offshore equipment rather than onshore equipment. These have different costs and specifications compared to offshore equipment, therefore these results do not represent reality, and should therefore be omitted from the analysis, aside from illustrative and verification purposes. The offshore location range of costs is between 4.41-4.82[€/kg]. The location of least electrolyzers correlates with the location of lowest delivered cost in 2050 (as well as lowest LCOH).

Total Runtime [min]	19.4
Average Runtime [s]	2.94
Max Runtime [s]	7.38
Min Runtime [s]	1.56

Table 4.10: Runtime Statistics for (j=1)

Year	2020	2023	2026	2029	2032	2035	2038	2041	2044	2047	2050
Cost per kg [€/kg]	6.06	5.58	5.30	5.08	4.92	4.80	4.69	4.60	4.53	4.47	4.41
Wind turbines	96	96	96	96	96	96	96	96	96	96	96
Solar platforms	34	34	34	34	34	34	34	34	34	34	34
Electrolyzers	53	53	53	53	53	53	53	53	53	53	53
Desalination equipment	51	51	51	51	51	51	51	51	51	51	51
Storage volume [m^3]	94100	94100	94100	94100	94100	94100	94100	94100	94100	94100	94100
Conversion devices	20	20	20	20	20	20	20	20	20	20	20
Reconversion devices	13	13	13	13	13	13	13	13	13	13	13
Transport medium	NH3 ship	NH3 ship	NH3 ship	NH3 ship	NH3 ship	NH3 ship	NH3 ship	NH3 ship	NH3 ship	NH3 ship	NH3 ship
FPSO volume [m^3]	955000	955000	955000	955000	955000	955000	955000	955000	955000	955000	955000
Distance sea [km]	440	440	440	440	440	440	440	440	440	440	440
Demand [kt/y]	121	121	121	121	121	121	121	121	121	121	121

Table 4.11: Results for optimal location (57.35, 7.78) for NH3 shipping (j=1)

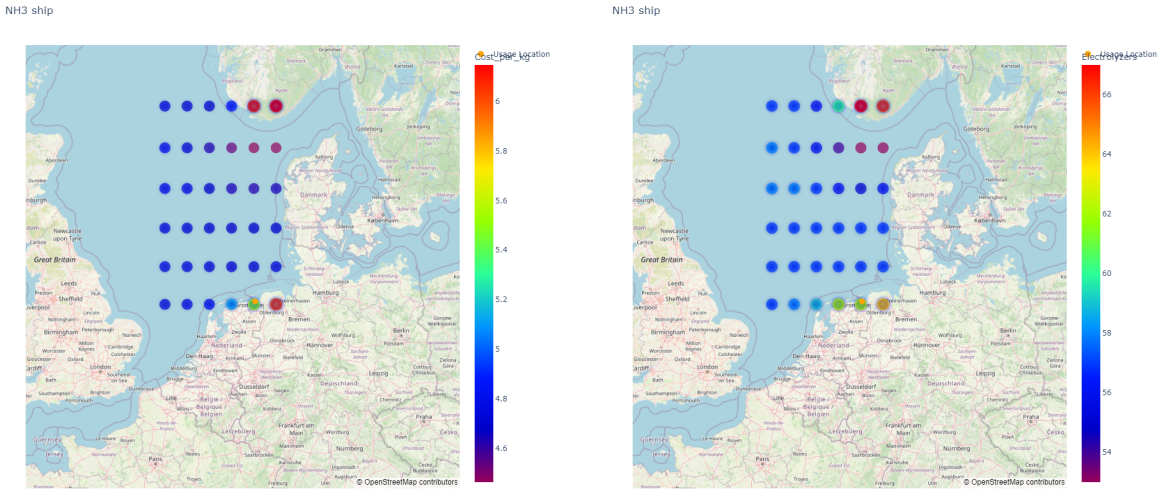

(a) Cost per kg in 2050 for NH3 Shipping

(b) Electrolyzer Number for NH3 Shipping

Figure 4.2: Map Plots for NH3 Shipping (j=1)

4.3.2. Scenario 2: LH2 Shipping (j=2)

The scenario for liquid hydrogen with shipping results in the same optimal location as in scenario 1, at coordinates (57.35, 7.78), as shown in the results Table C.1 in Appendix C. The LCOH value at this location is 6.521 [€/kg]. The total cost of across the time studied is 7,980[M€], with 104 wind turbines, 6 solar platforms, 51 electrolyzers, and 49 desalination units. The volume of the storage is 156,000 [m^3], while vessel volume is 1,130,000 [m^3]. Both the storage volume and vessel size are larger in the LH2 configuration as compared to the NH3 configuration. The cost of delivered hydrogen begins at 7.52 [€/kg] in 2020, and drops to 4.89 [€/kg] by 2050. If we consider the wind and solar equipment, the capacity of the energy generation units is 1.25[GW] to meet the demand of 121[kt].

The maps in Figures 4.3a and 4.3b follow a similar distribution as in the NH3 shipping case, with the absolute values being higher in the LH2 case. Again, the onshore locations illustrate the lowest weather availability for the wind and solar equipment, thus resulting in highest costs and equipment numbers, however these locations should not be included in analysis due to parameters not corresponding to reality. Considering all the locations while omitting onshore locations, the LCOH ranges between 7.217 and 6.521 [€/kg]. There is a large variation in solar platforms across the region due to certain locations having a significantly lower wind availability, and therefore being compensated by solar platforms which have comparatively lower associated costs.

Total Runtime [min]	24.6
Average Runtime [s]	3.73
Max Runtime [s]	48.7
Min Runtime [s]	1.51

Table 4.12: Runtime Statistics for (j=2)

Year	2020	2023	2026	2029	2032	2035	2038	2041	2044	2047	2050
Cost per kg [€/kg]	7.52	6.97	6.64	6.36	6.11	5.87	5.64	5.43	5.25	5.07	4.89
Wind turbines	104	104	104	104	104	104	104	104	104	104	104
Solar platforms	6	6	6	6	6	6	6	6	6	6	6
Electrolyzers	51	51	51	51	51	51	51	51	51	51	51
Desalination equipment	49	49	49	49	49	49	49	49	49	49	49
Storage volume [m^3]	156000	156000	156000	156000	156000	156000	156000	156000	156000	156000	156000
Conversion devices	20	20	20	20	20	20	20	20	20	20	20
Reconversion devices	13	13	13	13	13	13	13	13	13	13	13
Transport medium	LH2 ship	LH2 ship	LH2 ship	LH2 ship	LH2 ship	LH2 ship	LH2 ship	LH2 ship	LH2 ship	LH2 ship	LH2 ship
FPSO volume [m^3]	1130000	1130000	1130000	1130000	1130000	1130000	1130000	1130000	1130000	1130000	1130000
Distance sea [km]	440	440	440	440	440	440	440	440	440	440	440
Demand [kt/y]	121	121	121	121	121	121	121	121	121	121	121

Table 4.13: Results for optimal location (57.35, 7.78) for LH2 shipping (j=2)

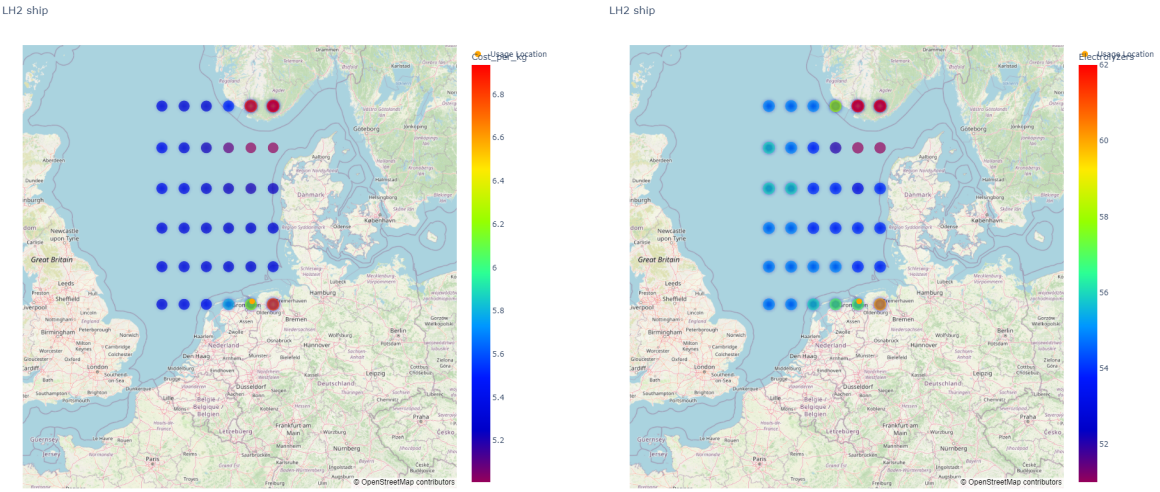

(a) Cost per kg in 2050 for LH2 Shipping

(b) Electrolyzer Number for LH2 Shipping

Figure 4.3: Map Plots for LH2 Shipping (j=2)

4.3.3. Scenario 3: GH2 Pipeline (j=3)

The scenario for compressed gaseous hydrogen transported through pipeline resulted in the optimal location at (54.35, 6.78), 102[km] from the Eemshaven port. The LCOH at this location is 4.052[€/kg]. The total cost for the time period of 2020 to 2050 in 3 year steps is 4,966[M€]. The equipment numbers include 93 wind turbines, 11 solar platforms, 55 electrolyzers, and 53 desalination units. No conversion nor reconversion units are present due to GH2 being the final product. The volume of the storage is 0[m^3] due to the assumption of storage in the pipeline, with the vessel size being 1,220,000[m^3]. The cost of delivered hydrogen begins at 4.81[€/kg] in 2020, and decreases to 3.20[€/kg] in 2050. Considering the energy generation equipment, the calculation arrives at a theoretical peak capacity of 1.12[GW].

The maps in Figure 4.4 show the delivered cost of hydrogen in 2050 and the number of electrolyzers required respectively, spread across the studied region. In contrast to the previous to scenarios, the optimal location cost-wise does not correspond to the location with minimum number of electrolyzers.

This suggests that the transport cost is dominant in determining location when considering pipeline transport. The LCOH in offshore locations ranges between 4.052 and 5.052[€/kg].

Total Runtime [min]	26.7
Average Runtime [s]	2.94
Max Runtime [s]	7.11
Min Runtime [s]	1.58

Table 4.14: Runtime Statistics for (j=3)

Year	2020	2023	2026	2029	2032	2035	2038	2041	2044	2047	2050
Cost per kg [€/kg]	4.81	4.34	4.06	3.84	3.68	3.57	3.46	3.37	3.31	3.25	3.20
Wind turbines	93	93	93	93	93	93	93	93	93	93	93
Solar platforms	11	11	11	11	11	11	11	11	11	11	11
Electrolyzers	55	55	55	55	55	55	55	55	55	55	55
Desalination equipment	53	53	53	53	53	53	53	53	53	53	53
Storage volume [m^3]	0	0	0	0	0	0	0	0	0	0	0
Conversion devices	0	0	0	0	0	0	0	0	0	0	0
Reconversion devices	0	0	0	0	0	0	0	0	0	0	0
Transport medium	GH2 pipe	GH2 pipe	GH2 pipe	GH2 pipe	GH2 pipe	GH2 pipe	GH2 pipe	GH2 pipe	GH2 pipe	GH2 pipe	GH2 pipe
FPSO volume [m^3]	1220000	1220000	1220000	1220000	1220000	1220000	1220000	1220000	1220000	1220000	1220000
Distance sea [km]	102	102	102	102	102	102	102	102	102	102	102
Demand [kt/y]	121	121	121	121	121	121	121	121	121	121	121

Table 4.15: Results for optimal location (54.35, 6.78) for GH2 pipeline (j=3)

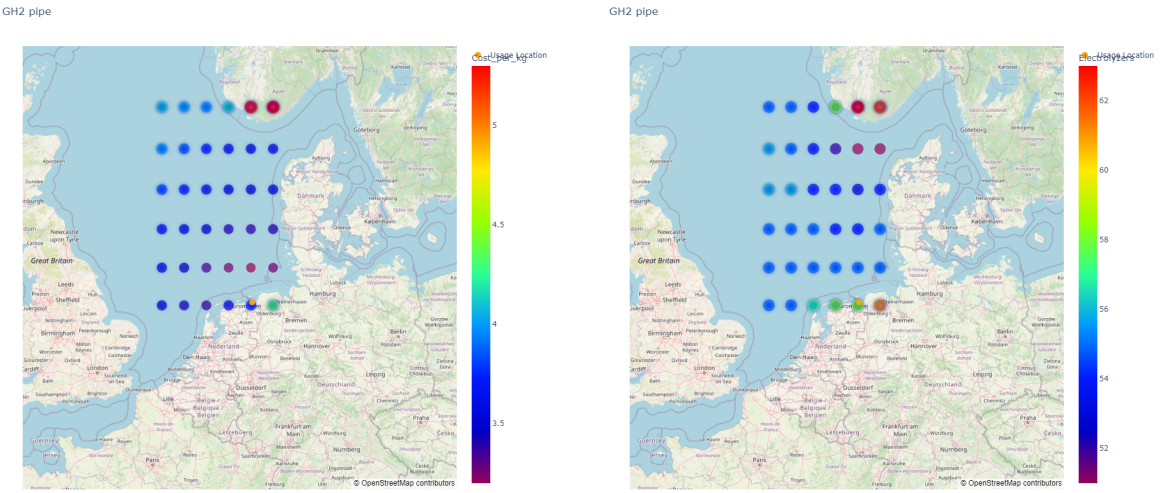

(a) Cost per kg in 2050 for GH2 Pipeline

(b) Electrolyzer Number for GH2 Pipeline

Figure 4.4: Map Plots for GH2 Pipeline (j=3)

4.3.4. Scenario 4: NH3 Pipeline (j=4)

The scenario ran for 19.4[min], with an average runtime of 2.94[s] for each run. The maximum runtime of 7.11[s] occurred for location (58.35, 2.78) at the 2029 timestep, while the lowest runtime of 1.58[s] occurred for location (58.35, 3.78) at the 2032 timestep. The runtime statistics are summarized in Table 4.16.

The final scenario investigates the ammonia pipeline supply chain configuration, finding the optimal location at (54.35, 6.78). This is the same location as the previous scenario involving the GH2 pipeline. The LCOH at this location is 5.494[€/kg], with the total cost across the 30 year time period reaching 6,860[M€]. The optimization model found the equipment to include 104 wind turbines, 7 solar platforms, 57 electrolyzers, 55 desalination units, 0[m^3] of storage volume (due to pipeline assumption), and an FPSO vessel size of 1,030,000[m^3]. The conversion and reconversion devices were again constant at

20 and 13 units respectively. The ammonia pipeline began at a delivered hydrogen cost of 6.31[€/kg] in 2020, reaching 4.58[€/kg] by 2050. Regarding energy generation, the theoretical capacity of the wind and solar equipment is 1.25[GW].

The maps shown in Figure 4.5 show the delivered cost in 2050 in (a) and electrolyzer number in (b). Similarly to the j=3 scenario, the lowest cost and lowest electrolyzer number do not correspond to the same location, which appears to be characteristic in the pipeline transport mode deployment. The elctrolyzer is lowest at the location corresponding to highest weather availability for energy generation. The LCOH in offshore locations ranges between 6.332 - 5.494 [€/kg].

Total Runtime [min]	19.4
Average Runtime [s]	2.94
Max Runtime [s]	7.11
Min Runtime [s]	1.58

Table 4.16: Runtime Statistics for (j=4)

Year	2020	2023	2026	2029	2032	2035	2038	2041	2044	2047	2050
Cost per kg [€/kg]	6.31	5.80	5.50	5.26	5.10	4.98	4.86	4.77	4.70	4.64	4.58
Wind turbines	104	104	104	104	104	104	104	104	104	104	104
Solar platforms	7	7	7	7	7	7	7	7	7	7	7
Electrolyzers	57	57	57	57	57	57	57	57	57	57	57
Desalination equipment	55	55	55	55	55	55	55	55	55	55	55
Storage volume [m^3]	0	0	0	0	0	0	0	0	0	0	0
Conversion devices	20	20	20	20	20	20	20	20	20	20	20
Reconversion devices	13	13	13	13	13	13	13	13	13	13	13
Transport medium	NH3 pipe	NH3 pipe	NH3 pipe	NH3 pipe	NH3 pipe	NH3 pipe	NH3 pipe	NH3 pipe	NH3 pipe	NH3 pipe	NH3 pipe
FPSO volume [m^3]	1030000	1030000	1030000	1030000	1030000	1030000	1030000	1030000	1030000	1030000	1030000
Distance sea [km]	102	102	102	102	102	102	102	102	102	102	102
Demand [kt/y]	121	121	121	121	121	121	121	121	121	121	121

Table 4.17: Results for optimal location (54.35, 6.78) for NH3 pipeline (j=4)

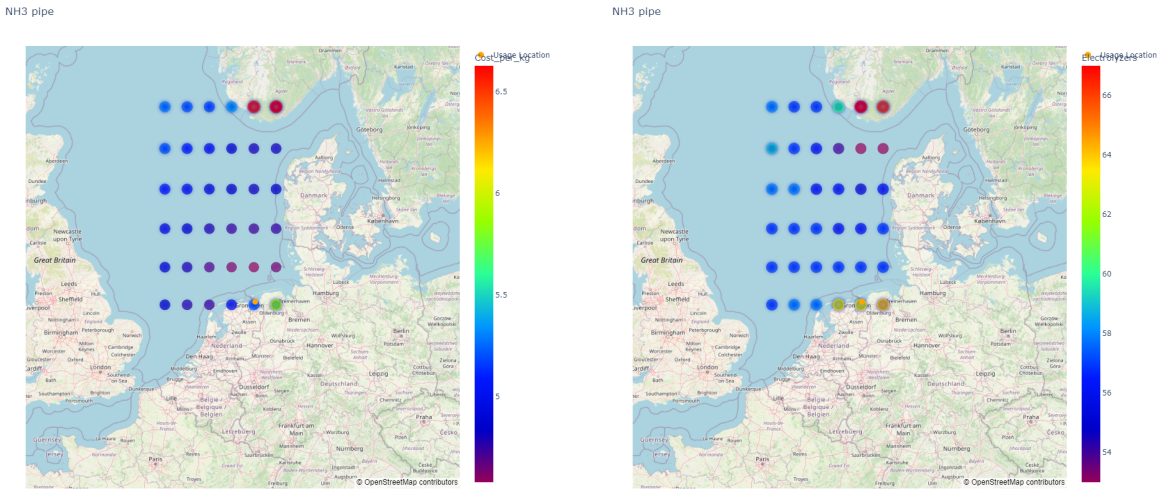

(a) Cost per kg in 2050 for NH3 Pipeline

(b) Electrolyzer Number for NH3 Pipeline

Figure 4.5: Map Plots for NH3 Pipeline (j=4)

4.4. Analysis

Now that the optimal locations based on LCOH from each scenario are determined, the configurations across scenarios can be compared. Figure 4.6 presents a plot of how the hydrogen cost develops over time in each scenario. It is clear that the compressed hydrogen in the pipeline configuration requires

the least cost at each time step. Overall, the LCOH is also the lowest for this configuration. The second lowest costs and LCOH are achieved by the NH3 shipping configuration. The NH3 pipeline appears to follow the same trend as its shipping counterpart, although at higher costs. The highest costs and LCOH are exhibited by the LH2 shipping configuration in scenario 2.

Looking at the energy generation part of the supply chain, the wind farm is largest in both LH2 shipping and NH3 pipeline, with 104 turbines involved. For NH3 shipping 96 turbines are chosen, while for GH2 pipeline there are 93. The ratio of wind turbine to solar platform is lowest in j=1, with 1 solar platform for every 2.8 wind turbine, followed by j=3 with a platform every 8.5 turbines, j=4 with 15 turbines per solar platform, and finally j=2 with 17 turbines for every solar platform. The hydrogen production in the scenarios spans 57 electrolyzers for the ammonia pipeline, 55 for compressed hydrogen pipeline, 53 electrolyzers for the ammonia shipping, and finally 51 electrolyzers for the liquefied hydrogen shipping. Interestingly, in the lowest cost scenario of j=3 the number of electrolyzers is higher at 55 compared to 51 in LH2 shipping. This suggests that production costs are not as dominant as energy generation costs. LH2 shipping is overall more expensive than NH3 shipping when comparing costs at corresponding locations, which is consistent with the findings of [49], where every scenario studied resulted in higher costs for LH2 compared to NH3 shipping.

The total yearly costs can be separated into cost components as shown in Figure 4.7, to allow for understanding how much each component contributes to the total costs in each year. What can be seen from the plot is that the liquid hydrogen shipping configuration is expected to have the greatest decrease in cost in the future. This is due to having the largest storage and transport costs, which are expected to diminish significantly as time progresses. This configuration was also assumed to have a learning rate for the conversion costs, which compound the decrease further. The wind and electrolyzer costs will drop at a similar rate for each configuration, therefore the number of units needed to satisfy the demand will drive the decision on most feasible deployment. Solar costs vary significantly between each configuration, which is due to the variation in number of platforms chosen in each scenario (ranging between 6-34 platforms). Desalination and FPSO size costs are constant across the time period for all configurations, as are conversion and transport costs for NH3 and GH2 configurations, due to previously established assumptions.

Percentage-wise, wind is the largest cost component of every configuration in every year, while conversion is the second largest component, excluding the GH2 scenario where conversion is not applied. In the GH2 case, the electrolyzer is the 2nd highest cost in 2020, shifting to the FPSO vessel in 2035 and 2050 when the PEM learning rate exhibits its effect. Furthermore, the wind costs for the GH2 case are roughly a half of the total costs throughout throughout the studied period. The smallest non-zero cost contributors to the total are desalination for j=1, solar for j=2, desalination in 2020 then solar in 2035 and 2050 for j=3, and finally solar for j=4.

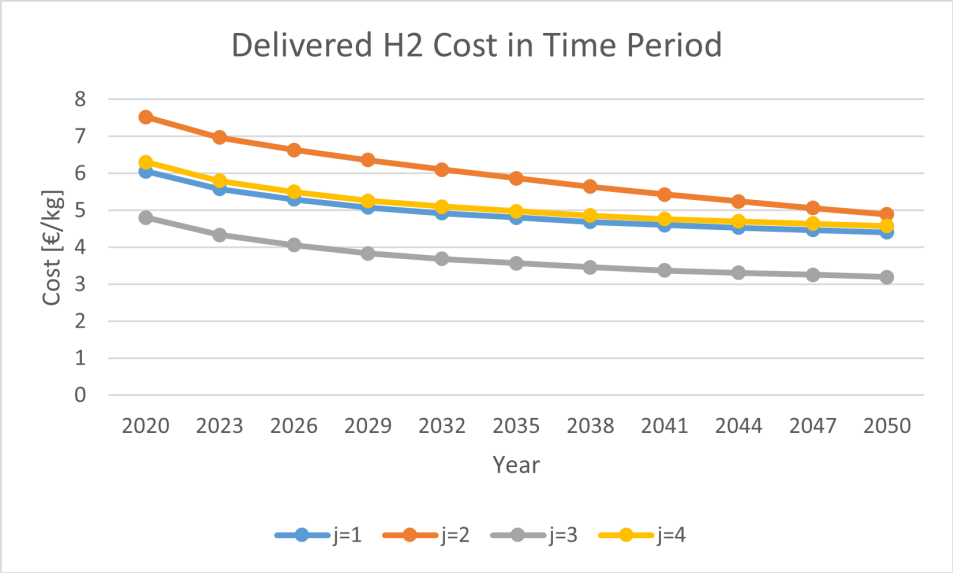

Figure 4.6: Cost of delivered hydrogen in the years within time period for optimal locations in Scenarios 1-4

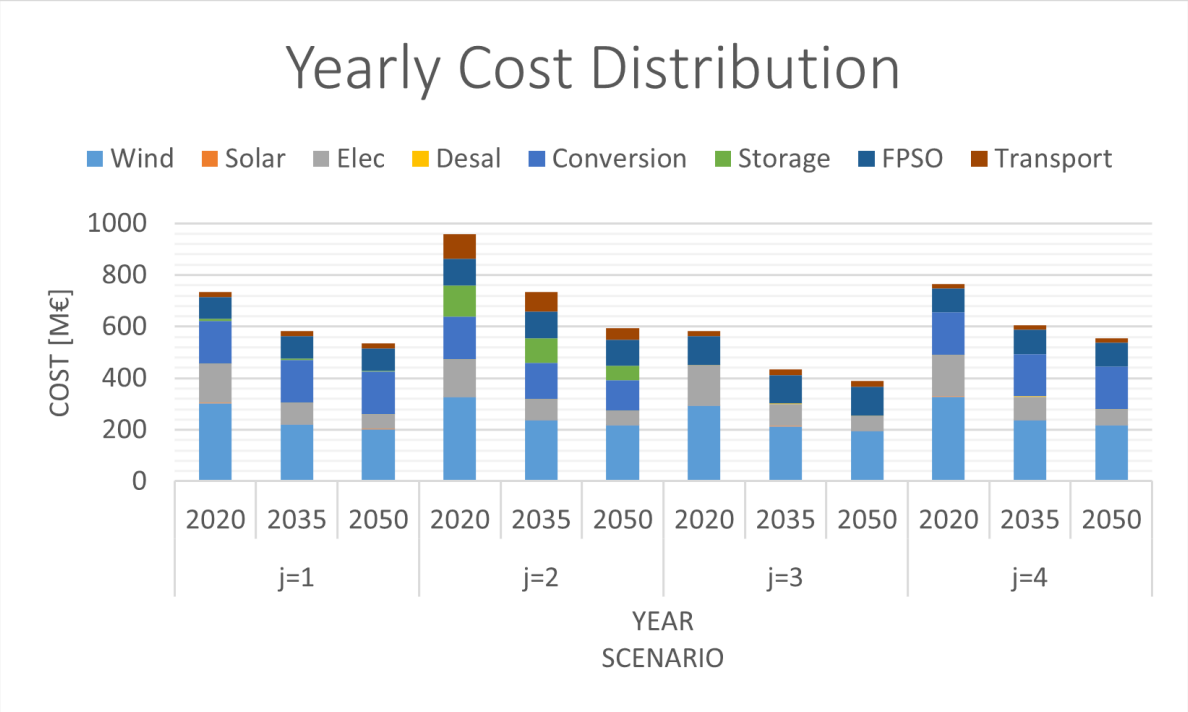

Figure 4.7: Cost distributions of scenarios at optimal locations for 2020, 2035, and 2050

The capacity factors from the weather dataset can be calculated for each location based on the actual power output from the sum of the hourly wind and solar functions, divided by the theoretical maximum power output across the time period. This results in the matrix in Figure 4.8 for each location. As can be seen, location (57.35, 7.78) has the highest energy generation due to weather with 66[%]. This also coincides with the optimal locations in the shipping scenarios. This can be explained by the fact that the optimal location in the shipping case is not restricted to the same degree by transport costs as the pipeline case.

		Longitude					
		2.78	3.78	4.78	5.78	6.78	7.78
Latitude	58.35	60%	61%	61%	58%	40%	38%
	57.35	59%	61%	62%	64%	66%	66%
	56.35	59%	60%	61%	62%	62%	62%
	55.35	60%	60%	61%	61%	61%	61%
	54.35	60%	60%	61%	61%	61%	60%
	53.35	60%	60%	59%	53%	48%	40%

Figure 4.8: Capacity factors for power output of single wind turbine and solar platform in study region based on 2020 weather data

The case for no solar can be applied for the optimal locations in the model to see the difference in cost when no solar platforms are implemented and only wind turbines are used to satisfy the demand. This results in the LCOH values of 5.296[€/kg] for j=1 with 97 wind turbines, 6.540[€/kg] for j=2 with 105 wind turbines, 4.068[€/kg] for j=3 with 94 wind turbines, and 5.512[€/kg] for j=4 with 105 wind turbines. In each scenario, the complete set of solar platforms are substituted with 1 additional wind turbine, improving the LCOH by 0.015[€/kg] on average. This suggests that the improvement is relatively low, which can be explained by the fact that 1 solar platform has a capacity which is approximately 21 times smaller than that of a wind turbine, while the cost of a solar platform is on average 2.36 times smaller per [MW] than a wind turbine. This suggests that 1 turbine can substitute 21 solar platforms, and only pay 2.36 times the amount for the 12[MW] of capacity it gains. At large scale capacities such as 700[MW] and upwards of 1[GW], this cost is relatively small if the amount of solar platforms chosen is below 21. Only j=1 resulted in 34 solar platforms selected, however this would still only result in approximately 20[MW] of the total capacity.

The case for no re-conversion for ammonia results in an LCOH of 5.148[€/kg] for j=1 and 5.352[€/kg] for j=4. This means a decrease of 0.147[€/kg] and 0.160[€/kg] respectively. This is quite a significant decrease in costs, however it does not affect the ranking of the configurations' LCOH values overall. As such, if the final demand can be delivered as ammonia instead of hydrogen, there is a significant cost saving potential for the value chain by eliminating the costs associated with re-conversion equipment.

4.5. Sensitivity

A sensitivity analysis is conducted to determine the influence of each cost parameter on the overall LCOH of the optimal locations in each scenario $j \in J$. The elements of each cost parameter A, B, C, and TC were varied by a 20[%] decrease and increase relative to the reference case from the results. Each cost component is multiplied by a sensitivity scale parameter to reflect this, with scale parameters SSP_A1, SSP_A2, SSP_B1, SSP_B2, SSP_B3, SSP_B4, SSP_C1, SSP_C2, and SSP_TC representing the multiplier for conversion, re-conversion, wind, solar, electrolysis, desalination, storage, vessel size, and transport cost respectively. The resulting LCOH values are summarized in Table 4.18, with sensitivity values shown in Table 4.19. These sensitivity values represent the % change in LCOH when adjusting the cost parameter by a 1% decrease or increase respectively. These sensitivity values are portrayed in Figures 4.9 and 4.10 to enable a visual comparison. Both figures suggest that parameter SSP_B1, or the sensitivity scale parameter for wind turbine cost has the greatest effect on the LCOH. This is consistent with the cost distribution analysis, where the wind turbine cost formed the largest component of the total cost. It is also consistent for each scenario, with an apparent correlation between the cost component fraction of total cost and sensitivity value, i.e j=3 for the GH2 pipeline has wind cost as the greatest component of total cost, as well as the highest sensitivity value for wind cost. It must be

noted that in the model the same cost per turbine is applied for every configuration, and therefore any variation in cost will affect each configuration at the same rate if the number of units selected remains the same. This means that within the context of this model, the ranking of configurations (when considering the selected locations) will not change based on a variation in the wind cost parameter, unless the number wind-solar ratio changes as well.

Range LCOH [€/kg]	**j = 1**	**j = 2**	**j = 3**	**j = 4**
Reference	5.290	6.521	4.052	5.494
SSP_A1	5.047 - 5.533	6.349 - 6.693	4.052 - 4.052	5.251 - 5.737
SSP_A2	5.262 - 5.318	6.499 - 6.543	4.052 - 4.052	5.466 - 5.522
SSP_B1	4.874 - 5.702	6.075 - 6.967	3.652 - 4.450	5.048 - 5.940
SSP_B2	5.286 - 5.293	6.520 - 6.522	4.048 - 4.053	5.493 - 5.495
SSP_B3	5.106 - 5.474	6.343 - 6.699	3.860 - 4.243	5.295 - 5.692
SSP_B4	5.289 - 5.291	6.520 - 6.522	4.050 - 4.053	5.493 - 5.495
SSP_C1	5.279 - 5.301	6.345 - 6.697	4.052 - 4.052	5.494 - 5.494
SSP_C2	5.148 - 5.433	6.352 - 6.690	3.869 - 4.234	5.341 - 5.647
SSP_TC	5.258 - 5.322	6.382 - 6.660	4.016 - 4.087	5.466 - 5.522

Table 4.18: Resulting ranges for LCOH at optimal locations when varying cost parameters by 20% below and above the reference case.

Sensitivity	**j = 1**	**j = 2**	**j = 3**	**j = 4**
SSP_A1	0.230 - 0.230	0.132 - 0.132	0.000 - 0.000	0.221 - 0.221
SSP_A2	0.027 - 0.027	0.017 - 0.017	0.000 - 0.000	0.026 - 0.026
SSP_B1	0.393 - 0.389	0.342 - 0.342	0.493 - 0.492	0.406 - 0.406
SSP_B2	0.004 - 0.003	0.001 - 0.000	0.004 - 0.001	0.001 - 0.001
SSP_B3	0.174 - 0.174	0.136 - 0.136	0.236 - 0.236	0.181 - 0.181
SSP_B4	0.001 - 0.001	0.001 - 0.001	0.001 - 0.001	0.001 - 0.001
SSP_C1	0.011 - 0.011	0.135 - 0.135	0.000 - 0.000	0.000 - 0.000
SSP_C2	0.135 - 0.135	0.130 - 0.130	0.225 - 0.225	0.139 - 0.139
SSP_TC	0.030 - 0.030	0.107 - 0.107	0.044 - 0.044	0.025 - 0.025

Table 4.19: Resulting sensitivity for LCOH at optimal locations. Each value represents a % change of LCOH when varying the corresponding cost parameter by 1%

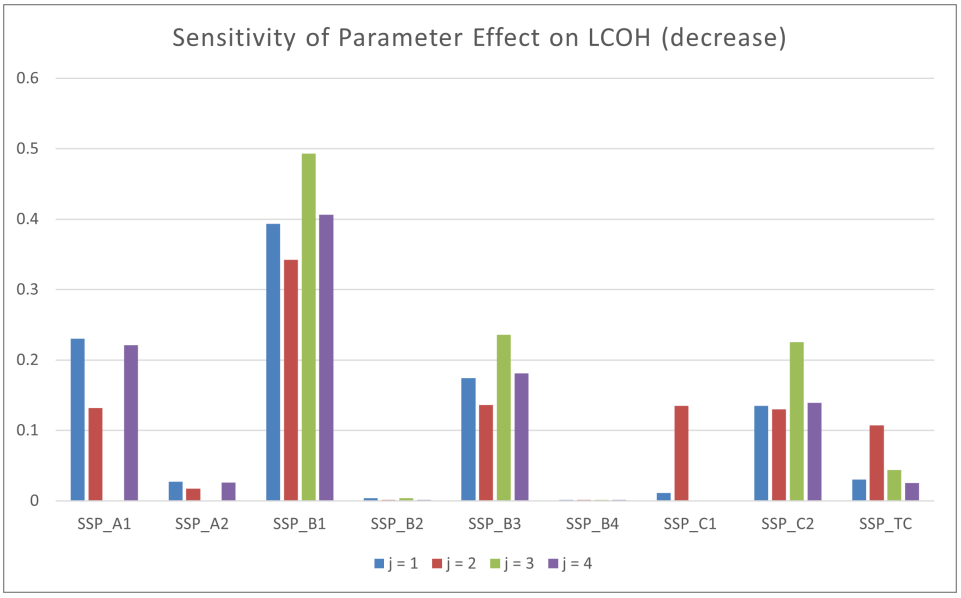

Figure 4.9: Sensitivity parameters and their corresponding effect on LCOH of each configuration when cost parameter is decreased by 1[%]

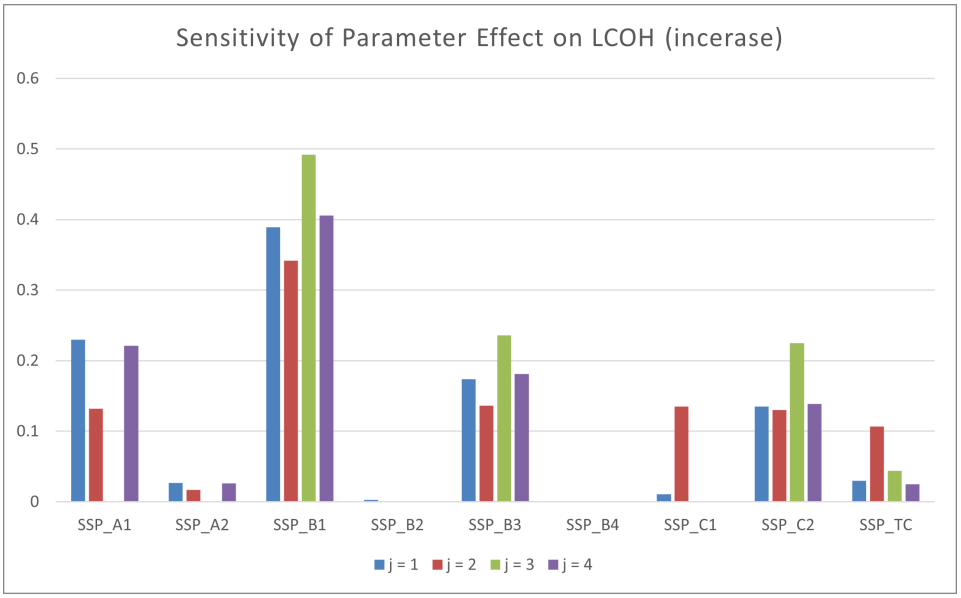

Figure 4.10: Sensitivity parameters and their corresponding effect when cost parameter is decreased by 1[%]

The ammonia based configurations are significantly more sensitive to conversion costs (SSP_A1) compared to the LH2 and GH2 configurations. Since the conversion process is different between these configurations, the variations in this parameter will behave differently depending on which conversion process has a change in cost. If the ammonia to hydrogen conversion process improves significantly, it would be possible for the ammonia configurations to become more competitive with the gaseous hydrogen pipeline configuration. For instance, if looking at Table 4.18, with a 20% reduction in conversion cost (SSP_A1) the LCOH of j=1 would become 5.047[€/kg], which is then within 1[€] range of the reference LCOH of j=3 of 4.052[€/kg].

For the liquid hydrogen shipping configuration, it can be seen that the storage (SSP_C1) and transport (SSP_TC) exhibit a higher sensitivity compared to other configurations. This suggests that if the storage and transport methods for liquid hydrogen are improved significantly in the future, it is possible that this configuration would become more competitive. If assuming linear behavior of the sensitivity value, a cost decrease of 70% of both the storage and transport simultaneously would yield an LCOH of 5.416[€/kg], allowing the configuration to outperform the reference case of the next best configuration, which is j=4 at 5.494[€/kg]. Generally, a cost reduction of more than half of both cost components (storage and transport) is required to reach the LCOH of nearest competitor. This is plotted in Figure 4.11, demonstrating the cost reduction in [%] required for storage and transport, such that the LCOH of the other configurations is attained.

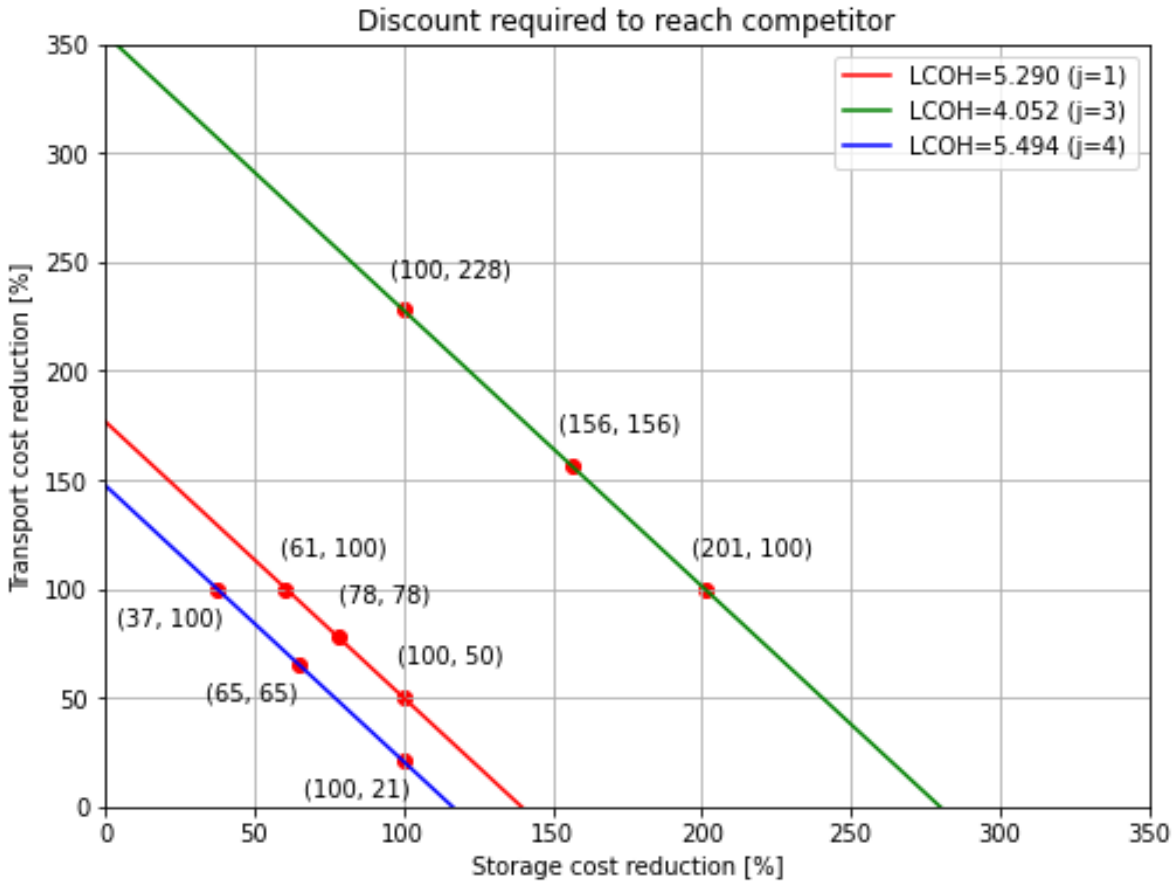

Figure 4.11: Percentages of cost reduction for storage and transport in configuration j=2 which would enable the LCOH to be reduced to that of the other configurations. Points are added on the plot representing the intercepts where cost reductions are equal, as well as where 100[%] reductions would be required

Similarly, we can see that SSP_A1 and SSP_A2 have a higher sensitivity for the ammonia configurations. This pertains to the conversion and reconversion cost components. Since j=1 has a higher sensitivity value, it is interesting to check how much of a reduction in cost is required to match the LCOH of the j=3 configuration. This is plotted in Figure 4.12. As can be observed, the plot is skewed due to conversion costs being a more sensitive parameter. If 100[%] of conversion costs are lifted, one would still need to reduce reconversion costs by 90[%], while a 15[%] reduction of conversion costs is required if the reconversion is completely eliminated. If both costs are reduced by 91[%], the LCOH would match that of j=3.

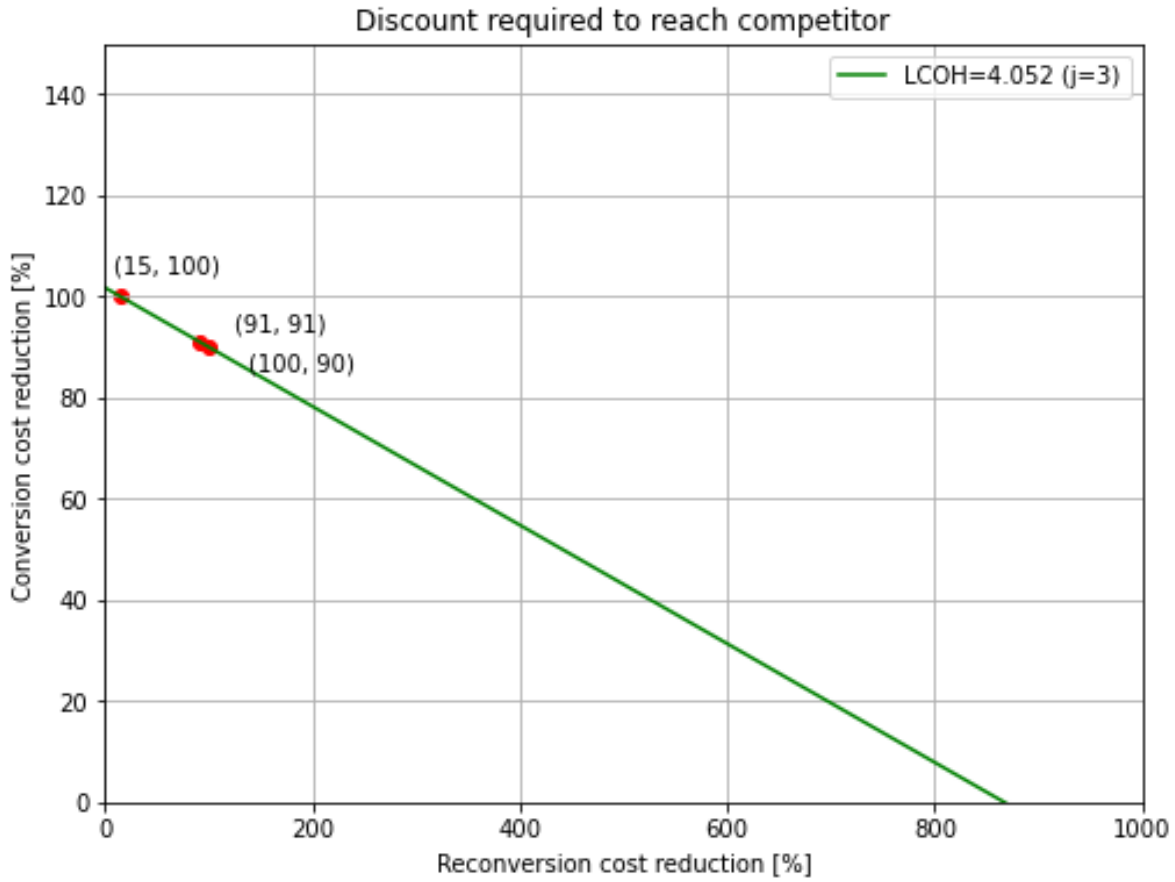

Figure 4.12: Percentages of cost reduction for conversion and reconversion in configuration j=1 which would enable the LCOH to be reduced to that of the j=3 configuration. Points are added on the plot representing the intercepts where cost reductions are equal, as well as where 100[%] reductions would be required

4.6. Discussion

The model assumes discrete points as locations when determining the weather and optimal costs. This means that the weather input for the whole wind and solar farm stems from a single point location, whereas in reality each wind turbine and solar panel will exist in a unique location point, with varying weather data, not captured in the model. Furthermore, most of the points vary in number of wind and solar equipment need, and thus would take up different amounts of space with their layout. The costs for the layout were considered in the wind CAPEX for cables required, scaling linearly with turbine number, however the area required for the wind and solar farm scales non-linearly with the equipment numbers.

The cost values in the results represent an amortized CAPEX and OPEX, where a learning rate has been applied to certain components. This means that the values presented show what the fraction of total CAPEX would be when considering the full lifetimes of the equipment if the project were started in the relevant year. In reality the CAPEX would be an upfront cost paid in the first year of development, but this is split into amortized fractions in order to allow for the model to determine the minimal cost in yearly time steps while considering the discount rate and improvements on cost depending on the year that the project started, as well as combining the costs of all equipment due to lifetimes varying per equipment. As such, the total yearly costs only consider a fraction of total CAPEX of equipment, and if looking at the complete span of the time period from 2020 to 2050 as the deployment of the supply chain, with 2020 as the starting year, the sum of the CAPEX would be lower than the total CAPEX in reality due to learning rate as time progresses, however higher when lifetimes of equipment are exceeded. In this case the assumption is that new equipment is implemented once lifetimes are exceeded, and thus a new CAPEX would be considered. As such, the total yearly costs, if summed

across time period, do not contain an actual representation of total CAPEX paid in reality, however it is an approximation done under the assumptions of amortization factor, interest rate, discount rate, and combination of equipment with varying lifetimes, to provide an aggregated value of the expenditures in a given year.

The demand in the model is considered constant, and matching the hydrogen production output of the GFPSO. In reality, the hydrogen demand will vary with time. Hydrogen demand is relatively ”non-existent” in current the total energy demand of the EU, which matches the global trends [12]. The final energy demand in the EU has remained relatively constant from 1990 to 2020, at around 10,500[TWh] (which would be equivalent to 315[Mt] of H2) [12]. Hydrogen demand is expected to remain at under or around 1[%] up to 2030 by most studies, and is estimated to rise to an average of 18[Mt] by 2040 and 32[Mt] by 2050 in the EU [12].

The business case chosen in this research was a near offshore scenario with the north sea, whereas the model by [49] was originally designed for the purpose of investigating far offshore scenarios. This means that the assumptions of the original model may apply directly to near offshore scenarios. This was identified in the parameters, where the offshore wind turbine costs had to be changed from floating to fixed-bottom specifications due to water depth in the region. The solar platform was kept as floating, due to the [17] pilot being applied in a near offshore case already, which suggests that the technology can be applicable to both far and near offshore cases. The electrolyzer, desalination, and conversion equipment’s technical and cost parameters were assumed to remain consistent between far and near offshore. One important consideration differentiating the far and near offshore cases would be the possibility for using subsea cables and connecting the energy generation to onshore production. This supply chain configuration has been studied to an extent in literature, for instance in scenario (i) of [19] where GH2 is produced onshore, assuming constant electricity market price. Including the possibility for onshore production from offshore generation introduces additional cost parameters for HVDC terminals offshore and at the port, as well as the subsea cables with efficiency losses. [19] suggests that the cost contribution of these components could be between 19.5[%]-47[%] of the total costs. The sensitivity analysis from [19] looked at power output and distance to shore combinations in the scenarios of 150[MW] at 60[km], 500[MW] at 200[km], 1[GW] at 1000[km], and 12[GW] at 1000[km], and 12[GW] at 10,000[km]. These combinations do not directly translate to the optimal locations and supply chain configurations studied here, however the findings indicate that for every power-distance combination and supply chain configuration the LCOH is higher than the highest LCOH found in the optimal locations in this study except for LH2 shipping (5.60[€/kg] is lowest LCOH found at 150[MW] and 60[km] in 2050 for onshore GH2 production). The only case where [19] found lower LCOH for onshore production was for the optimistic scenario in 2050 for combination 150[MW] at 60[km] having an LCOH of 3.88[€/kg] and for 500[MW] at 200[km] having LCOH of 4.13[€/kg]. The former suggests a lower cost than that found in the optimal case of GH2 pipeline (j=3) in this study, however at a closer distance to shore and significantly lower plant capacity. As such it is not possibly to definitively state whether onshore production would perform better than the GH2 pipeline in the GFPSO, however the research of [19] itself finds GH2 pipelines more cost effective in each case than the onshore production. At the same time, the electrolyzers would be placed onshore, removing the need for offshore production, storage, and offloading, effectively changing the concept from a GFPSO to simply onshore production, storage and distribution. While not fitting into the scope of a GFPSO supply chain, it is still relevant to discuss such a configuration as an alternative for an optimal hydrogen supply chain deployment strategy for comparison, however it should be reserved for a future extension of the model due to such a comparison introducing further complexities for consideration, including potential grid connectivity and electricity pricing.

The weather data considered was from a single year (2020). Additionally, the weather data was only available for a 9 months due to website dataset download size restrictions [24]. The resulting cost data is simply scaled to 12 months, however in reality the final 3 months of the year are not entirely represented by an average of the prior 9 months. If the final 3 months exhibit poor wind and solar conditions, the resulting cost may be higher, however if wind and solar conditions are better, the cost may be lower than estimated. To have an idea on the variation from year to year, the capacity factors at the different locations can be plotted, as portrayed in Figures 4.13 and 4.14. The weather conditions do change somewhat from year to year, therefore it could be the case that the optimal location would shift again. This could particularly be the case for the shipping mode configurations, since the LCOH

appears to depend significantly on energy generation costs. It does not seem reasonable to move locations from year to year due to the infrastructure of wind being fixed, therefore an actual optimal location in reality would have to consider where weather would be sufficiently good to provide highest energy yield across a long term time span.

		Longitude					
		2.78	3.78	4.78	5.78	6.78	7.78
Latitude	58.35	52%	54%	56%	52%	34%	31%
	57.35	52%	54%	57%	61%	62%	60%
	56.35	51%	53%	55%	57%	58%	56%
	55.35	52%	54%	55%	56%	56%	55%
	54.35	53%	53%	53%	54%	55%	55%
	53.35	52%	53%	52%	46%	41%	33%

Figure 4.13: Capacity factors for power output of single wind turbine and solar platform in study region based on 2021 weather data

		Longitude					
		2.78	3.78	4.78	5.78	6.78	7.78
Latitude	58.35	65%	65%	64%	59%	40%	35%
	57.35	63%	64%	65%	66%	66%	63%
	56.35	62%	62%	63%	64%	64%	61%
	55.35	60%	61%	61%	62%	62%	60%
	54.35	58%	58%	58%	58%	58%	57%
	53.35	56%	55%	54%	48%	44%	37%

Figure 4.14: Capacity factors for power output of single wind turbine and solar platform in study region based on 2022 weather data

The depth was considered uniform, however in reality the depth will affect the cost of material and installation of a bottom-fixed wind turbine, and for depths exceeding 60[m], as some northern points in the region considered do, floating wind turbines would be required. To verify water depth, an interpolation to calculate depth based on bathymetry data from [21] for each location was performed, as visualized in Figure 4.15. Given this, the costs should be recalculated in the locations exceeding 60[m] (rounding up from the deepest fixed-bottom turbine at 58.6[m] [18]). To do this, the parameters for floating wind from [49] can be applied and the model can run for this. When these parameters are applied, this results in the costs distributed as shown in Figure 4.16. It is clear that the cost becomes significantly lower when the floating wind turbines are applied compared to the fixed-bottom structure. Although it is possible that at some point in the future floating wind turbines become cheaper than fixed, based on estimations from [65] this is not likely. If the floating wind parameters and calculations from [49] are applied for depths above 60[m], while fixed wind parameters from [65] are applied for depths under 60[m], there is an inconsistency between the methods of cost estimation and learning rate, since the former applied a linear learning rate based on time, while the latter uses exponential decay with learning rate based on cumulative capacity. To ensure a consistent comparison, the approach from [65] is applied in the model for the floating wind case. This is done by taking Equation 4.1 and applying values from [65] for learning rate of 11.5[%], an initial CAPEX of 9,120[€/kW], as well as capacities of $\approx$0[GW] in 2020 and 30[GW] in 2035, yielding an annual capacity increase of $\approx$ 2[GW/y]. The OPEX is then taken as 222[€/kW/y] from [65]. This results in the costs shown in Figure 4.17, where overall location distribution of costs is relatively consistent, however the absolute value decreases from 4.41[€/kg] to 4.27[€/kg]. The LCOH for j=1 would be 5.030[€/kg], while the LCOH for j=2 would become 6.354[€/kg], corresponding to a

cost decrease of 0.260[€/kg] and 0.167[€/kg] respectively. This is not significant enough to impact the ranking for LCOH, however it is useful to note when considering the sensitivity analysis.

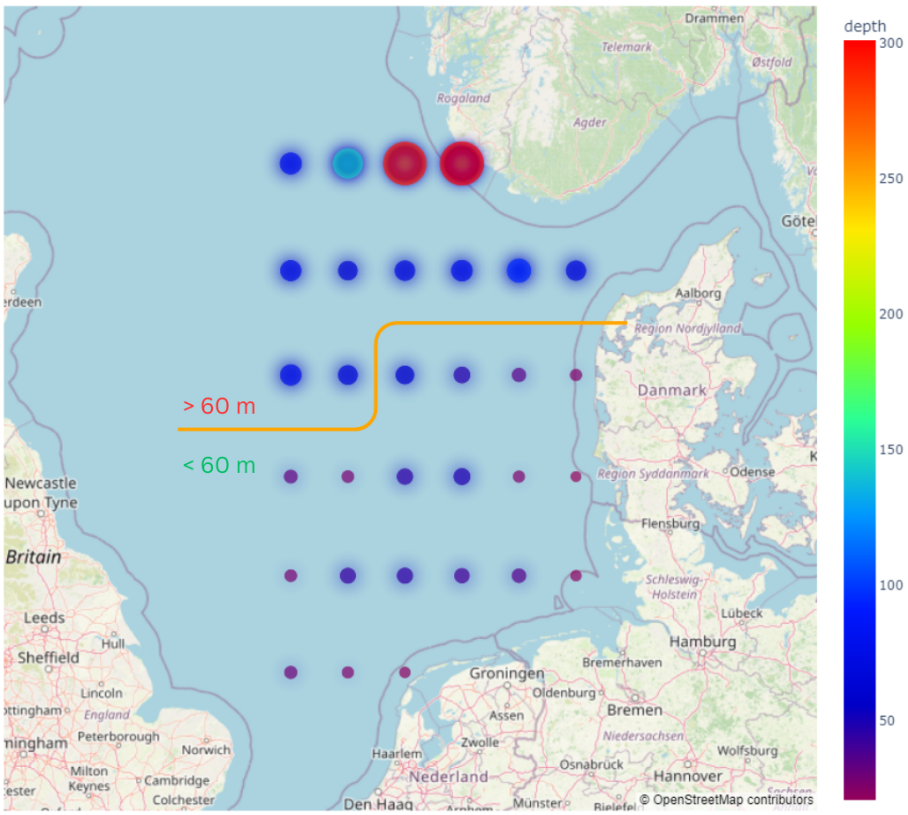

Figure 4.15: Water Depth at each location in North Sea

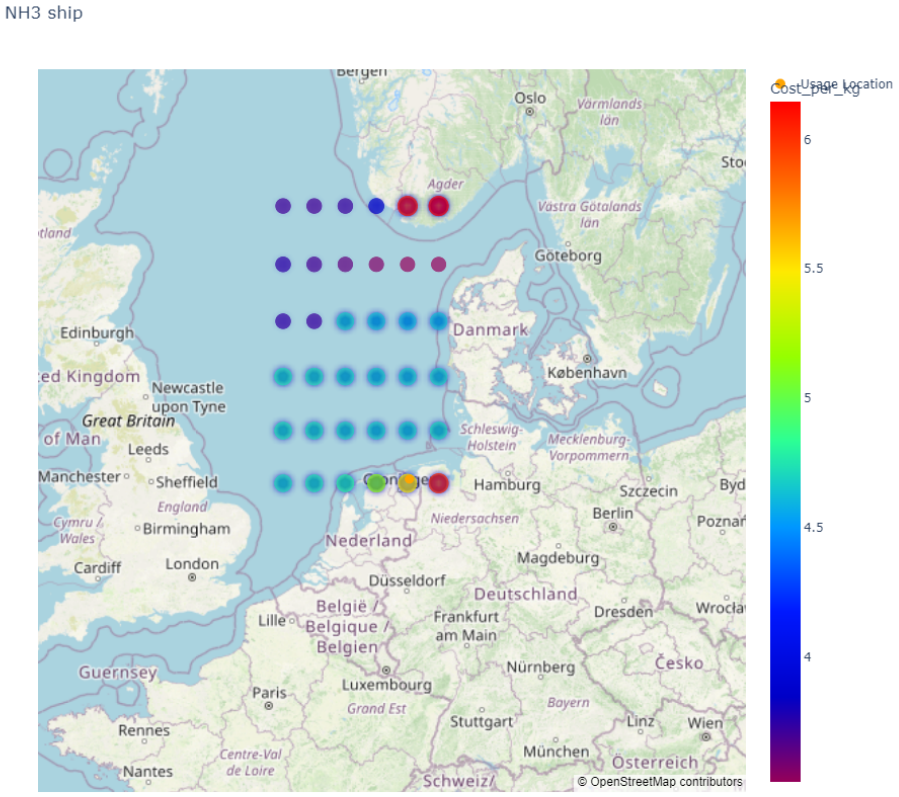

Figure 4.16: Cost per kg in 2050 for j=1, with floating wind parameters from [49] above 60[m] water depth

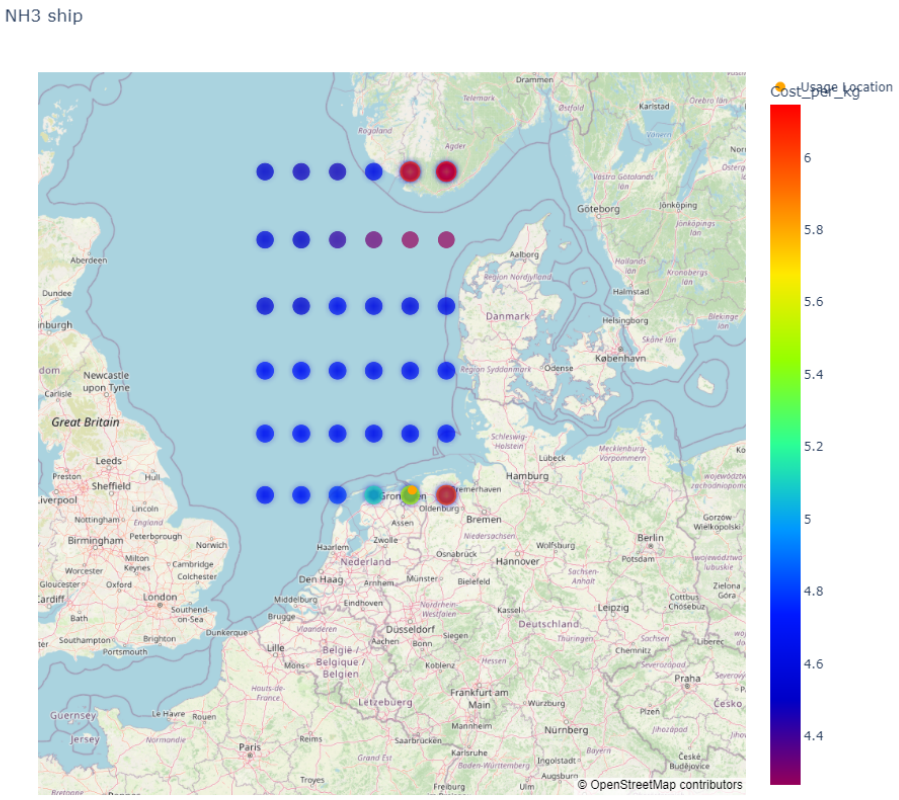

Figure 4.17: Cost per kg in 2050 for j=1, with floating wind parameters from [65] above 60[m] water depth

The layout of the wind and solar farm would also play a role in the LCOH in reality. In the model the energy generation layout is simplified to a single discrete point, considering the weather data measurement at this point to represent the weather of the entire farm. In reality the weather would differ for each separate wind turbine and solar platform location. With the wind turbine results arriving in the order of 100 units, this would allow for a spacing between turbines of approximately 12.3[km] spacing between the turbines. This is due the following reasoning: given that 1 degree of latitude, as well as 1 degree of longitude span 111[km] each, that allows for 111[km^2] of space without overlap. If we arranged 100 wind turbines in a square grid such that they are equally spaced, we have 9 spaces between each turbine vertically and horizontally. $\frac{111[km]}{9} = 12.3[km]$. According to [66], a regularly spaced wind farm requires a spacing distance of 8.88 rotor diameters, considering a 10[MW] turbine with a rotor size of 190.8[m]. Assuming we scale up to a 12[MW] turbine, we can consider the specification of a ”GE Vernova GE Haliade-X 12 MW” which has 220[m] rotor diameter. As such, the minimum spacing ought to be $8.88 \cdot 220[m] = 1.95[km]$. As such, the wind farm may fit without overlap in the regions specified in the study.

Another limitation is that of the geodesic. A geodesic is used to calculate the distance for the transport to occur. The transport costs are dependent on this distance to the demand node. In reality, the path traveled by the ship, as well as the constructed pipeline would not match a geodesic exactly, and thus the costs are a lower bound of the actual costs in this case. However, the transport costs make up of approximately 2-10[%] depending on the year and configuration, with the highest share being in the liquid hydrogen configuration. The ranking is not impacted significantly by the transport cost, with the most sensitive configuration of j=2 requiring an approximate 150[%] reduction in transport cost to match the LCOH of the next best alternative (j=4). It could be possible to create an upper bound on the transport cost, applying a Manhattan distance instead of a geodesic, however due to the sensitivity analysis it is likely not necessary.

4.6.1. Validation

The results from the modeling in this study an be compared to values found in literature to validate the results. The study by [19] is able to provide LCOH values for the North Sea case, without including solar energy generation. They also indicate the LCOH values for scenarios based on discrete values for capacity and distance to shore. As such, the difference in assumptions ought to be considered, however a comparison can still be made. In [19], the reference scenario concerns the GH2 pipeline, scenario (ii) looks at the LH2 shipping configuration, scenario (iii) looks at NH3 shipping, and finally scenario (iv) considers NH3 pipelines. Since these scenarios correspond to the scenarios in this study, the resulting LCOH values can be compared. The values in [19] consider an optimistic and a pessimistic case for the costs, therefore the LCOH values are provided as ranges. The ranges for power outputs between 150-1000[MW] and 60-1000[km] were considered due to being most closely related to the study done here. The ranges and values from this study are presented in Table 4.20. All of the resulting LCOH values in this study fall within the ranges provided by [19], with the exception of the GH2 pipeline LCOH which falls below the range for a project started in 2025, and the LH2 shipping LCOH exceeding the range for a 2050 project. The first instance could be due to solar generation and the scenario discrepancy, with the combination of power output and distance in the optimal GH2 pipeline location being 1.12[GW], and 102[km], whereas the lowest LCOH in [19] is achieved with 500[MW] at 200[km], with solar energy generation also contributing to the improved cost. For the second instance where LH2 shipping LCOH exceeds the range, this could be due to the different time periods used for calculation. In this study, the LCOH is based on a 30 year time period from 2020-2050. When considering projects starting at later times, while keeping yearly production constant, the LCOH decreases due to the discount and learning rates applied in future years. Therefore if we do not consider the costs in the time period for 2047 and below, the LCOH would be estimated as the cost of delivered hydrogen, which is 4.89[€/kg] for LH2 shipping in 2050, which does fall within the range. Other sources suggest competition will be able to provide costs below 2[€/kg] in 2050 [58][33]. Due to this, cost developments should be monitored when ultimately determining the strategy.

Year	Configuration	LCOH min [€/kg]	LCOH max [€/kg]	LCOH Model [€/kg]	Delivered H2 Cost [€/kg]
2025*	GH2 pipe	4.42	9.12	4.05	4.06
	LH2 ship	4.03	20.97	6.52	6.64
	NH3 ship	5.15	11.60	5.29	5.3
	NH3 pipe	5.20	10.90	5.49	5.5
2035	GH2 pipe	3.44	7.10	4.05	3.57
	LH2 ship	2.58	9.74	6.52	5.87
	NH3 ship	3.39	8.26	5.29	4.8
	NH3 pipe	3.44	7.67	5.49	4.98
2050	GH2 pipe	2.33	6.27	4.05	3.19
	LH2 ship	1.32	5.53	6.52	4.89
	NH3 ship	1.80	6.41	5.29	4.41
	NH3 pipe	1.83	5.98	5.49	4.58

Table 4.20: Comparison of scenario results from [19] to model results from current analysis. *For the Year 2025 row, the delivered cost of H2 results from the model are actually for the time step of 2026 due to the manner in which the time steps are divided for the modeling results.

Based on the research from [59], it is suggested that utilizing offshore wind for the energy generation in a hydrogen production context requires a selling price of 5.5[$/kg], or 5.09[€/kg], to turn a profit. Comparing the model results for delivered hydrogen cost per kg each time step to the suggested price from [59], it can be seen in Figure 4.6 that each configuration achieves a cost below this mark, however at different rates. Referring to the results tables for each scenario provided in Section 4.3, it can be determined that for j=1 this is 2029 at 5.08[€/kg], for j=2 this is 2047 at 5.07[€/kg], for j=3 this is from 2020 with 4.81[€/kg], and for j=4 this is 2035 with 4.98[€/kg].

4.7. Evaluation based on Criteria Framework

Having looked at the results from the techno-economic model, the supply chain configurations can be evaluated against the previously established criteria to contextualize the supply chain deployment at a higher level. Some of the criteria can be evaluated directly based on quantitative model results, while others are based on literature and qualitative reasoning. For the economic criteria, the LCOH values from the model can be used, while the CRI values must be considered based on literature. The technological criteria of TRL and EoI, the environmental criterion of CO2 reduction should also be determined based on literature and decisions made for the configurations in the modeling. The geopolitical criteria of access can be based on model results, while regulations again based on literature.

4.7.1. Economic

The LCOH values for the configurations are available from the calculated model scenarios. These are 5.290[€/kg] for j=1, 6.521[€/kg] for j=2, 4.052[€/kg] for j=3, and 5.494[€/kg] for j=4. As such, the GH2 pipeline ranks 1st, followed by the NH3 shipping configuration, the NH3 pipeline configuration, and finally the LH2 shipping configuration, as summarized in Table 4.23. Although it is possible that a variation in certain cost components can affect the LCOH and thus change the ranking of the configurations (such as the transport and storage costs illustrated in Figure 4.11), the cost difference required is significant and therefore the LCOH values are taken directly from the results for the ranking.

The CRI requires the TRL value to be at least 8 for a CRI of 2, and 9 for a CRI of 2-6 (as can be seen in Figure 3.3). The CRI for shipping of ammonia is at the highest level of 6, due to ammonia being a commodity in an industry which is commercially mature, being used primarily for fertilizers and chemicals. The infrastructure, regulations, and commercial models are well-established globally. The shipping of liquid hydrogen has a TRL below 8, therefore CRI is limited to 1. The business models, cost structures, and supporting infrastructures are still being developed. The pipeline for transporting gaseous hydrogen is at a level between 4-5, since instances of gaseous hydrogen pipelines exist for refining and chemical plants, however widespread application of long-distance pipelines is still in the process of being scaled up. While commercial applications do exist, they are not at the stage where they would be competitive in the energy industry. As the regulatory frameworks and new projects become introduced, such as the European Hydrogen Backbone, the CRI is expected to increase in the years leading up to 2050. The ammonia pipeline can be expected to have a CRI of 5-6, with thousands of kilometers of onshore ammonia pipelines already existing in the United States. However, subsea pipelines are not as mature, therefore the commercial readiness is not at a maximum yet.

4.7.2. Technological

The TRL for ammonia shipping is 9 according to [60], considering how this transport and energy combination has been applied in the fertilizer industry, where ammonia is used for acquiring nitrogen, with onboard storage being at a commercially successful level. The only difference is transporting ammonia for the purpose of energy, and generating the energy in a green manner, however this should not require equipment which is not already available. Conversion of hydrogen to ammonia is also presently ready using the Haber-Bosch process [55]. In contrast, the shipping of liquid hydrogen is far earlier in it's stages of development. Sources suggest a TRL of 6 [38], and 7 [41]. There have been developments such as with the first LH2 ship called the Suiso Frontier by Kawasaki Heavy Industries in 2019 [47], however the challenges of low temperature storage, low energy density, boil-off, terminal infrastructure, leak detection and safety are still holding this configuration back. Regarding the gaseous hydrogen pipeline, sources suggest that onshore pipelines are at a TRL of 9 [39]. GH2 pipelines do not come without challenges, notably material corrosion (also known as hydrogen embrittlement), high pressures, leak detection, as well as installation complexity. Finally, the ammonia pipeline is also at a level of 9 for onshore according to [39]. Similarly to the ammonia shipping case, the industrial application for transporting ammonia in order to satisfy fertilizer demand is currently applied in industry.

Focusing on the EoI criterion, shipping typically requires less infrastructural development in comparison to pipelines. In shipping it would be possible to charter vessels to transport the product, not requiring to consider construction of proprietary transport vessels. A pipeline would require a complete procedure for deployment, from surveying and design to construction. Regarding energy medium, ammonia shipping does not require extreme temperatures for storage, and therefore would be easier to imple-

ment and control than liquid hydrogen. This reasoning would suggest that ammonia shipping is the easiest to implement. Liquid hydrogen is also transported by ship in the considered configurations, however as mentioned previously, vessels with the ability to store LH2 have not yet been commercially demonstrated. Ammonia subsea pipelines have been applied already, and again require less extreme temperatures to maintain the product, therefore ammonia pipelines should be ranked 2nd in EoI. Considering gaseous hydrogen also does not require such extreme conditions, therefore ranking above the LH2 configuration.

4.7.3. Environmental

Considering CO2 emission reduction, scope 1, 2 and 3 emissions can be considered when evaluating each configuration. Scope 1 pertains to the direct emissions from using fuel in operation of the project. Scope 2 are indirect emissions due to the electricity, with the emissions coming from the fuel used to provide this electricity. Finally, scope 3 emissions pertain to the emissions which exist further upstream and downstream in relation to the project. For the ammonia shipping case, the scope 1 emissions are assumed to be due to the fuel used by the vessels transporting the hydrogen. This assumption remains the same for the liquid hydrogen configuration. For the pipelines for gaseous hydrogen and ammonia configurations, the energy used for the compression and pumping stations are considered respectively. Regarding scope 2 emissions, the energy used for conversion processes is considered, and storage for j=1 and j=2. Finally in scope 3 we consider the reconversion emissions at the terminal downstream, and materials used to construct the pipelines.

For scope 1, the specifications of a fully refrigerated LPG carrier was considered from International Contract Engineering Marine Design [14] for transporting ammonia, the Suiso Frontier vessel from Kawasaki Heavy Industries [28] for transporting liquid hydrogen, for the gaseous hydrogen pipeline 2 separate calculations were done from [6] and [15], and finally for the hydrogen pipeline the values from [6] were considered. For scope 2, the values from [49] were taken for the power consumption of conversion and storage. Lastly, in scope 3 the reconversion power was based on the conversion, and scaled by 13/20 due to the number of units in the scenarios. For pipeline materials, X70 API 5L steel was considered, with the wall thickness matching the diameter based on the API 5L code. All of the values are summarized in Table 4.21, with all the estimated values being yearly emissions of CO2 in [ktCO2] for the given demand, with the exception of pipeline materials in scope 3 being a one-off cost.

Some of the emissions have the potential to be eliminated if fossil fuels are not used as the energy source. This leads the totals in Table 4.21 in the last 2 columns. The total gray energy is the sum of all of the previous emissions, with the total green column excluding values which are assumed to be substituted by green energy sources. For j=1, the vessels chosen for the estimations were diesel powered, therefore not being able to be substituted by green sources currently, however it is possible that this will not be the case forever. Similarly, emissions associated with the steel manufacturing in j=3 and 4 are not removed in the green case since currently most steel manufacturing does not use green energy sources, and these are one-off emissions. If the project were started at a future point where steel manufacturing is sustainably sourced, this value would be subject to change.

The results from the estimations in Table 4.21 suggest that in the gray case j=3 would lead to least emissions, followed by j=4, j=1, and finally j=2. In the green case the ranking would switch, with j=1 being the lowest emission configuration, followed by j=3 and j=4, and finally j=2. In both cases liquid hydrogen requires the largest amount of emissions, likely due to the high energy cost of refrigeration in storage. Additionally, the LH2 vessel has a much smaller capacity than the ammonia vessel, therefore significantly more trips are required. For the final values for the ranking the gray energy total is assumed, since in theory all of the energy could be greenly sourced eventually, however the gray case provides a greater idea about how much possible emissions could be created (or potentially saved).

Scenario		Scope 1 [ktCO2]	Scope 2 [ktCO2]	Scope 3 [ktCO2]	Total Grey [ktCO2]	Total Green [ktCO2]
j=1	NH3 ship	2.28	277	171	450	2.28
j=2	LH2 ship	14.4	682	419	1,115	14.4
j=3	GH2 pipe	32.7 [15] 23.8 [6]	-	2.8	35.5	2.8*
j=4	NH3 pipe	10.1	264	174* (incl. 2.8)	448	2.8

Table 4.21: CO2 Emission Estimations for each scope of every scenario considered. *The scope 3 emissions in the pipeline have a one-off emission of 2.8[ktCO2] for the materials, and a yearly recurring 171[ktCO2/y] for the reconversion.

4.7.4. Geopolitical

The access to a location based on political borders of the North-Sea can be discussed by overlaying the points in study over the a map of the borders as shown in Figure 4.18. Looking at the business case from the perspective of the government of the Netherlands, the simplest location access would come from within the Dutch Exclusive Economic Zone (EEZ). The coordinates of the locations investigated in the study which overlap with this Dutch EEZ are listed in Table 4.22. Unfortunately, none of the optimal solutions found in Section 4.3 are within this EEZ, and location 7 and 8 are onshore. In fact the shipping optimal location (57.35, 7.78) is found in the Norwegian EEZ, while the pipeline optimal location (54.35, 6.78) is found in the German EEZ. Unless some sort of agreement can be reached for permitting the government of the Netherlands to make use of the external EEZs, the only feasible locations for a Dutch North Sea case would be the ones within the Dutch EEZ territory. In order to quantify the access criterion, the LCOH results from the model can be considered when looking at locations strictly within the Dutch EEZ region. This results in 5.612[€/kg] for j=1, 6.943[€/kg] for j=2, 4.195[€/kg] for j=3, and 5.613[€/kg] for j=4. All of the lowest LCOH values are found at (54.35, 4.78), or location 4 on Figure 4.18.

Considering the regulatory frameworks in place to support the hydrogen supply chain, the ammonia medium has already been commercially transported by ship and by pipeline, with existing standards and regulation for such endeavors. In contrast, regulation surrounding commercial transport of liquid and gaseous hydrogen has not been fully established. Considering the existing frameworks, the EU follows the IGC code for ships carrying liquefied gases in bulk from the International Maritime Organization (IMO) [54]. Pipelines on the other hand have design codes to ensure safety, as listed in [4], including ASME B31, ISO DIS 13623, API RP1111, DNV Pipeline Rules, and ABS 2000 Guide. The regulatory framework is being updated, with IMO having made progress on drafting guidelines for hydrogen and ammonia fuel in shipping for safety [73]. The EU is supporting electrolysis scale-up by allowing the signing of ”power purchase agreements”, to ensure that hydrogen productions matches the scale of electricity generation capacities [70]. This should benefit each configuration equally. Ammonia is classified as a hazardous material, therefore adherence to the international convention on the prevention of pollution from ships (MARPOL) is required. For gaseous hydrogen, there is significant support in the EU Hydrogen Strategy, with the initiative for establishing infrastructure through the hydrogen backbone [3]. Ammonia pipelines are not as common in Europe as in the U.S., however the pipeline regulations covering hazardous material handling apply here. Liquid hydrogen shipping faces the greatest number of regulatory gaps, due to the technology level being relatively lower. Overall, ammonia by ship has the strongest regulatory framework support currently, followed by GH2 pipelines, due to there being a strategic focus on infrastructure development within the EU, then NH3 pipeline which has regulations in place but does not have the same strategic support as gaseous hydrogen, and finally liquid hydrogen shipping which is still emerging.

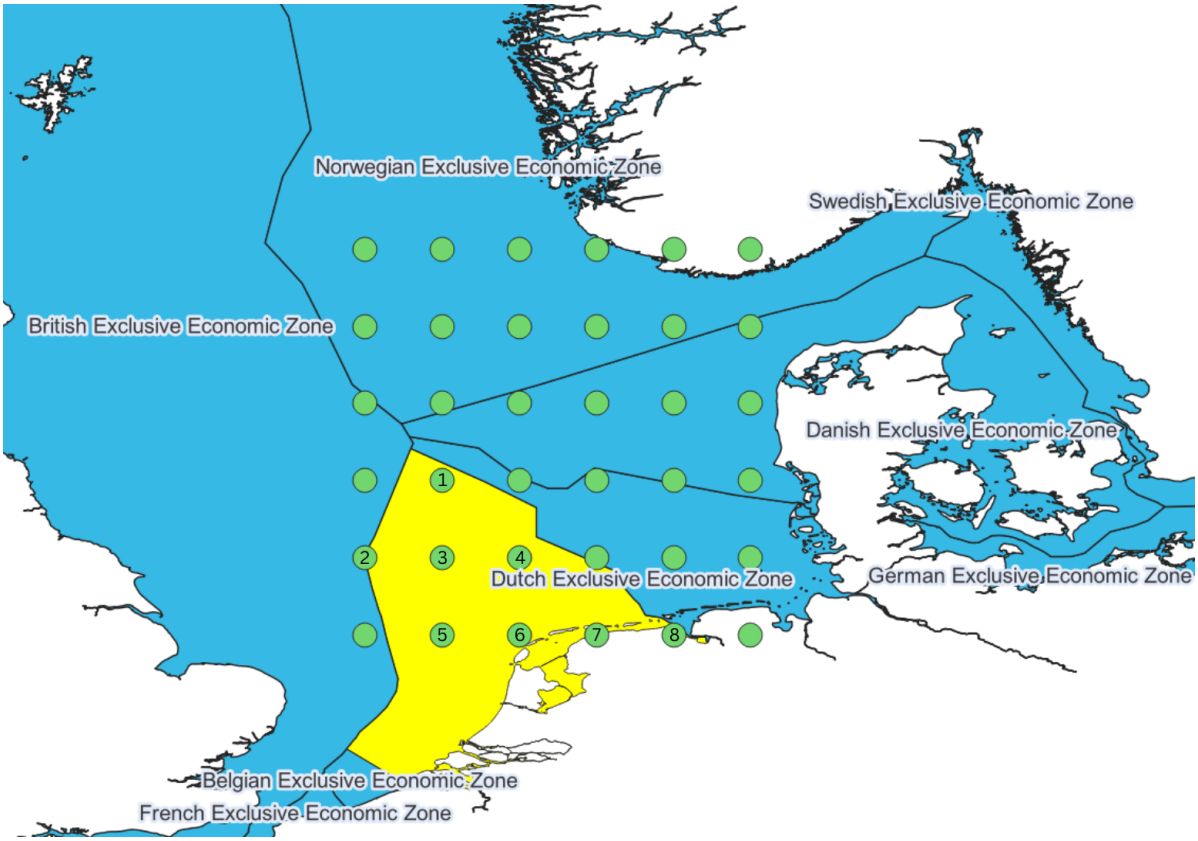

Figure 4.18: North-Sea map including political borders from [29], with green points added to mark studied locations and yellow region highlighting the Dutch Exclusive Economic Zone. Numbered marks represent locations within the Dutch EEZ.

Location	Latitude	Longitude
1	55.35	3.78
2	54.35	2.78
3	54.35	3.78
4	54.35	4.78
5	53.35	3.78
6	53.35	4.78
7	53.35	5.78
8	53.35	6.78

Table 4.22: Coordinates of locations within Dutch EEZ

4.8. Strategy and Implications

In this section the results are compiled and re-formulated into a coherent strategy for deployment of the supply chain, considering feasible outcomes. Such a feasible strategy is conditional on several factors which form assumptions in the research. The factors are examined in Section 4.6, with most relevant ones summarized as follows:

- Weather conditions
- Farm Layout
- Technical and economic parameters
- Hydrogen demand
- Grid connectivity and electricity pricing
- Location availability
- Water depth
- Transport distance

Written concisely, weather conditions are based on data from a single year, with a layout modeled at a discrete point, cost and technology parameters are based on various sources, hydrogen demand is assumed constant, grid connectivity and electricity pricing are excluded, all locations are assumed to be available, at water depths under 60m and transport distances based on a geodesic.

Under the assumptions made, the findings of the optimization model output suggest that the GH2 pipeline provides the lowest LCOH out of the configurations, at 4.052[€/kg]. This is followed by NH3 shipping at 5.29[€/kg], then NH3 pipeline at 5.494[€/kg], and finally LH2 shipping with the highest LCOH of 6.521[€/kg]. The optimal location for the shipping configurations matched the location with greatest weather availability for power generation at a distance of 440[km], while the pipeline configurations were closer to the shore at 102[km] from the demand location. The largest cost component for all of the scenarios in every time step was the wind turbine cost parameter, making up between 33-51[%] of the total cost. The conversion costs were another significant component of the total costs across the scenarios, which is why gaseous hydrogen appears to exhibit lower LCOH. When including the additional solution of the solar platforms, the model found that the cost can be reduced by 0.015[€/kg] on average. If ammonia is considered as the final demand medium, eliminating the reconversion process and associated costs, a decrease of 0.147[€/kg] and 0.160[€/kg] in LCOH can be observed for shipping and pipeline respectively.

Considering the sensitivity, in every scenario the LCOH is most sensitive to wind costs, which can also be reasoned from the cost distribution results. Wind and solar costs, as well as PEM and desalination should benefit similarly from cost improvements, since all supply chain configurations make use of these technologies. The liquid hydrogen configuration could benefit from a reduction in transport and storage costs, which it is relatively most sensitive to. The reduction in costs in these components would affect the configuration independently. As such it was found that cost reduction of 65[%], 78[%], and 156[%] would be required (if both transport and storage are reduced equally) to match the LCOH of the ammonia pipeline configuration, the ammonia shipping configuration, and finally the gaseous hydrogen

pipeline configuration. Regarding conversion and reconversion, the ammonia shipping configuration would require a 91[%] decrease in both cost components to achieve equal LCOH to gaseous hydrogen pipeline configuration.

Considering the criteria framework, the NH3 shipping appears to be the dominant solution if all weights are equal, exhibiting best performance in 4 metrics, followed by GH2 pipeline with 3 metrics, and NH3 pipeline with 1 metric. Despite the model suggesting that the gaseous pipeline offers the lowest LCOH, if considering CRI, TRL, EoI and Regulatory frameworks, NH3 shipping appears to be preferable for deployment.

Depending on the weights of the criteria as they pertain to the entity responsible for supply chain deployment, the most feasible strategy can vary. Despite this fact, there are 2 strategies which clearly emerged as dominant based on the previous evaluation. As such, these 2 strategies are formulated based on the key decisions identified involving equipment, energy medium, transport mode, and logistics decisions.

The most feasible strategy for deployment under the given assumptions, one which results in most feasible outcomes for LCOH, CO2 emissions, and location access, consists of fixed wind and floating solar panels, and PEM electrolyzers for equipment. The energy medium is gaseous hydrogen, transported using a pipeline. Regarding logistics decisions, the energy generation location should be at coordinate (54.35, 6.78) at 102[km] from the shore. The network topology would be a considered a ”line”, from production location node to demand location node at the Eemshaven port. Allocation and routing are not considered in the current scope. This strategy is suitable if cost, emissions and/or accessibility permissions are significantly more important than the other criteria.

The most feasible strategy for deployment for satisfying outcomes of commercial and technological readiness, ease of implementation, and existing regulation, would consist of fixed wind, floating solar panels, PEM electrolyzers, conversion and reconversion devices as well as storage tanks on the FPSO regarding equipment. The energy medium would be liquid ammonia, transported with tanker vessels. Regarding logistics decisions, the production location would be at (57.35, 7.78) and demand location at Eemshaven, amounting to a distance of 440[km] from shore. The network topology would again be a ”line” from node to node, with allocation and routing being out of scope. This strategy offers the ability to pivot toward the ammonia market, offering flexibility for demand, and utilizing more established technologies regarding technological and commercial readiness. Additional flexibility is gained by not requiring (initially) expensive pipeline infrastructure.

Category	Criterion	Value j=1	Value j=2	Value j=3	Value j=4	Rank j=1	Rank j=2	Rank j=3	Rank j=4	Final
Economic	LCOH [€/kg]	5.29	6.52	4.05	5.49	2	4	1	3	j=3
	CRI	6	1	4-5	5-6	1	4	3	2	j=1
Technological	TRL	9	6-7	8-9	9	1	3	2	1	j=1 & j=4
	EoI	(Qualitative)				1	4	3	2	j=1
Environmental	CO2 Emissions [kt]	450	1,115	35.5	448	3	4	1	2	j=3
Geopolitical	Access [€/kg]	5.612	6.943	4.195	5.613	2	3	1	2	j=3
	Regulations	(Qualitative)				1	4	2	3	j=1

Table 4.23: Results for Framework for Evaluating Supply Chain Configurations

5

Conclusion

The GFPSO supply chain deployment strategy has been investigated for a North Sea business case. Relevant literature has been considered, a mathematical model was formulated and applied to the business case, the criteria for a feasible deployment strategy have been examined, and the key decisions for the strategies have been specified. Returning to the overarching aim denoted in Chapter 1, articulated as to ”Determine a feasible strategy for implementation of an offshore GFPSO supply chain by developing an accessible holistic techno-economic assessment model and applying it in a comprehensive business case spanning until 2050”, as well as the main research question ***What strategy could be used to deploy a GFPSO supply chain and ensure techno-economically feasible outcomes?***, the answer is discussed in the following section.

The strategies considered in the study were comprised of decisions on which equipment should be selected, as well as the location for energy collection to take place. The strategies shared similar equipment in terms of energy generation, namely offshore wind turbines and solar platforms as well as PEM electrolyzers. This is both due to model results and literature. The strategies varied in the selection of the energy vector and transport mode to deliver this vector to the demand node, selected as the port in Eemshaven in the North Sea case. These variations were compiled into 4 separate combinations to be studied as scenarios/configurations of the supply chain in the model. Additionally, the criteria which were not quantified by the model were estimated through qualitative lens. Whether the outcomes of a strategy satisfy techno-economic feasibility can depend on the value placed on the attributes by the entity responsible for implementing the supply chain, and as such the performed study offers insight into the relatively most feasible strategy within these competing configurations. Under the assumptions and given the limitations of the approach (including weather, hydrogen demand, location availability, and technological improvements of equipment), there were 2 strategies which emerged dominant after analysis.

The cost-driven solution involves the gaseous hydrogen energy medium, using pipeline transport from the farm to the port. In this strategy, the location of the farm would be in the South-East section of the studied region. This strategy offered stronger outcomes in the carbon emission and access criteria, as well as the final LCOH. If these attributes have significantly greater relative importance to the stakeholder, then such a solution is recommended, keeping in mind the key weaknesses of hydrogen embrittlement, greater upfront cost, and thus also lower flexibility of the FPSO asset.

The balanced approach involves ammonia as the energy vector produced, with shipping vessel for transport, with energy generation located in the North-East of the region. This strategy sacrifices overall LCOH in favor of the technological readiness of the equipment used, which has seen greater commercial application in reality. The risk is also reduced, since the asset can be moved to a different location if required, without losses due to immobility of the pipeline infrastructure. Additionally, there may be a possibility to tap into ammonia demand aside from hydrogen, however this requires further investigation.

If further cost reductions were to be prioritized for the elements in the strategy of the GFPSO supply

chain deployment, it would be recommended to emphasize the offshore wind turbines, as suggested by the cost distributions and sensitivity analysis. Additionally, if conversion costs can be sufficiently reduced relative to other costs in the supply chain, the decision to utilize ammonia as the vector becomes more strategically attractive.

The recommendations extracted from the study can be summarized in the following key points:

- If an established demand, flexibility, early start, and technological maturity are prioritized then the deployment strategy involving ammonia shipping has more preferable criteria outcomes.
- A reduction of the conversion process costs for hydrogen to ammonia would improve competitiveness of ammonia shipping as an alternative strategy.
- If cost-competitiveness, emission reductions, and geopolitical access are prioritized, then the strategy should involve the gaseous hydrogen pipeline configuration.
- Liquid hydrogen transport and storage technologies need significant improvement in cost before they can enable a competitive supply chain. The cost developments should continue to be monitored.

5.1. Research Question Evaluation

SQ1. What key decisions must be made in a GFPSO supply chain deployment strategy?
The corroborative knowledge type in this sub-question is descriptive. The key decisions involved in the strategy have been described in Section 3.1.1, ensuring that the answer is suitable to the question. A strategy is typically defined as a plan of action for a long-term aim, and the key decisions pertain to equipment, energy medium, transport mode, and logistics.

SQ2. What criteria can be used to evaluate the success of the GFPSO deployment strategy in a business case?
The knowledge type is descriptive in this sub-question as well, thus a description of the criteria is presented. The criteria are categorized by economic, technological, environmental, and geopolitical considerations, and are discussed in Section 3.1.2.

SQ3. What model can be used to easily, effectively, and efficiently determine a realistic techno-economic feasibility at varying locations on a large-scale?
The model proposed by [49] can be modified, as shown in Section 3.2, to investigate techno-economic feasibility of supply chain configurations at varying locations. The model reduces the number of variables and compiles parameters into matrices, improving the ease of model use. The effectiveness is verified through matching previous to current model behavior, ensuring variables exhibit values corresponding to expectations, as well as validating further contributions against literature. The efficiency is demonstrated through the reduction in computation time by a factor of approximately 100, due to lifting quadratic constraints and parameterizing certain variables, as well as reducing constraints. This speed increase enables the comparison of supply chain configurations at several spatial and temporal dimensions in a reasonable amount of time.

SQ4. To what extent can additional solutions enhance techno-economic potential of GFPSO?
The impact on LCOH due to the inclusion of solar platforms was described in Section 4.6, with an average LCOH reduction of 0.015[€/kg] observed through modeling (by constraining solar platforms to zero in the optimization). Additionally, gaseous pipeline and ammonia pipeline were introduced as solutions to deliver hydrogen in the supply chain. In comparison to the liquid hydrogen shipping configuration, the LCOH of GH2 pipeline showed a reduction of 2.469[€/kg], while NH3 pipeline presented a reduction of 1.027[€/kg]. For the ammonia shipping solution, only the gaseous hydrogen pipeline provided a reduction, that being 1.238[€/kg].

SQ5. Which transport mode and energy medium combinations offer optimal outcomes?
Gaseous hydrogen energy medium with the pipeline transport mode in the configuration exhibited the lowest costs at optimal locations in the investigated scenarios.

SQ6. What are the preferable scenarios for deployment of a GFPSO?
Considering the criteria framework, the most preferable scenario involves the NH3 shipping configuration based on CRI, TRL, EoI and regulations, followed by the GH2 pipeline configuration based on the LCOH, CO2 emissions, and geopolitical access. Ammonia pipeline is performs equally well on its TRL value compared to the shipping counterpart, however is outperformed in each other metric. Finally, LH2 shipping is the least preferable in terms of the criteria considered.

5.2. Future Research

Due to the limitations of the model, as well as the uncertainties emerging from renewable energy generation, production technologies, hydrogen demand, and further innovation in the energy transition, additional research ought to be performed to develop sufficient understanding for GFPSO supply chain deployment. The NPV could be calculated for each scenario by modeling revenue streams through price forecasting. The price can be applied to the production output from the supply chain to determine the monetary value of the investment based on cash flows. There was an attempt to incorporate intermediate battery storage in the optimization model, however completion of this additional solution became unreasonable for the scope of this project. As such, it is suggested to investigate this solution in future research to see the potential of load balancing with a battery in a GFPSO context. It is recommended to perform such an investigation with a model external to the model used here. As ammonia and hydrogen as fuel for maritime vessels progresses in technology and adoption increases, the potential for tapping into this demand should be investigated and the possibility of strategic advantages of an GFPSO supply chain should be evaluated. While PEM was chosen due to support in prior literature, the current large scale hydrogen energy projects make use of AWE. This technology could be substituted into the model by changing the electrolyzer cost parameter, and the other parameters affected by the new technological parameters (such as storage and FPSO vessel size). Based on literature, PEM appears to have advantages over AWE making it preferable, however this could be modeled explicitly to have greater confidence. A demand-based model should be researched to gain a further understanding of how a GFPSO supply chain would function in the renewable hydrogen market. Other regions could be considered aside from the North Sea, enabling a business case which may reveal different results for configurations, and possibly different wind-solar unit ratios.

References

[1] E. B. Agyekum, C. Nutakor, A. M. Agwa, and S. Kamel. “A critical review of renewable hydrogen production methods: factors affecting their scale-up and its role in future energy generation”. In: *Membranes* 12.2 (2022), page 173.

[2] ARENA. *Commercial Readiness Index for Renewable Energy Sectors*. 2014. URL: https://arena.gov.au/assets/2014/02/Commercial-Readiness-Index.pdf.

[3] European Hydrogen Backbone. *The European Hydrogen Backbone (EHB) initiative*. 2024. URL: https://ehb.eu/.

[4] Y Bai. *Subsea pipelines and risers*. Elsevier Ltd, 2005.

[5] M. Ball and M. Weeda. “The hydrogen economy–vision or reality?” In: *International Journal of Hydrogen Energy* 40.25 (2015), pages 7903–7919.

[6] J. R. Bartels. *A feasibility study of implementing an Ammonia Economy*. Iowa State University, 2008.

[7] S. Baufumé et al. “GIS-based scenario calculations for a nationwide German hydrogen pipeline infrastructure”. In: *International Journal of Hydrogen Energy* 38.10 (2013), pages 3813–3829. ISSN: 0360-3199. DOI: https://doi.org/10.1016/j.ijhydene.2012.12.147. URL: https://www.sciencedirect.com/science/article/pii/S0360319913000670.

[8] G. Brändle, M. Schönfisch, and S. Schulte. “Estimating long-term global supply costs for low-carbon hydrogen”. In: *Applied Energy* 302 (2021), page 117481. ISSN: 0306-2619. DOI: https://doi.org/10.1016/j.apenergy.2021.117481. URL: https://www.sciencedirect.com/science/article/pii/S0306261921008667.

[9] G. Calado, R. Castro, A. J. Pires, and M.J. Marques. “Assessment of hydrogen-based solutions associated to offshore wind farms: The case of the Iberian Peninsula”. In: *Renewable and Sustainable Energy Reviews* 192 (2024), page 114268.

[10] M. Carmo, D. L. Fritz, J. Mergel, and D. Stolten. “A comprehensive review on PEM water electrolysis”. In: *International Journal of Hydrogen Energy* 38.12 (2013), pages 4901–4934. ISSN: 0360-3199. DOI: https://doi.org/10.1016/j.ijhydene.2013.01.151. URL: https://www.sciencedirect.com/science/article/pii/S0360319913002607.

[11] CFI. *Levelized Cost of Energy (LCOE)*. 2022. URL: https://corporatefinanceinstitute.com/resources/valuation/levelized-cost-of-energy-lcoe/.

[12] European Commission, Joint Research Centre, and D. Tarvydas. *The role of hydrogen in decarbonisation energy scenarios – Views on 2030 and 2050*. Publications Office of the European Union, 2022. DOI: doi/10.2760/899528.

[13] Marine Environment Protection Committee. *RESOLUTION MEPC.377(80)*. 2023. URL: https://wwwcdn.imo.org/localresources/en/OurWork/Environment/Documents/annex/MEPC%2080/Annex%2015.pdf.

[14] International Contract Engineering Marine Desing. *84,000m3 FULLY REFRIGERATED LPG CARRIER*. 2018. URL: https://www.icedesign.info/wp-content/uploads/ICE-84000-cu-m-LPG-Carrier-Design-2018.pdf.

[15] N. G. Díez, S. van der Meer, J. Bonetto, and A. Herwijn. *North Sea Energy: Technical assessment of Hydrogen transport, compression, processing offshore*. 2020. URL: https://north-sea-energy.eu/static/7ffd23ec69b9d82a7a982b828be04c50/FINAL-NSE3-D3.1-Final-report-technical-assessment-of-Hydrogen-transport-compression-processing-offshore.pdf.

[16] Q. V. Dinh, P. H. Todesco Pereira, V. Nguyen Dinh, A. J. Nagle, and P. G. Leahy. “Levelised cost of transmission comparison for green hydrogen and ammonia in new-build offshore energy infrastructure: Pipelines, tankers, and HVDC”. In: *International Journal of Hydrogen Energy* 62 (2024), pages 684–698. ISSN: 0360-3199. DOI: https://doi.org/10.1016/j.ijhydene.2024.03.066. URL: https://www.sciencedirect.com/science/article/pii/S0360319924008553.

[17] Solar Duck. *Merganser Pilot*. 2024. URL: https://solarduck.tech/merganser-pilot/.

[18] A. Durakovic. “Deepest Ever Fixed-Bottom Wind Turbine Foundation Stands Offshore Scotland”. In: *offshoreWIND.biz* (2023).

[19] A. Giampieri, J. Ling-Chin, and A. P. Roskilly. “Techno-economic assessment of offshore wind-to-hydrogen scenarios: A UK case study”. In: *international journal of hydrogen energy* 52 (2024), pages 589–617.

[20] A. Gonzalez-Arceo et al. “Techno-economic assessment of far-offshore hydrogen-carrying energy vectors off the Iberian Peninsula”. In: *Energy Conversion and Management* 300 (2024), page 117915.

[21] GEBCO Compilation Group. *GEBCO 2024 Grid*. 2024. DOI: doi:10.5285/1c44ce99-0a0d-5f4f-e063-7086abc0ea0f.

[22] Hatenboer-Water. URL: https://www.hatenboer-water.com/products/reverse-osmosis-proteus/.

[23] M. Héder. “From NASA to EU: the evolution of the TRL scale in Public Sector Innovation”. In: *The Innovation Journal* 22.2 (2017), pages 1–23.

[24] H. Hersbach et al. *ERA5 hourly data on single levels from 1940 to present*. 2023. DOI: https://doi.org/10.24381/cds.adbb2d47. (Visited on 06/28/2024).

[25] O. S. Ibrahim, A. Singlitico, R. Proskovics, S. McDonagh, C. Desmond, and J. D. Murphy. “Dedicated large-scale floating offshore wind to hydrogen: Assessing design variables in proposed typologies”. In: *Renewable and sustainable energy reviews* 160 (2022), page 112310.

[26] IEA. *The Future of Hydrogen*. IEA, 2019. URL: https://www.iea.org/reports/the-future-of-hydrogen.

[27] IEA. *The Role of Low-Carbon Fuels in the Clean Energy Transitions of the Power Sector*. Paris: OECD Publishing Éditions OCDE, 2021. ISBN: 9789264533684. DOI: 10.1787/a92fe011-en. URL: https://doi.org/10.1787/a92fe011-en.

[28] Kawasaki Heavy Industries. *World’s First Liquefied Hydrogen Carrier SUISO FRONTIER Launches Building an International Hydrogen Energy Supply Chain Aimed at Carbon-free Society*. 2019. URL: https://global.kawasaki.com/en/corp/newsroom/news/detail/?f=20191211_3487.

[29] Flanders Marine Institute. Maritime Boundaries Geodatabase, version 12. 2023. DOI: https://doi.org/10.14284/628. URL: https://www.marineregions.org/.

[30] Yara International. *The world’s first clean ammonia-powered container ship*. 2023. URL: https://www.yara.com/corporate-releases/the-worlds-first-clean-ammonia-powered-container-ship/.

[31] IPOC. “Climate change 2007: The physical science basis”. In: *Agenda* 6.07 (2007), page 333.

[32] J. Janissen. *Energy transition at mixed business parks: A case study and guideline for consultants, government officials and entrepreneurs*. 2024. URL: http://resolver.tudelft.nl/uuid:8ebbd0b5-5faa-4ebc-8697-f03d10317b9e.

[33] J. L.L.C.C. Janssen, M. Weeda, R. J. Detz, and B. van der Zwaan. “Country-specific cost projections for renewable hydrogen production through off-grid electricity systems”. In: *Applied Energy* 309 (2022), page 118398. ISSN: 0306-2619. DOI: https://doi.org/10.1016/j.apenergy.2021.118398. URL: https://www.sciencedirect.com/science/article/pii/S0306261921016342.

[34] P. Kaczmarek. *GFPSO Supply Chain Model*. 2024. URL: https://github.com/PiotrKaczmarekEng/PiotrThesis.

[35] G. K. Karayel and I. Dincer. “A study on green hydrogen production potential of Canada with onshore and offshore wind power”. In: *Journal of Cleaner Production* 437 (2024), page 140660.

[36] G. K. Karayel and I. Dincer. “Green hydrogen production potential of Canada with solar energy”. In: *Renewable Energy* 221 (2024), page 119766.

[37] A. Kim, H. Kim, C. Choe, and H. Lim. “Feasibility of offshore wind turbines for linkage with onshore green hydrogen demands: A comparative economic analysis”. In: *Energy Conversion and Management* 277 (2023), page 116662. ISSN: 0196-8904. DOI: https://doi.org/10.1016/j.enconman.2023.116662. URL: https://www.sciencedirect.com/science/article/pii/S0196890423000080.

[38] A. Kim, Y. Yoo, S. Kim, and H. Lim. “Comprehensive analysis of overall H2 supply for different H2 carriers from overseas production to inland distribution with respect to economic, environmental, and technological aspects”. In: *Renewable Energy* 177 (2021), pages 422–432. ISSN: 0960-1481. DOI: https://doi.org/10.1016/j.renene.2021.05.127. URL: https://www.sciencedirect.com/science/article/pii/S0960148121008107.

[39] H. Kim, A. Kim, M. Byun, and H. Lim. “Comparative feasibility studies of H2 supply scenarios for methanol as a carbon-neutral H2 carrier at various scales and distances”. In: *Renewable Energy* 180 (2021), pages 552–559. ISSN: 0960-1481. DOI: https://doi.org/10.1016/j.renene.2021.08.077. URL: https://www.sciencedirect.com/science/article/pii/S0960148121012453.

[40] U. Krien, G. Plessmann, S. Günther, B. Schachler, S. Boschand, and C. Kaldemeyer. *feedinlib (oemof) - creating feed-in time series - v0.0.12*. Zenodo. 2019. DOI: 10.5281/zenodo.2554102.

[41] H. Lee, G. Roh, S. Lee, C. Choung, and H. Kang. “Comparative economic and environmental analysis of hydrogen supply chains in South Korea: Imported liquid hydrogen, ammonia, and domestic blue hydrogen”. In: *International Journal of Hydrogen Energy* 78 (2024), pages 1224–1239. ISSN: 0360-3199. DOI: https://doi.org/10.1016/j.ijhydene.2024.06.367. URL: https://www.sciencedirect.com/science/article/pii/S0360319924026077.

[42] J. Lee, B. Park, K-.H. Kim, and W.-S. Ruy. “Multi-objective optimization of liquid hydrogen FPSO at the conceptual design stage”. In: *International Journal of Naval Architecture and Ocean Engineering* 15 (2023), page 100511. ISSN: 2092-6782. DOI: https://doi.org/10.1016/j.ijnaoe.2022.100511. URL: https://www.sciencedirect.com/science/article/pii/S2092678222000772.

[43] S. Lensink and I. Pisca. *WIND OP ZEE*. 2018. URL: https://www.rvo.nl/sites/default/files/2022-11/Rekenmodel-basisbedrag-Wind-op-zee.xlsx.

[44] S. Lensink and I. Pisca. *Costs of offshore wind energy 2018*. 2019. URL: https://www.pbl.nl/en.

[45] A. Van den Noort M. Vos J. Douma. 2020. URL: https://www.gie.eu/wp-content/uploads/filr/2598/DNV-GL_Study-GLE-Technologies-and-costs-analysis-on-imports-of-liquid-renewable-energy.pdf.

[46] MARIN. *Beyond the horizon: Strategy 2022-2025*. 2022. URL: https://www.marin.nl/en/about/strategy.

[47] Baird Maritime. *VESSEL REVIEW | Suiso Frontier – Japanese LH2 carrier sets the pace in hydrogen transport*. 2021. URL: https://www.bairdmaritime.com/shipping/gas/vessel-review-suiso-frontier-japanese-lh2-carrier-sets-the-pace-in-hydrogen-transporth.

[48] A. Martinez and G. Iglesias. “Mapping of the levelised cost of energy from floating solar PV in coastal waters of the European Atlantic, North Sea and Baltic Sea”. In: *Solar Energy* 279 (2024), page 112809. ISSN: 0038-092X. DOI: https://doi.org/10.1016/j.solener.2024.112809. URL: https://www.sciencedirect.com/science/article/pii/S0038092X24005048.

[49] T. Melles. *Global Techno-Economic Feasibility of Far Offshore Green Hydrogen Production towards 2050*. 2024. URL: http://resolver.tudelft.nl/uuid:a6873511-f046-423a-8378-db2b1cf89c30.

[50] United Nations. *Convention on the Continental Shelf*. Geneva. 1958. URL: http://treaties.un.org/Pages/CTCs.aspx (visited on 09/04/2024).

[51] R.M. Nayak-Luke, C. Forbes, Z. Cesaro, R. Bañares-Alcántara, and K.H.R. Rouwenhorst. “Chapter 8 - Techno-Economic Aspects of Production, Storage and Distribution of Ammonia”. In: *Techno-Economic Challenges of Green Ammonia as an Energy Vector*. Edited by A. Valera-Medina and R. Banares-Alcantara. Academic Press, 2021, pages 191–207. ISBN: 978-0-12-820560-0. DOI: https://doi.org/10.1016/B978-0-12-820560-0.00008-4. URL: https://www.sciencedirect.com/science/article/pii/B9780128205600000084.

[52] Government of the Netherlands. *Offshore wind energy*. 2024. URL: https://www.government.nl/topics/renewable-energy/offshore-wind-energy.

[53] thyssenkrupp nucera. *Green Hydrogen Solutions*. 2024. URL: https://thyssenkrupp-nucera.com/green-hydrogen-solutions/.

[54] International Maritime Organization. *IGC Code*. 1986. URL: https://www.imo.org/en/ourwork/safety/pages/igc-code.aspx (visited on 10/28/2024).

[55] D. D. Papadias, J.-K. Peng, and R. K. Ahluwalia. “Hydrogen carriers: Production, transmission, decomposition, and storage”. In: *International Journal of Hydrogen Energy* 46.47 (2021). ISSN: 0360-3199. DOI: https://doi.org/10.1016/j.ijhydene.2021.05.002. URL: https://www.sciencedirect.com/science/article/pii/S0360319921016815.

[56] Algemeen Nederlands Persbureau. *Shell cuts 200 jobs in renewable energy branch*. 2023. URL: https://nltimes.nl/2023/10/26/shell-cuts-200-jobs-renewable-energy-branch.

[57] S. Ramakrishnan, M. Delpisheh, C. Convery, D. Niblett, M. Vinothkannan, and M. Mamlouk. “Offshore green hydrogen production from wind energy: Critical review and perspective”. In: *Renewable and Sustainable Energy Reviews* 195 (2024), page 114320.

[58] Goldman Sachs Research. *Green Hydrogen: The Next Transformational Driver of the Utilities Industry*. Technical report. Goldman Sachs, 2020. URL: https://www.goldmansachs.com/insights/goldman-sachs-research/green-hydrogen.

[59] C. Ríos, P. Molina, C. Martínez de León, and J.J. Brey. “Simulation of the optimal plant size to produce renewable hydrogen based on the available electricity”. In: *International Journal of Hydrogen Energy* 52 (2024), pages 1325–1337.

[60] A. S. Rojas, P. Miltrup, and S. Rueda. *Ammonia Transport & Storage*. Technical report. German Federal Ministry for Economic Affairs and Climate Action (BMWK), 2024. URL: https://ptx-hub.org/wp-content/uploads/2024/01/International-PtX-Hub_202401_Ammonia-transport-and-storage.pdf.

[61] RVO.nl. *Holland Hydrogen 1*. 2022. URL: https://data.rvo.nl/subsidies-regelingen/projecten/holland-hydrogen-1.

[62] E. Saborit, E. García-Rosales Vazquez, M. D. Storch de Gracia Calvo, G. M. Rodado Nieto, P. Martínez Fondón, and A. Abánades. “Alternatives for Transport, Storage in Port and Bunkering Systems for Offshore Energy to Green Hydrogen”. In: *Energies* 16.22 (2023), page 7467.

[63] N. Salmon and R. Bañares-Alcántara. “A global, spatially granular techno-economic analysis of offshore green ammonia production”. In: *Journal of Cleaner Production* 367 (2022), page 133045. ISSN: 0959-6526. DOI: https://doi.org/10.1016/j.jclepro.2022.133045. URL: https://www.sciencedirect.com/science/article/pii/S0959652622026361.

[64] R. Seitz. “Bright water: hydrosols, water conservation and climate change”. In: *Climatic Change* 105.3 (2011), pages 365–381.

[65] M. Shields, P. Beiter, and J. Nunemaker. *A Systematic Framework for Projecting the Future Cost of Offshore Wind Energy*. Technical report. National Renewable Energy Laboratory, 2022.

[66] M. Sickler, B. Ummels, M. Zaaijer, R. Schmehl, and K. Dykes. “Offshore wind farm optimisation: a comparison of performance between regular and irregular wind turbine layouts”. In: *Wind Energy Science* 8.7 (2023), pages 1225–1233.

[67] T. Stehly, P. Duffy, and D. Mulas Hernando. *2022 Cost of Wind Energy Review*. 2023. URL: https://www.nrel.gov/docs/fy24osti/88335.pdf.

[68] K. Takahashi. “Transportation of Hydrogen by pipeline”. In: *Energy Carriers And Conversion Systems With Emphasis On Hydrogen-Volume II* 8 (2009), page 148.

[69] TNO. *HyDelta: WP 7B - D7B.1: Technical Analysis of H2 Supply Chains*. 2022. URL: https://zenodo.org/records/6469569#.Yl6godNByUk.

[70] European Union. *Renewable Hydrogen*. 2024. URL: https://energy.ec.europa.eu/topics/energy-systems-integration/hydrogen/renewable-hydrogen_en#:~:text=Renewable%20hydrogen%20is%20promoted%20in,June%202023%202%20delegated%20acts..

[71] G. Varras and M. Chalaris. "Critical Review of Hydrogen Production via Seawater Electrolysis and Desalination: Evaluating Current Practices". In: *Journal of Electrochemical Energy Conversion and Storage* 21.4 (2024).

[72] M. Velasquez-Jaramillo, J.-G. García, and O. Vasco-Echeverri. "Techno Economic Model to Analyze the Prospects of Hydrogen Production in Colombia". In: *International Journal of Thermofluids* 22 (2024), page 100597.

[73] Det Norske Veritas. *IMO CCC 10: Interim guidelines for ammonia and hydrogen as fuel*. 2024. URL: https://www.dnv.com/news/imo-ccc-10-interim-guidelines-for-ammonia-and-hydrogen-as-fuel/.

[74] P. Verschuren, H. Doorewaard, and M. J. Mellion. *Designing a research project*. Volume 2. The Hague: Eleven International Publishing, 2010.

[75] M. De Vries, B. Albers, S. Goossens, and B. Van Dongen. *Innovate and industrialize: How Europe's offshore wind sector can maintain market leadership and meet the continent's energy goals*. Technical report. Roland Berger, 2021.

[76] T. Weenk. *Smart grid-integrated vessel through a shore power system*. 2023. URL: http://resolver.tudelft.nl/uuid:eedf3cb6-6079-4a86-bf2b-3b4043227a09.

A

Corroborative Knowledge Types

The ranked corroborative knowledge types from [74] are shown in Table A.1.

Table A.1: Corroborative Knowledge Types Basic Summary, adapted from [74]

Knowledge type	Description
1. Descriptive	Comprehensive and accurate overview of a certain research object
2. Explanatory	Demonstrates causality, and generalizable laws which can be applied
3. Predictive	Makes a prediction about the future, based on past or current situation
4. Evaluative	Assesses the value of a research object, judging it positively or negatively
5. Prescriptive	Instructs on change of a situation

B

Parameters for Model Input

B.1. Cost Parameters

l	Year	$A_{l,i=1,j=1}$	$A_{l,i=2,j=1}$	$A_{l,i=1,j=2}$	$A_{l,i=2,j=2}$	$A_{l,i=1,j=3}$	$A_{l,i=2,j=3}$	$A_{l,i=1,j=4}$	$A_{l,i=2,j=4}$
0	2020	7.37E+06	1.33E+06	7.25E+06	1.45E+06	0.00E+00	0.00E+00	7.37E+06	1.33E+06
1	2023	7.37E+06	1.33E+06	7.03E+06	1.41E+06	0.00E+00	0.00E+00	7.37E+06	1.33E+06
2	2026	7.37E+06	1.33E+06	6.81E+06	1.36E+06	0.00E+00	0.00E+00	7.37E+06	1.33E+06
3	2029	7.37E+06	1.33E+06	6.59E+06	1.32E+06	0.00E+00	0.00E+00	7.37E+06	1.33E+06
4	2032	7.37E+06	1.33E+06	6.39E+06	1.28E+06	0.00E+00	0.00E+00	7.37E+06	1.33E+06
5	2035	7.37E+06	1.33E+06	6.19E+06	1.24E+06	0.00E+00	0.00E+00	7.37E+06	1.33E+06
6	2038	7.37E+06	1.33E+06	6.00E+06	1.20E+06	0.00E+00	0.00E+00	7.37E+06	1.33E+06
7	2041	7.37E+06	1.33E+06	5.80E+06	1.16E+06	0.00E+00	0.00E+00	7.37E+06	1.33E+06
8	2044	7.37E+06	1.33E+06	5.61E+06	1.12E+06	0.00E+00	0.00E+00	7.37E+06	1.33E+06
9	2047	7.37E+06	1.33E+06	5.41E+06	1.08E+06	0.00E+00	0.00E+00	7.37E+06	1.33E+06
10	2050	7.37E+06	1.33E+06	5.22E+06	1.04E+06	0.00E+00	0.00E+00	7.37E+06	1.33E+06

Table B.1: Cost Parameter A_{lij}

l	Year	$B_{l,k=1}$	$B_{l,k=2}$	$B_{l,k=3}$	$B_{l,k=4}$
0	2020	3.16E+06	7.19E+04	2.84E+06	1.23E+04
1	2023	2.73E+06	6.31E+04	2.53E+06	1.23E+04
2	2026	2.55E+06	5.76E+04	2.23E+06	1.23E+04
3	2029	2.44E+06	5.37E+04	1.92E+06	1.23E+04
4	2032	2.36E+06	5.02E+04	1.72E+06	1.23E+04
5	2035	2.30E+06	4.73E+04	1.57E+06	1.23E+04
6	2038	2.25E+06	4.48E+04	1.42E+06	1.23E+04
7	2041	2.21E+06	4.27E+04	1.30E+06	1.23E+04
8	2044	2.17E+06	4.08E+04	1.22E+06	1.23E+04
9	2047	2.14E+06	3.81E+04	1.15E+06	1.23E+04
10	2050	2.11E+06	3.65E+04	1.07E+06	1.23E+04

Table B.2: Cost Parameter B_{lk}

l	Year	$C_{l,n=1,j=1}$	$C_{l,n=1,j=2}$	$C_{l,n=1,j=3,4}$	$C_{l,n=2,j}$
0	2020	8.28E+01	7.82E+02	0.00E+00	9.06E+01
1	2023	8.03E+01	7.58E+02	0.00E+00	9.06E+01
2	2026	7.78E+01	7.35E+02	0.00E+00	9.06E+01
3	2029	7.53E+01	7.11E+02	0.00E+00	9.06E+01
4	2032	7.08E+01	6.68E+02	0.00E+00	9.06E+01
5	2035	6.52E+01	6.16E+02	0.00E+00	9.06E+01
6	2038	5.96E+01	5.63E+02	0.00E+00	9.06E+01
7	2041	5.40E+01	5.10E+02	0.00E+00	9.06E+01
8	2044	4.84E+01	4.57E+02	0.00E+00	9.06E+01
9	2047	4.28E+01	4.04E+02	0.00E+00	9.06E+01
10	2050	3.72E+01	3.52E+02	0.00E+00	9.06E+01

Table B.3: Cost Parameter C_{lnj}

C

Model Results for Scenarios in Business Case

Latitude	Longitude	LCOH [€/kg] (j=1)	LCOH [€/kg] (j=2)	LCOH [€/kg] (j=3)	LCOH [€/kg] (j=4)
58.35	2.78	5.642	6.986	4.966	6.222
58.35	3.78	5.584	6.921	4.871	6.136
58.35	4.78	5.575	6.899	4.834	6.105
58.35	5.78	5.821	7.217	5.052	6.332
58.35	6.78	7.545	9.200	6.620	8.033
58.35	7.78	7.691	9.315	6.740	8.187
57.35	2.78	5.722	7.085	4.874	6.166
57.35	3.78	5.614	6.952	4.724	6.027
57.35	4.78	5.501	6.810	4.579	5.894
57.35	5.78	5.370	6.628	4.423	5.731
57.35	6.78	5.293	6.524	4.337	5.650
57.35	7.78	***5.290***	***6.521***	4.344	5.653
56.35	2.78	5.702	7.061	4.705	6.034
56.35	3.78	5.669	7.025	4.608	5.951
56.35	4.78	5.575	6.905	4.475	5.826
56.35	5.78	5.519	6.820	4.378	5.732
56.35	6.78	5.497	6.795	4.353	5.709
56.35	7.78	5.519	6.822	4.377	5.732
55.35	2.78	5.644	6.983	4.511	5.873
55.35	3.78	5.635	6.972	4.426	5.800
55.35	4.78	5.593	6.916	4.311	5.698
55.35	5.78	5.572	6.896	4.256	5.655
55.35	6.78	5.571	6.898	4.238	5.641
55.35	7.78	5.592	6.915	4.261	5.658
54.35	2.78	5.647	6.987	4.424	5.804
54.35	3.78	5.637	6.974	4.314	5.716
54.35	4.78	5.612	6.943	4.195	5.613
54.35	5.78	5.592	6.922	4.098	5.534
54.35	6.78	5.589	6.909	***4.052***	***5.494***
54.35	7.78	5.626	6.957	4.119	5.560
53.35	2.78	5.628	6.964	4.383	5.764
53.35	3.78	5.660	7.006	4.299	5.702
53.35	4.78	5.720	7.087	4.245	5.685
53.35	5.78	6.154	7.624	4.539	6.016
53.35	6.78	6.656	8.193	4.897	6.428
53.35	7.78	7.497	9.087	5.729	7.339

Table C.1: LCOH for each scenario in every location calculated by model. Lowest LCOH found in each column is is highlighted in bold and italic font.